universität wien

MASTERARBEIT

„Macrocyclic systems based on dinuclear organometallic cores"

Verfasser

Leo Schranzhofer B.Sc.

Angestrebter akademischer Grad

Master of Science (M.Sc.)

Wien 2012

Studienkennzahl lt. Studienblatt:	A 066 086
Studienrichtung lt. Studienblatt:	Masterstudium Chemie
Betreuerin/Betreuer:	O. Univ.-Prof. Dr. Dr. Bernhard K. Keppler

universität wien

MASTERTHESIS

„Macrocyclic systems based on dinuclear organometallic cores"

Leo Schranzhofer B.Sc.

Submitted in part fulfillment of the requirements for the degree

Master of Science (M.Sc.)

Supervisor

O. Univ.-Prof. Dr. Dr. Bernhard K. Keppler

"Früher starben die Menschen mit 35,
heute schimpfen sie bis 95 auf die Chemie"
Carl H. Krauch

"Wer sich Steine zurechtlegen kann, über die er stolpert,
hat Erfolg in den Naturwissenschaften.“
Erwin Chargaff

Acknowledgements

At this place I want to thank the following people

O. Univ.-Prof. Dr. Dr. Bernhard K. Keppler for the opportunity to work in his workgroup and to do my master thesis.

Many thanks go to my supervisors Dr. Christian Hartinger, who provided me with this interesting topic, Dr. Wolfgang Kandioller for his great support during the whole work and to Dr. Muhammad Hanif for his help during my first days in the working group.

Furthermore I want to thank the whole NMR-Team (Mag. Sergey Abramkin, Dr. Wolfgang Kandioller, Dipl.-Chem. Paul-Steffen Kuhn, Mag. Verena Pichler, Mag. Michael Primik as well as Ao. Univ.-Prof. Dr. Markus Galanski) for the daily NMR measurements.

Ing. Alexander Roller and Ao.-Univ. Prof. Dr. Vladimir Arion for x-ray data collection and structure refinement.

Special thanks to Mag. Elfriede Limberger for her administrative work.

Then I want to thank my Lab 6 colleagues Andrea, Mario, Britta, Masha, Stefan and Filip for their daily support, fun and entertainment.

All the members of the working group especially Michi, Lukas, Paul, Jelena, Sam, Amitava, Alex, Norbert and Verena for the good atmosphere and daily conversations and Sonja for assisting and helping me with the synthesis.

A special thanks to my friends Thomas Herzog, René Elsner, Kevin Rambek, Anna-Maria Müller and Ingrid Krumphals for spending time together.

Many thanks to my family for their ceaseless support in daily life during my years in Vienna, especially to my mother and her husband Peter.

Last but not least, I want to thank my beloved Tanja for her support and for always being at my side.

For financial support:

Abstract

Metal-based drugs such as cisplatin, carboplatin and oxaliplatin are clinically applied in approximately 50% of all cancer treatments. However, these platinum(II)-complexes have shown various severe side effects. Therefore extensive research for novel non-platinum-based compounds acting as chemotherapeutics has been done over the last decades. In clinical studies ruthenium(III)-based drugs like KP1019 and NAMI-A exhibited very promising activity and it is supposed that the active species of these complexes is the analogous ruthenium(II) complex, formed under hypoxic conditions inside the tumor cell (“Activation by Reduction” hypothesis). The oxidation state +II of the ruthenium metal core can be stabilized by coordination of an arene moiety yielding a so called "piano-stool" configuration. A new strategy to improve the cytotoxicity is based on the binding of biological active chelating ligands to the metal center.

4-Pyrones (maltol, kojic acid, etc.) are known to possess a high affinity towards metal ions and a favorable toxicity profile. Related structures of this ligand system are 2- and 4-pyridones. It has been shown by Kay Severin and coworkers that ruthenium(II)-arene-complexes bearing 2,3-dihydroxypyridones as chelating ligands are able to form metallomacrocycles which could potentially protect the complex from cleavage of the bidentate ligand. During this master thesis a set of dinuclear organometallic systems based on 2,3-hydroxypyridone-derived ligands and ruthenium(II), osmium(II) and rhodium(III)-arene complexes were synthesized and characterized by NMR spectroscopy and in some cases by X-ray diffraction analysis. The stability and reactivity towards biomolecules was investigated. Additionally, the potential of these macrocyclic compounds as ionophores in aqueous solution in the presence of Li^+, Na^+ and K^+ ions was studied.

Zusammenfassung

Heutzutage werden in einem von zwei Fällen platinbasierende Medikamente wie Cisplatin, Carboplatin und Oxaliplatin als Chemotherapeutika in Kliniken eingesetzt. Aufgrund der großen Anzahl von Nebenwirkungen dieser Platin(II) Verbindungen wurde in den letzten Jahrzehnten verstärkt nach neuen nicht-platinhältigen Verbindungen geforscht, die in der Krebstherapie eingesetzt werden können. Hierzu zeigen Ruthenium(III) Komplexe wie KP1019 und NAMI-A vielversprechende Ergebnisse in klinischen Studien. Als aktive Spezies werden deren Ruthenium(II) Analoga angenommen, welche im hypoxischen Milieu des Tumors entstehen ("Activation by Reduction" Hypothese). Durch die Koordination eines Arenliganden kann die Oxidationsstufe +II stabilisiert werden. Dies führt zu einer "piano-stool" Konfiguration des Komplexes. Um deren Zytotoxizität weiter zu steigern, können biologisch aktive Moleküle als Chelatliganden an das Metallzentrum koordiniert werden.

4-Pyrone (Maltol, Kojisäure, usw.) sind bekannt für ihre hohe Affinität zu Metallionen und weisen außerdem ein sehr günstiges Toxizitätsprofil auf. Verwandte Strukturen dieses Ligandensystems stellen 2- und 4 Pyridone dar. Es wurde von Kay Severin und Mitarbeitern gezeigt, dass Ruthenium(II)-Aren Komplexe mit 2,3-Dihydroxypyridin-derivaten als Liganden Makrozyklen bilden können, welche dadurch vor einer möglichen Abspaltung des zweizähnigen Chelats geschützt ist. Im Rahmen dieser Masterarbeit wurden eine Reihe von zweikernigen organometallischen Systemen basierend auf 3-Hydroxy-2-pyridon-derivatiesierten Liganden koordiniert an Ruthenium(II), Osmium(II) und Rhodium(III) Zentren synthetisiert und mittels NMR Spektroskopie und Röntgendiffraktometrie charakterisiert. Die Stabilität in wässriger Lösung und deren Interaktion mit Biomolekülen wurde untersucht, sowie deren möglichen ionophoren Eigenschaften gegenüber Lithium, Natrium und Kaliumionen.

Table of Contents

Abbreviations

°C	degree Celsius
2,3-DHP	2,3-dihydroxypyridine
brs	broad singlet (NMR)
CD_3OD	deuterated methanol
$CDCl_3$	deuterated chloroform
cp*	pentamethyl-cyclopentadiene
cym	*p*-cymene
d	doublet (NMR)
D_2O	deuterated water
d^6-DMSO	(deuterated) dimethyl sulfoxide
e.g.	example given
eq	equivalent
Et_2O	diethyl ether
etc.	et cetera
EtOH	ethanol
g	gram
Hz	hertz
IC_{50}	drug concentration that causes 50% inhibition (of cell growth)
M	molar
m	multiplet (NMR)
MeOH	methanol
mg	milligram
NaOMe	sodium methoxide
NMR	nuclear magnetic resonance
pD	pondus deuterii (power of deuterium)
pH	pondus hydrogenii (power of hydrogen)
pK_a	negative decadic logarithm of the acid dissociation constant

pK_{a^*}	negative decadic logarithm of the acid dissociation constant for deuterium
ppm	parts per million
q	quartet (NMR)
s	singlet (NMR)
t	triplet (NMR)
δ	chemical shift (NMR)

1. Introduction

1.1. Cancer

In economically developed countries cancer after cardiovascular diseases is the second most leading cause of death. In 2010 19.757 people died due to this disease in Austria.[1]

Cancer is known for a broad range of different tissues, for example lung or breast cancer and is classified according to WHO guidelines[2] that show a wide spectrum of malignant neoplasm (see figure 1).[3]

The most frequent incident for men is prostate cancer and for women breast cancer (see figure 1).

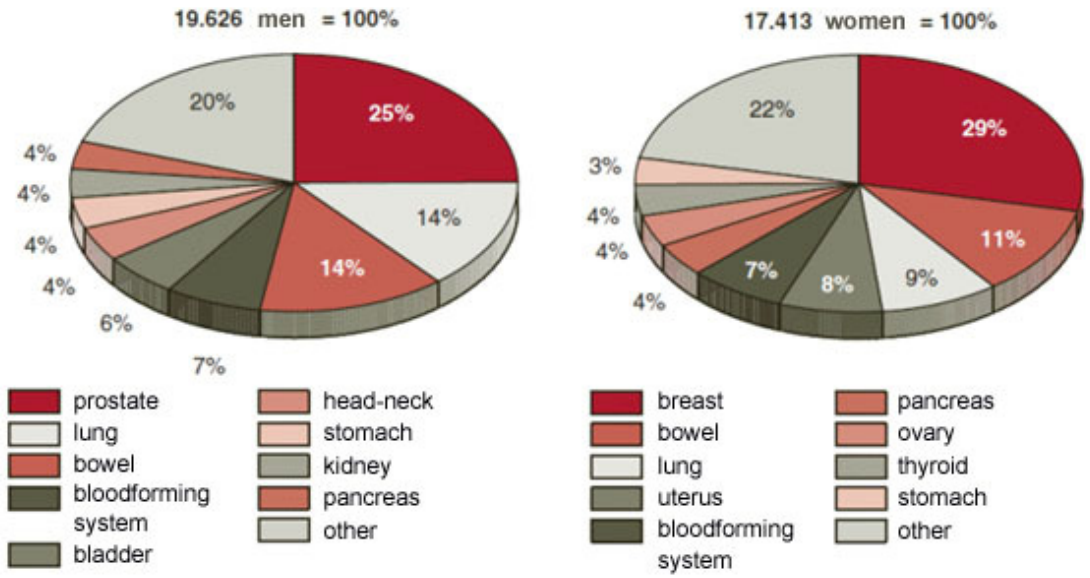

Figure 1 - Most common tumor types for men and women (2009)[3]

[1] Statistik Austria
[2] http://apps.who.int/classifications/icd10/browse/2010/en#/II
[3] http://www.statistik.at/web_de/wcmsprod/groups/b/documents/webobj/020524.gif

An early diagnosis of the disease is important for the therapy and therefore for survival of the patient. Characteristics of cancer cells include uncontrolled growth, invasion of nearby tissue and often formation of metastases.

1.2. Carcinogenesis

Gene mutations can arise spontaneously or can be induced. Spontaneous mutations naturally occur in all cells, whereas induced mutations are produced by mutagens or mutagenic agents, which are the predominant factor for gene mutations. Mutagens can be of chemical, physical (radiation) or biological (bacteria, viruses) origin. They are able to act by at least three different mechanisms. A nucleobase of the DNA can be replaced, altered (so that it specifically mispairs with another base) or damaged (so that it can't interact with its counterpart anymore). Most of these mutations have no effect, because of the degenerative coding of the DNA, due to the repair mechanisms of the cell or the recessive characteristic of the mutation. The repair mechanisms of cells take some time and cancer cell proliferation is usually faster than cell repair. This characteristic is important for cancer therapy.[4]

The complex multi-step process in which a normal healthy cell transforms into a malignant tumor cell is called carcinogenesis. The different progress stages are called initiation, promotion, conversion and finally the progression step (see figure 2).
In the initiation step a gene is modified spontaneously or by a mutagen. If cell division happens before the repair mechanism of the DNA and/or the programmed cell death occurs, the mutation is given to the next cell generation.
During the promotion step cell proliferation is either accelerated or the DNA is indirectly damaged by endogenous and exogenous substances (e.g. hormones, alcohol, tobacco smoke, etc.). These substances have to be present for some

[4] Anthony J.F. Griffiths et al, *An Introduction to Genetic Analysis,* W.H. Freeman an Company, New York, 7th Edithion, **2000**.

time (from weeks to years) to show an effect on the initiated cells. The so grown preneoplastic cell population is called a benign tumor, which has not invaded other tissue. Until this point, the whole process is reversible and apoptosis can occur.

Further mutations lead to the formation of a malignant tumor (conversion). It is possible that the second mutation can follow right after the initiation step. During the last step, the malignant tumor cells proliferate uncontrolled and start to invade other organs or tissue and spreading metastasis.[5,6]

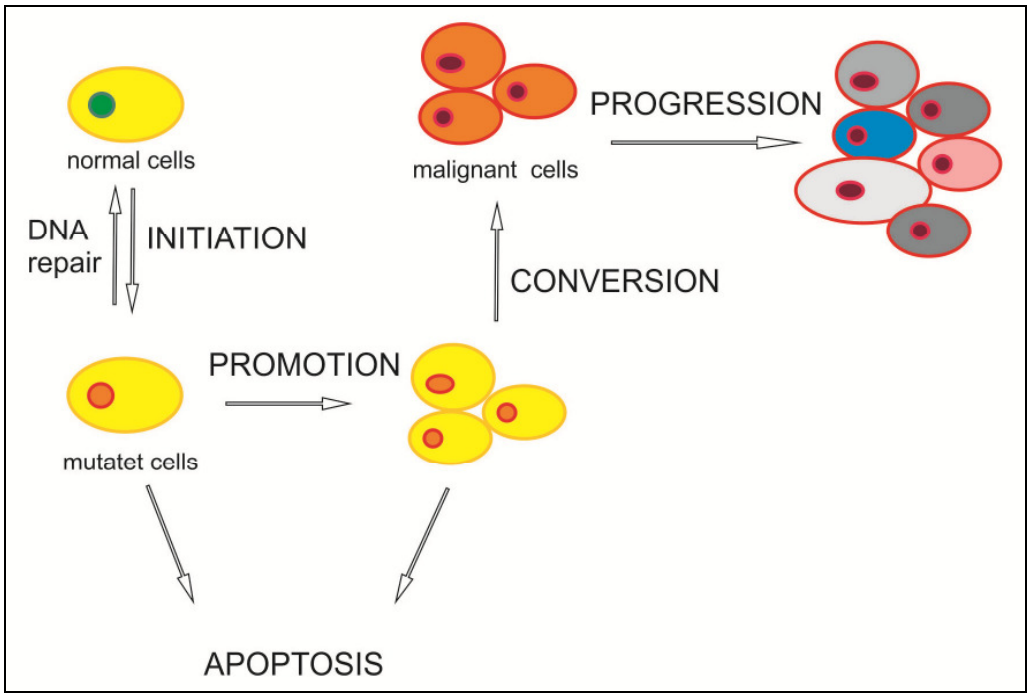

Figure 2 - Steps during carcinogenesis

[5] C. M. Haskell, *Cancer Treatment*, Saunders, Philadelphia **2000.**
[6] P. A. Oliveira, A. Colaço, R.I Chaves, H. Guedes-Pinto, L.F. De-La-Cruz, P. Carlos Lopes, *An Acad Bras Cienc*, **2007**, *79* (4), 593-616.

1.3. Cancer Therapy

A single cure for cancer is not possible due to the fact that cancer describes a variety of different diseases. The treatment is different for each patient and tumor type and depends on his/her health conditions as well as on the class and the progression of the tumor. The three main therapies are surgery, radiation therapy and chemotherapy. A combination of the three types is often practiced in modern cancer therapy.

Surgery is used for solid tumors, which are at an early stage or after chemo- or radiation therapy, when the size of tumor tissue has been decreased. Generally an additional cycle of medication or radiation treatment follows.

Radiation therapy uses ionizing radiation (x-ray or gamma ray, radioactive radiation) to harm and destroy the cancer cells. However, due to the induced damage to healthy cells, severe side effects can occur, which depend on the irradiated tissue (e.g. flush, mucositis, diarrhea, impairment of lung function, etc.).[7]

Chemotherapy: uses synthetic or natural chemical substances with low molecular weight for cancer treatment. Such compounds can interfere with the DNA replication of malignant tumor cells, inhibit proteins involved in the cell cycle or damage the cell in another way. As with radiation therapy, severe side effects occur during the treatment (e.g. hemogram changes, hair loss, nausea, mucositis, etc.)

[7] http://www.krebshilfe-wien.at/Strahlentherapie.106.0.html?&L=myqrgfkmkdnnpk#c358

Most of the applied chemotherapeutics can be divided in following classes:

- Alkylating and intercalating agents: alter DNA, can induce strain breaks or cross-link DNA, inhibit RNA and proteins to hinder transcription and translation of the DNA. Examples are triazines (e.g. *dacarbazine*), nitrogen mustardes (e.g. *cyclophospamide*), alkyl sulfonates (e.g. *busulfan*) and platinum(II) complexes (e.g. *Cisplatin*, *Carboplatin*)
- Anti-metabolites: mimic nucleobases and can be implemented to the DNA or RNA of the cancer cell to stop transcription and translation. Examples are folic acid analogues (e.g. *methotrexate*), pyrimidine analogues (e.g. *5'-flourouracil, floxuridine*), purine analogues (e.g. *tioguanine*) and topoisomerase inhibitors (e.g. *topotecan*, *etoposide*).
- Mitosis Inhibitors: are plant alkaloids and terpenoids that prevent cell division by interfering with the microtubule function. Examples are vinca alkolids and taxanes.

Additional classes of chemotherapeutics include hormone inhibitors, cytotoxic antibiotics (e.g. *anthracycline*, *mitoxantrone*, *bleomycine*), antibodies, signal transduction inhibitors and enzyme inhibitors.[5]

1.4. Metal based Drugs

Since ancient times metals play an important role for mankind, not only in making tools and weapons, but also for medicine. Metals were used as salts or in elementary state for medication. For example arsenic salts were applied in ancient Greece for treating asthma.[8] Mercury, was also used for treating gastro-intestinal diseases and is still used as amalgam for dental filing in modern times.

[8] D. Doyle, *British Journal of Haematology* **2009**, 145, 309-317.

Nowadays metal based drugs are established and widely used (e.g. cisplatin, auranofin, lithium).

During an investigation in the 1960's of the effects of electric fields on bacterial growth Barnett Rosenberg discovered that in the presence of platinum (from the electrodes), ammonium chloride and sunlight *E. coli* bacteria didn't proliferate. Instead they formed long filaments (up to 300 times bigger). The under these conditions generated *cis*-diamminedichloridoplatinum(II) (*cisplatin*), was responsible for the arrest of cell division.[9] This feature of cisplatin was of high importance for new metal based anti-cancer drugs. The huge success of cisplatin started the research for other platinum and non-platinum metal based drugs.
Nowadays platinum compounds are widely used as chemotherapeutics and cisplatin, carboplatin and oxaliplatin (see figure 3) are in worldwide clinical use.

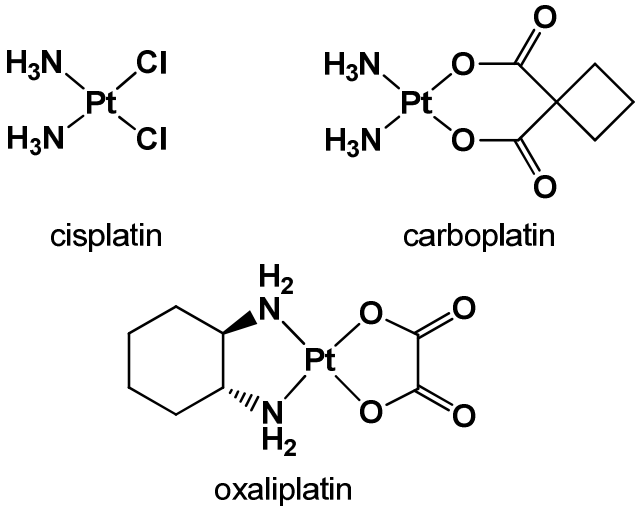

Figure 3 - Platinum-based anticancer drugs in clinical use

Cisplatin coordinates to the DNA and hinders the DNA replication by bending the DNA strain. The mode of action is as follows: cisplatin is transported into the cell, is hydrolyzed in the cytoplasma and transported to the cells core. There the

[9] B. Rosenberg, L. Van Camp, T. Krigas, *Nature* **1965**, *205*, 698-699.

DNA-cisplatin-adduct can be formed, but it can also bind to RNA and sulfhydryl groups of proteins, which is supposed to inactive the compound.[10] Oxaliplatin and carboplatin shows a similar mode of action. Oxaliplatin is also effective against certain types of cancer, for where cisplatin shows less to no activity (e.g. colon cancer).

Platinum compounds are used for about 50% of cancer treatments nowadays, but not every tumor type is sensitive to them. Due to the numerous side effects (e.g. nephrotoxicity, neurotoxicity for cisplatin) and the intrinsic and acquired resistances of some tumors, researchers focus on the development of novel (non-)platinum based chemotherapeutics.

1.4.1. Ruthenium based Drugs

During the last decades a broad range of metal complexes have been developed and investigated for their anticancer potential and ruthenium complexes have shown very promising results *in vitro* and *in vivo*.[11] These compounds possess a similar ligand exchange rate compared to platinum(II)-compounds, are stable at different oxidation states (II, III, IV) under physiological conditions and features an octahedral ligand geometry. Because of the similarity of ruthenium to iron, they can also bind to transport proteins (albumin, transferrin), leading to an improved selectivity and lower toxicity, indicating a different mode of action compared to platinum-based drugs.
Two pathophysiological characteristics of solid tumors are an overexpression of iron transporting protein receptors (transferrin-receptors)[12] and a surrounding

[10] Robert R. Crichton, *Biological Inorganic Chemistry An Introduction*, Elsevier B. V., Netherlands, 1st Edition, **2008**.
[11] C.G. Hartinger, M.A. Jakupec, S.Zorbas-Seifried, M. Groessl, A. Egger, W. Berger, H. Zorbas, P.J. Dyson, B.K. Keppler, *Chemistry and Biodiversity* **2008**, *5*, 2140-2155.
[12] F. Kratz, B. K. Keppler, M. Hartmann, L. Messori, M. R. Berger, *Metal-based Drugs* **1996**, *3*(1), 15-23.

reductive milieu, based on the insufficient nutrient and blood supply (hypoxic milieu).[13] The ruthenium(III)-complex is supposed to be reduced to the more reactive ruthenium(II) species under these conditions. This step is called "activiation by reduction" and was first postulated by Clarke in the 1980's.[14]

The most promising compounds so far are KP1019 (respective the sodium salt KP1339) and NAMI-A (see figure 4), which are currently investigated in clinical trials.

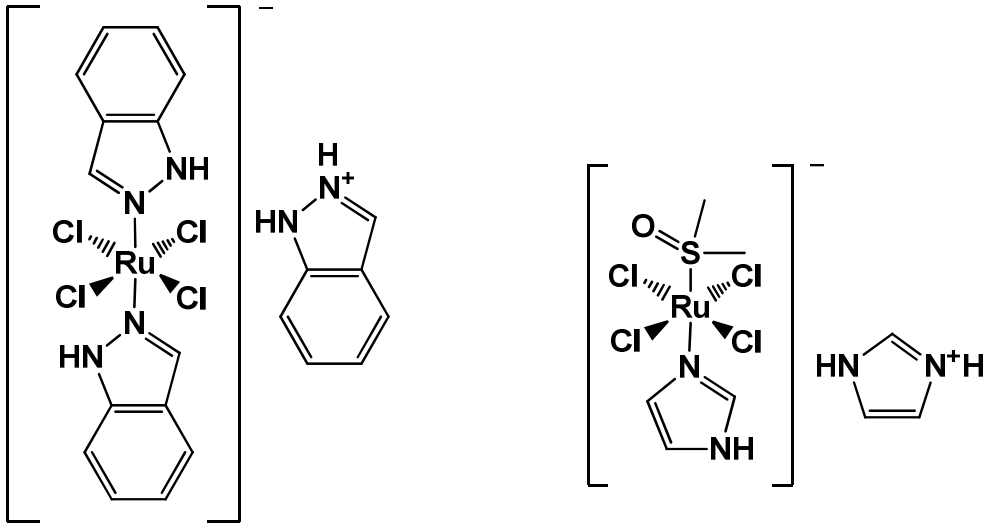

Figure 4 - Ruthenium(III) compounds in clinical phase I

After intravenous formulation of KP1019 a fast binding to the blood proteins albumin and transferrin can be observed and the formed adducts are accumulated within the tumor cell, where after reduction the active ruthenium(II)-analog can interact with biological targets. Experiments in freshly explanted human tumor samples, including specimens with resistance to standard antineoplastic agents showed activity in a broader spectrum of tumors.

[13] S. Kapitza, M. Pongratz, M. Jakupec, W. Berger, L. Lackinger, B.K. Keppler, B. Marian, *Journal of Cancer Research and Clinical Oncology* **2004**, *131*(2), 101-110.
[14] M. J. Clarke, *Met. Ions. Biot. Syst.* **1980**, *11*, 231.

NAMI-A on the other hand showed only minor activity against primary tumors but possess some antimetastatic potential. Both compounds already passed clinical phase I and KP1339 will enter clinical phase II soon. Investigations on the potential biological targets are in progress.[15]

As a consequence of the "activation by reduction" hypothesis by Clarke, ruthenium (II) complexes were studied for their cytotoxicity. The oxidation state +II can be stabilized by coordination of an arene moiety (e.g. benzene, biphenyl, dihydroanthracene, *p*-cymene, etc.). The three remaining binding sites of the so called "piano-stool" configuration (position X, Y, Z, see Figure 5) can contain various mono-, di- or tridentate ligands.

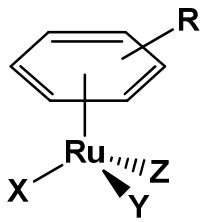

Figure 5 - Ruthenium(II)-complex geometry - "piano-stool" configuration

The positions X and Y are often occupied by a chelating ligand, e.g. ethylenediamine, which can provide additional stability, whereas in position Z halido ligand is often coordinated to the metal center, which acts as a leaving group. Hydrolysis of the Ru-halido bond appears to be important for activation, yielding the highly reactive aqua species, which can interact with the biological target, implying a different mode of action as for ruthenium(III)-compounds.[16,17,18]

---

[15] M. Galanski, B.K. Keppler, *Tumorhemmende Metallverbindungen*, Pharm. Unserer Zeit, **2/2006** (35).
[16] A. Habtemariam, M. Melchart, R. Fernandez, S. Parsons, I.D.H. Oswald, A. Parkin, F.P.A. Fabbiani, J.E. Davidson, A. Dawson, R.E. Aird, D.I. Jodrell, P.J. Sadler, *J. Med. Chem.* **2006**, *49*, 6858–6868.
[17] W. H. Ang, A. Casini, G. Sava, P.J. Dyson, *Journal of Organometallic Chemistry* **2011**, *696*, 989-998.
[18] D.J.M. Snelders, A. Casini, F. Edafe, G. van Koten, R.J.M. Klein Gebbink, P. J. Dyson, *Journal of Organometallic Chemistry* **2011**, *696*, 1108-1116.

Sadler and coworkers studied the influence of the arene ligand on biological activity of the ruthenium(II) complexes with the general form [Ru(η^6-arene)(en)X] (en = ethylenediamine, X = Cl, Br, I). It was found that the cellular uptake increase with the lipophilicity of the arene ligand.[19] *p*-Cymene is often used as arene ligand.

Alteration of the first reported Ruthenium(II)-arene complex ([$RuCl_2$(DMSO)(η^6-C_6H_6)] [20] led to the development of the PTA (= 1,3,5-triaza-7-phospha-adamantane) based family of RAPTA complexes (see figure 6), which exhibits an increased aqueous solubility, antimetastatic effects as well as a lower general toxicity, comparable to NAMI-A.[21]

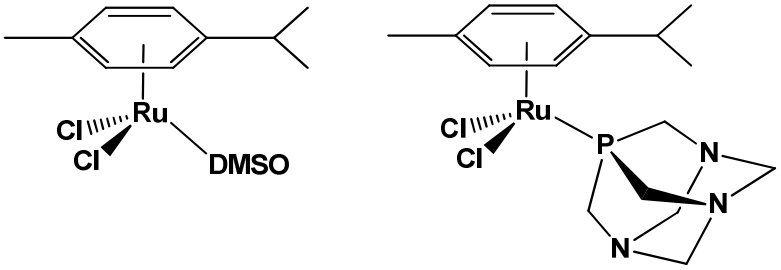

Figure 6 - [$RuCl_2$(DMSO)(C_6H_6)] and RAPTA-C

The tendency today is to develop metal-complexes bearing biologically active compounds, which can induce synergetic effects due to the coordination.[22]

3-Hydroxy-4-pyrones as natural products with a low toxicity profile offer a broad range of different derivatisation possibilities. They can be used as chelating

[19] R. E. Aird, J. Cummings, A. A. Ritchie, M. Muir, R. E. Morris, H. Chen, P. J. Sadler, D. I. Jodrell, *Br. J. Cancer* **2002**, *86*, 1652-1657.
[20] L.D. Dale, J.H. Tocher, T.M. Dyson, D.I. Edwards, D.A. Tocher, *Anti-Cancer Drug Design* **1992**, *7*(1), 3-14.
[21] C. Scolaro, A. Bergamo, L. Brescacin, R. Delfino, M. Cocchietto, G. Laurenczy, T.J. Geldbach, G. Sava, P.J. Dyson, *J. Med. Chem.* **2005**, *48*, 4161-4171.
[22] M.A. Jakupec, M. Galanski, V.B. Arion, C.G. Hartinger, B.K. Keppler, *Dalton Trans.* **2008**, 183-194.

ligands due to their high affinity to metal ions yielding highly stable complexes. Some examples of pyrone-ligands are shown in figure 7.[23,24]

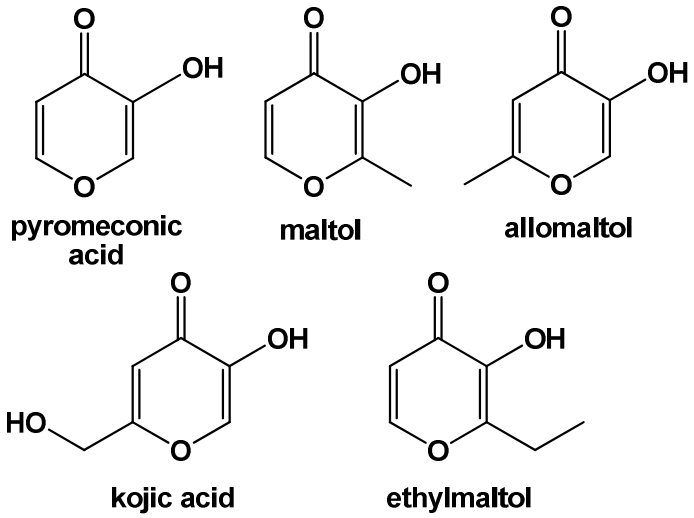

Figure 7 – Examples for common 3-hydroxy-4-pyrones

Pyrone-based Ruthenium(II) complexes were reported in literature during the last years.[23] As an example, the maltolato-based ruthenium and osmium complexes were investigated by Sadler and co-workers for their behavior in aqueous solution and their cytotoxicity in A2780 and A2780^{cis} cell lines. It was observed that the ligand exchange (Cl to H_2O) was too fast to be monitored by NMR spectroscopy. After some time, the maltolato-ligand seemed to be cleaved in aqueous solution and a stable but inactive dimeric hydroxido complex of the general structure $[Ru_2(cym)_2(OH)_3]^+$ was formed (see scheme 1). The IC_{50}-values were determined and no significant *in vitro* cytotoxicity was observed.[25]

[23] W. Kandioller, A. Kurzwernhart, M. Hanif, S.M. Meier, H. Henke, B.K. Keppler, C.G. Hartinger, *Journal of Organometallic Chemistry*, **2011**, *696*, 999-1010.
[24] W. Kandioller, C. G. Hartinger, A. A. Nazarov, C. Bartel, M. Skocic, M. A. Jakupec, V. B. Arion, B. K. Keppler, *Chem. Eur. J.* **2009**, *15*, 12283-12291.
[25] A.F.A. Peacock, M. Melchart, R.J. Deeth, A. Habtemariam, S. Parsons, P.J. Sadler, *Chem. Eur. J.* **2007**, *13*, 2601-2613.

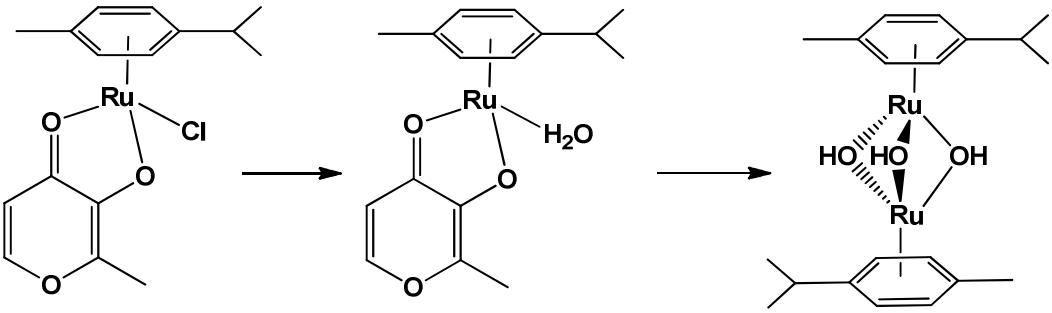

Scheme 1 – Hydrolysis of maltolato-cymene-ruthenium(II)-complex forming hydroxido dimer

To stabilize the ruthenium(II) pyronato system, various modified complexes were reported.[24,26,27,28] For all complexes, a quick aquation to the corresponding aqua species by exchange of the halido ligand was observed. Derivatisation at position two of the pyrone backbone leads to moderate IC_{50}-values, whereas thionation of the 4-oxygen led to IC_{50}-values in the low micromolar range.

1.4.2. Osmium and Rhodium based Drugs

Other elements of the platinum-group are also known for their cytotoxic activity, but were only minor investigated during the last decades.

Due to the similarity to ruthenium, osmium can be another candidate for metal-based drugs. Like ruthenium, osmium complexes are stable at different oxidation states (II, III, IV) under physiologic conditions and several cytotoxic osmium(II) analogues of ruthenium(II) arene complexes were reported.[29,30,31] A general

[26]W. Kandioller, C.G. Hartinger, A.A. Nazarov, M.L. Kuznetsov, R.O. John, C. Bartel, M.A. Jakupec, V.B. Arion, B.K. Keppler, *Organometallics* **2009**, *28*, 4249-4251.
[27] M. Hanif, P. Schaaf, W. Kandioller, M. Hejl, M.A. Jakupec, A. Roller, B.K. Keppler, C.G. Hartinger, *Aust. J. Chem*. **2010**, *63*, 1521-1528.
[28] J.H. Kasser, W. Kandioller, C.G. Hartinger, A.A. Nazarov, V.B. Arion, P.J. Dyson, B.K. Keppler, *Journal of Organometallic Chemistry* **2010**, *695*, 875-881.
[29] A.F.A. Peacock, S. Parsons and P.J. Sadler, *J. Am. Chem. Soc.* **2007**, *129*, 3348–3357.
[30] A.F.A Peacock, A. Habtemariam, R. Fernandez, V. Walland, F.P.A. Fabbiani, S. Parsons, R.E. Aird, D.I. Jodrell, P.J. Sadler, *J. Am. Chem. Soc*. **2006**, *128*, 1739–1748.

distinction between the activity of osmium and ruthenium as central metal is not possible, because of the large influence of the ligand system. Besides the ruthenium analogues other osmium complexes were reported, e.g. osmium(VI)-nitrido complexes, which exhibited an *in vitro* activity in the micromolar range.[32]

Rhodium in its oxidation states +I, +II and +III was only of little interest in the last decades for anti-cancer drug design. Rhodium(I) complexes are generally known for their use as catalysts for hydrogenation or hydroformylation (e.g. Willkinson catalyst[33]). However, rhodium was one of the first transition metals that was investigated for its cytotoxic activity.[9] There are a few compounds reported as possible anti-cancer agents in oxidation state +III.[34,35,36,37] Some of them are similar to ruthenium(II) complexes with piano-stool configuration of general composition [Rh(cp*)(X)Cl] (X = chelating ligand).[35] Dimeric acetato complexes of Rh(II) as well as monomeric Rh(I) and Rh(III) complexes have shown interesting anticancer properties.[36,38]

---

[31] L.K. Filak, G. Mühlgassner, M.A. Jakupec, P. Heffeter, W. Berger, V.B. Arion, B.K. Keppler, *J Bio.l Inorg. Chem.* **2010**, *15*, 903–918.
[32] Wen-Xiu Ni, Wai-Lun Man, Shek-Man Yiu, Man Ho, Myra Ting-Wai Cheung, Chi-Chiu Ko, Chi-Ming Che, Yun-Wah Lam, Tai-Chu Lau, *Chem. Sci.* **2012**, *3*, 1582–1588.
[33] A. F. Holleman, N. Wiberg, *Lehrbuch der Anorganischen Chemie*, 102. Auflage **2007**, Walter de Gruyter & Co, Berlin.
[34] R. Bieda, I. Kitanovic, H. Alborzinia, A. Meyer, I. Ott, S. Wölfl, W.S. Sheldrick, *Biometals* **2011**, *24*, 645-661.
[35] Y. Geldmacher, R. Rubbiani, P. Wefelmeier, A. Prokop, I. Ott, W.S. Sheldrick, *Journal of organometallic Chemistry* **2011**, *696*, 1023-1031.
[36] M. Carneiro, E. Nunes, R. Peixoto, R. Oliveira, L. Lourenço, I. da Silva, A. Simioni, A. Tedesco, A. de Souza, Z. Lacava, S. Báo, *Journal of Nanobiotechnology* **2011**, *9*, 11.
[37] S. Wirth, C.J. Rohbogner, M. Cieslak, J. Kazmierczak-Baranska, S. Donevski, B. Nawrot, I.P. Lorenz, *J Biol Inorg Chem* **2010**, *15*, 429-440.
[38] N. Katsaros, A. Anagnostopoulou, *Crit Rev Oncol Hematol* **2002**, *42*, 297-308.

1.5. 3-Hydroxypyridones

Protected 3-hydroxy-4-pyrones can be converted easily to their corresponding 3-hydroxypyridones by reaction with ammonia or primary amines (including amino acids) in high yields (see scheme 2). As an example for their high affinity to metal ions, the relatively non-toxic deferiprone (1,2-dimethyl-3-hydroxy-4(*1H*)-pyridone) can be used for the treatment of iron overload.[39]

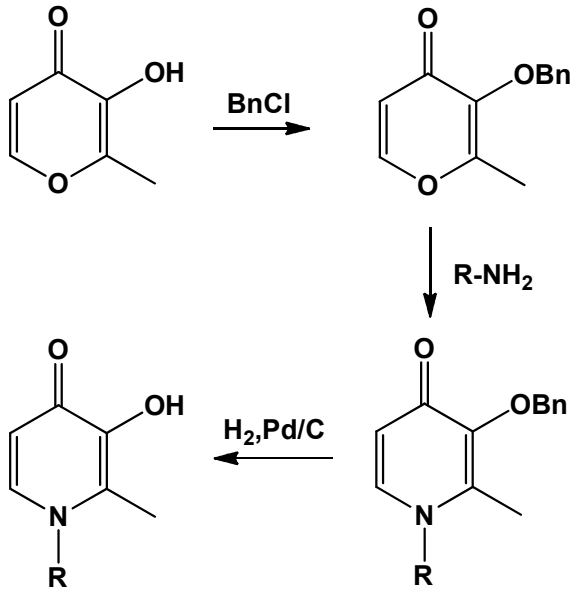

Scheme 2 - Conversion of maltol to the corresponding pyridone

Ruthenium and osmium complexes were investigated for their antiproliferative potential, whereas di- or trinuclear complexes bearing 3-hydroxy-4-pyridones (see figure 8) were synthesized with very promising *in vitro* antitumor activity was.[40]

[39] A.V. Hoffbrand, A. Cohen, C. Hershko, *Blood* **2003,** *102* 17-24.
[40] M.G. Mendoza-Ferri, C.G. Hartinger, A.A. Nazarov, R.E. Eichinger, M.A. Jakubec, K. Severin, B.K. Keppler, *Organometallics* **2009**, *28*(21), 6260-6265.

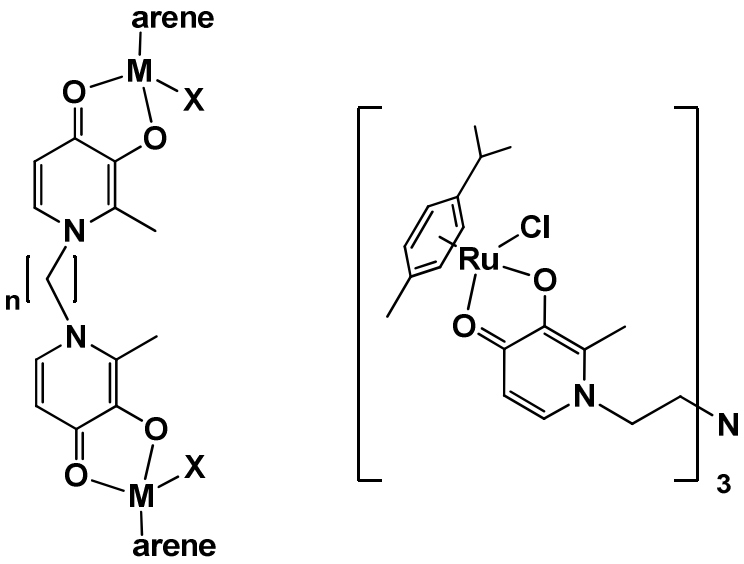

Figure 8 - Dinuclear and trinuclear metal complexes (M = Ru, Os; X = Cl, Br, I; n = 6, 8; arene = p-cymene, biphenyl)

The isomeric 3-hydroxy-2-pyridones can by synthesized by using the commercially available 2,3-DHP. As their close analogues (3-hydroxy-4-pyridones) they provide many possibilities for derivatisations, e.g. substitution on position 4 and 6, thionation or alkylation of the hydroxy group (see figure 9).

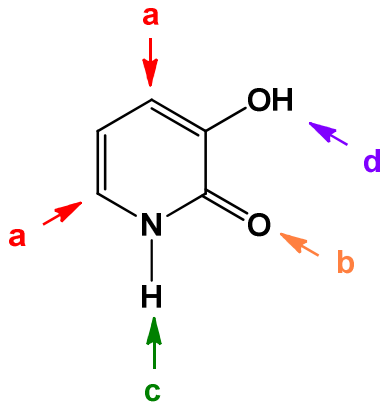

Figure 9 - Possible modification sites of the 2-pyridone scaffold; a: mannich reaction, substitution, b: thionation, c: N-alkylation, d: alkylation

Both types of pyridones can be easily functionalized at the nitrogen atom or at different positions of the pyridone system, which provides an opportunity for fine-

tuning chemical and biological properties such as lipophilicity, bioavailability, chelating ability, etc.[23,41,42].

Metal complexes bearing 3-hydroxy-2-pyridone derivates as bidentate ligands were investigated for a broad range of biological application, e.g. as potential enzyme inhibitors against tuberculosis[43], as metal chelators of Al(III) against Alzheimer disease[44] and gadolinium complexes as potent MRI-contrast agents and also for their cytotoxic potential. [45,46,47] These complexes showed a fast hydrolyses to the respective aqua species, which is stable for at least five days without forming of dimeric hydroxido-ruthenium arene species. However, the aqua-complexes react quickly with different amino acids leading to the loss of the hydroxypyridone ligand. The osmium compounds seem to be more stable than their corresponding ruthenium complexes. The interaction with the DNA-model compound 5'-GMP was investigated and coordination of the *N7* atom of the purine base was observed. The formed adduct was found to be stable for more than 24 hours. Unfortunately these compounds showed no *in vitro* cytotoxic activity against the human tumor cell lines CH1 (human ovarian cancer), SW480 (colon cancer) and A549 (non-small cell lung cancer).

1.5.1. Metal Cages

A special feature of metal complexes bearing 3-hydroxy-2-pyridones is the possibility to form macrocyclic systems. Kay Severin and coworkers described a

---

[41] R.C. Fox, P.D. Taylor, *Synthetic Communications*, **1998**, *28*(9), 1563-1574.
[42] Deng Ruey Hwang, J. S .Driscoll, *Journal of Pharmaceutical Sciences* **1979**, *68*(7), 816-819.
[43] S.L. Williams, C.A.F. de Oliveira, H. Vazquez, J.A. McCammon, *Chem. Bio. Drug Des*. **2011**, *77*, 117-123.
[44] K.H. Thompson, C.A. Barta, C. Orvig, *Chem. Soc. Rev*. **2006**, *35*, 545-556.
[45] E.J. Werner, J. Kozhukh, M. Botta, E.G. Moore, S. Avedano, S. Aime, K.N. Raymond, *Inorg. Chem.* **2009**, *48*, 277-286.
[46] V.C. Pierre, M. Botta, S. Aime, K.N. Raymond, *J. Am. Chem. Soc*. **2006**, *128*, 5344-5345.
[47] M. Hanif, H. Henke, S.M. Meier, S. Martic, M. Labib, W. Kandioller, M.A. Jakubec, V.B. Arion, H.B. Kraatz, B.K. Keppler, C.G. Hartinger, *Inorg. Chem*. **2010**, *49*, 7953-7963.

metallomacrocyclic ionophore which is sensitive for alkali metals. The trimeric complex can be easily obtained by self-assembly using ruthenium-cymene precursor and 2,3-DHP.[48] The alkali metal fits in the cavity of this metallocrown ether and is stabilzed *via* the oxygen atoms (see figure 12). Other macrocycles were reported by modifying the hydroxypyridone scaffold[49,50] or by coordination of other ligand systems[51] to increase the number of metal cores of the cages, which can be selective for metal ions or are able to intercalate organic molecules, e.g. coronene or perylene.[52]

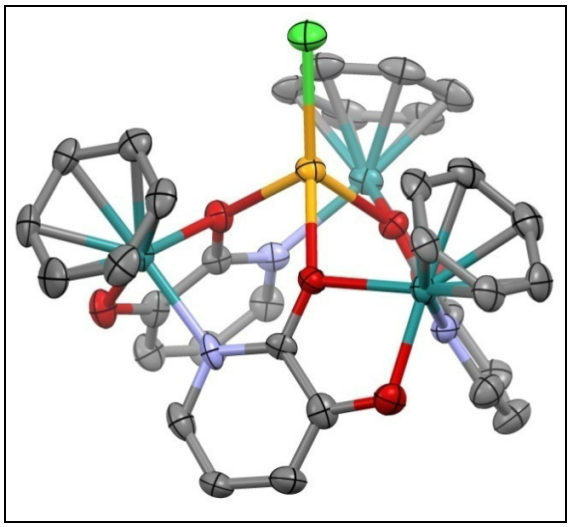

Figure 10 - Molecular structure of [η^6-p-cymene)(3-oxo-κO-2-(*1H*)-pyridonato-κO)ruthenium]$_3$·NaCl without hydrogens and methyl and isopropyl substitutes of the arene ring

[48] H. Piotrowski, K. Polborn, G. Hilt, K. Severin, *J. Am. Chem. Soc.* **2001**, *123*, 2699-2700.
[49] Zacharias Grote, Simone Bonazzi, Rosario Scopelliti, Kay Severin, *J. Am. Chem. Soc.* **2006**, *128*, 10382-10383.
[50] A. Granzhan, T. Rüs-Johannessen, R. Scopelliti, K. Severin, *Angew. Chem. Int. Ed.* **2010**, *49*, 5515-5518.
[51] S. Mirtschin, E. Krasniqi, R. Scopelliti, K. Severin, *Inorganic Chemistry* **2008**, *47*(14), 6375-6381.
[52] B. Therrien, *Eur. J. Inorg. Chem* **2009**, 2445-2453.

2. Results and Discussion

The aim of this master thesis was the synthesis of novel piano-stool configured dimeric Ru(II)-(η^6-p-cymene), Os(II)-(η^6-p-cymene) and Rh(III)-(η^5-cp*) complexes bearing different *N*-functionalized 3-hydroxy-2-pyridones as chelating ligands. The compounds were characterized by NMR spectroscopy, elemental analysis, melting point, water solubility and for some complexes by crystal structure analysis and mass spectrometry.

2.1. Synthesis and Characterization of Metal Complexes bearing 3-Hydoxy-2-pyridone Ligands

2.1.1. Synthesis

Two different methods were performed to obtain chain length of the spacer with one (C1-spacer) or two carbon atoms (C2-spacer) between the nitrogen atom of the pyridone ring and the ester group (see scheme 3). Compound **1a** (1-Ethoxycarbonylmethyl-3-hydroxy-2(*1H*)-pyridone) was synthesized by *N*-alkylation of 2,3-DHP according to literature procedure.[53]

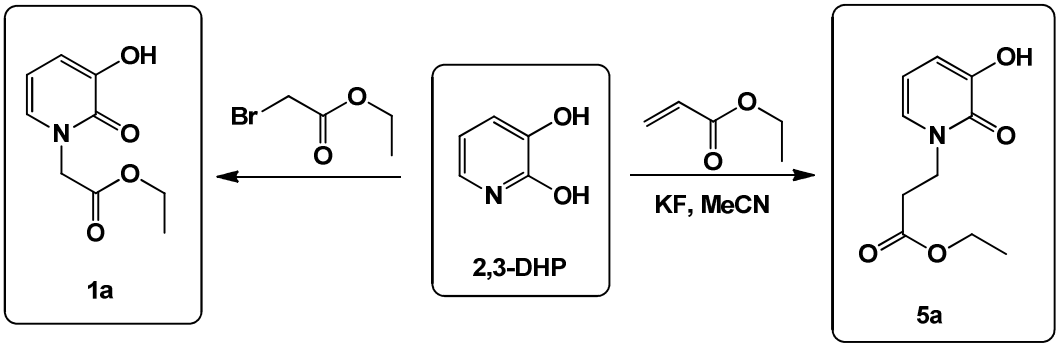

Scheme 3 - Synthesis of intermediates of C1 and C2 spacer

[53] M. Streater, P.D. Taylor, R.C. Hider, J. Porters, *J. Med. Chem.* ***1990,*** *33,* 1749-1755.

For a chain length of two carbon atoms (C2-spacer) a Michael-addition was performed, using 2,3-DHP and ethyl acrylate as reagents and potassium fluoride as the catalyst resulting in compound **5a** with an excellent yield of 90%. [54]

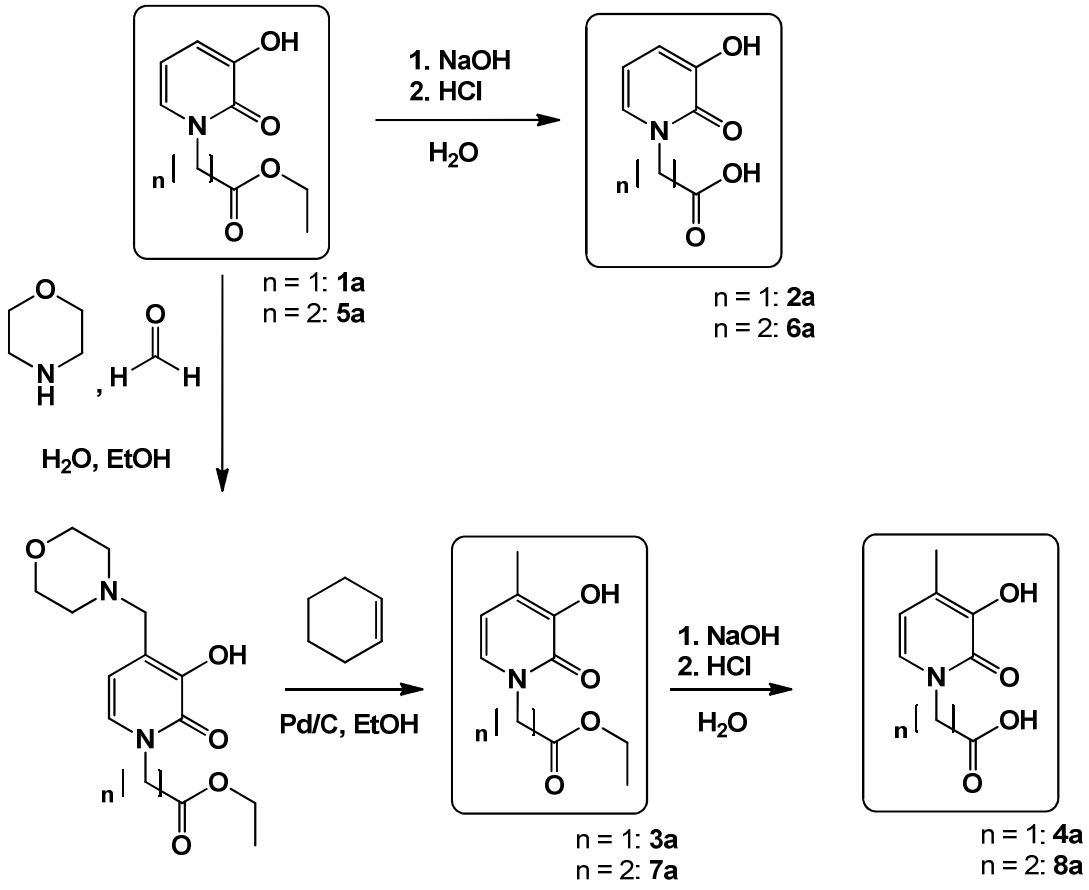

Scheme 4 - Synthesis of C1 and C2 spacer ligands

Both *N*-functionalized hydroxypyridones were further modified according to literature procedure (scheme 4). [55] Compound **1a** (respectively **5a**) was methylated on position 4 in two steps. In the first step the intermediate was modified by Mannich reaction using morpholine and formaldehyde. The isolated compound **1i** (respectively **5i**) was reduced with cyclohexene as a hydrogen

[54] J.H. Clark, *Chem. Rev.*, **1980**, *80*, 429-452.
[55] R.C. Fox, P.D. Taylor, Synthetic Communications, **1998**, *28*(9), 1563-1574.

source and in the presence of Pd on charcoal as catalyst yielding compound **3a** (respectively **7a**). Afterwards, hydrolysis of the ester moiety of **1a** and **3a** (respectively **5a** and **7a**) led to the free acids **2a** and **4a** (respectively **6a** and **8a**).

The obtained ligands **1a–8a** were converted to their corresponding metal complexes under alkaline conditions (as described in section 3.2.2. general procedure for pyridone metal complexes) using different dimeric metal precursors (bis[(η^6-p-cymene)dichlorido ruthenium(II)] - **p1**, bis[(η^6-p-cymene)dichlorido osmium(II)] - **p2**, Bis[dichlorido(η^5-pentamethylcyclopentadiene) rhodium(III)] - **p3**). By using ligands with carboxylic acid, the formation of dimers of the metal complexes was observed (see scheme 5).

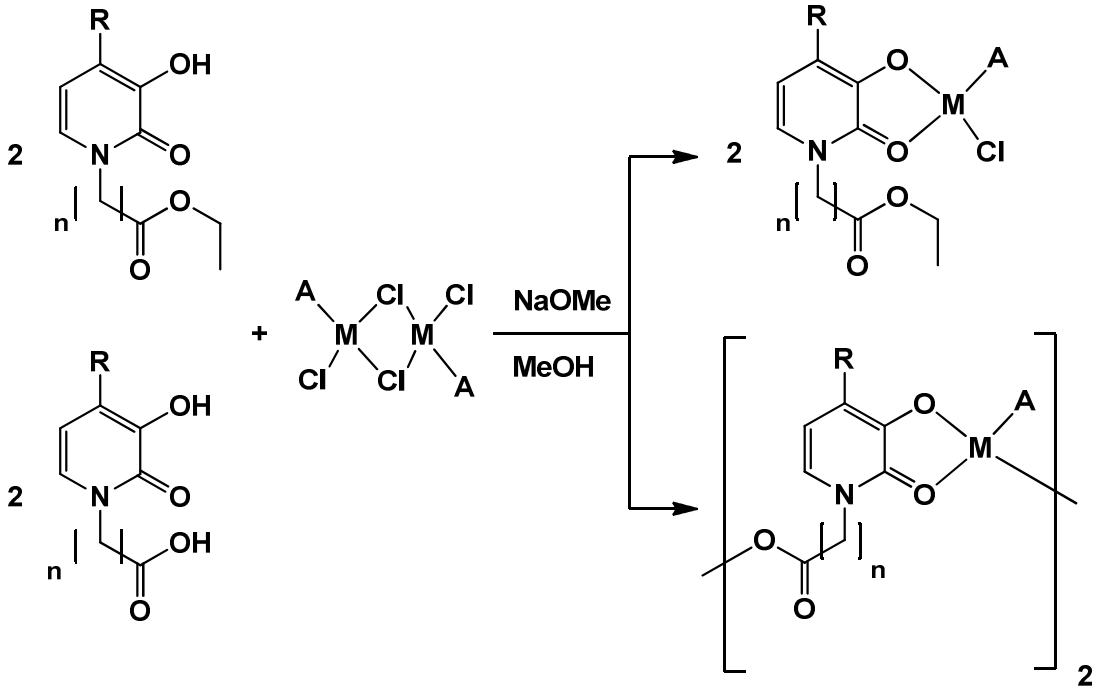

Scheme 5 - Complexation (A = cym, cp*, M = Ru(II), Os(II), Rh(III), n = 1, 2, R = H, CH_3)

A series of different complexes was obtained with variation of the metal center, the coordinated arene, mono and dinuclear organometallics and with different ligand systems modified at position 4 and various spacer lengths (see table 1).

Table 1 - Different ruthenium(II), osmium(II) and rhodium(III) complexes

Complex ID	Ligand ID	R	A	M
1b	**1a**	H	cym	Ru
1c	**1a**	H	cym	Os
1d	**1a**	H	cp*	Rh
2b	**2a**	H	cym	Ru
2c	**2a**	H	cym	Os
2d	**2a**	H	cp*	Rh
3b	**3a**	CH_3	cym	Ru
3c	**3a**	CH_3	cym	Os
3d	**3a**	CH_3	cp*	Rh
4b	**4a**	CH_3	cym	Ru
4c	**4a**	CH_3	cym	Os
4d	**4a**	CH_3	cp*	Rh
5b	**5a**	H	cym	Ru
5d	**5a**	H	cp*	Rh
6b	**6a**	H	cym	Ru
6d	**6a**	H	cp*	Rh
7b	**7a**	CH_3	cym	Ru
7c	**7a**	CH_3	cym	Os
7d	**7a**	CH_3	cp*	Rh
8b	**8a**	CH_3	cym	Rh
8d	**8a**	CH_3	cp*	Rh

2.1.2. Characterization by NMR Spectroscopy

All ligands and complexes were characterized by ^{1}H-NMR spectroscopy. For novel compounds ^{13}C-NMR measurements were performed. The aliphatic area of the proton spectra of the ligands **1a** and **5a** were compared (see figure 11). The green marked peaks show the CH_2-groups of the C1 spacer (bottom spectra, one

singlet) and the C2-spacer (top spectra, two triplets). 2D-NMR (HSQC, HMBC, ^{1}H-COSY and ^{1}H-TOCSY) was performed for ligand **5a** for correct peak assignment. Through the HMBC experiment two ^{3}J(C,H) couplings to the pyridone ring were observed for the peak at 4.13 ppm, while for the peak at 2.75 ppm no coupling to the aromatic area was monitored. The peak at lower ppm shift can therefore be assigned to the CH_2 group near the ester moiety and the one at higher shift to the CH_2-group neighboring the nitrogen atom.

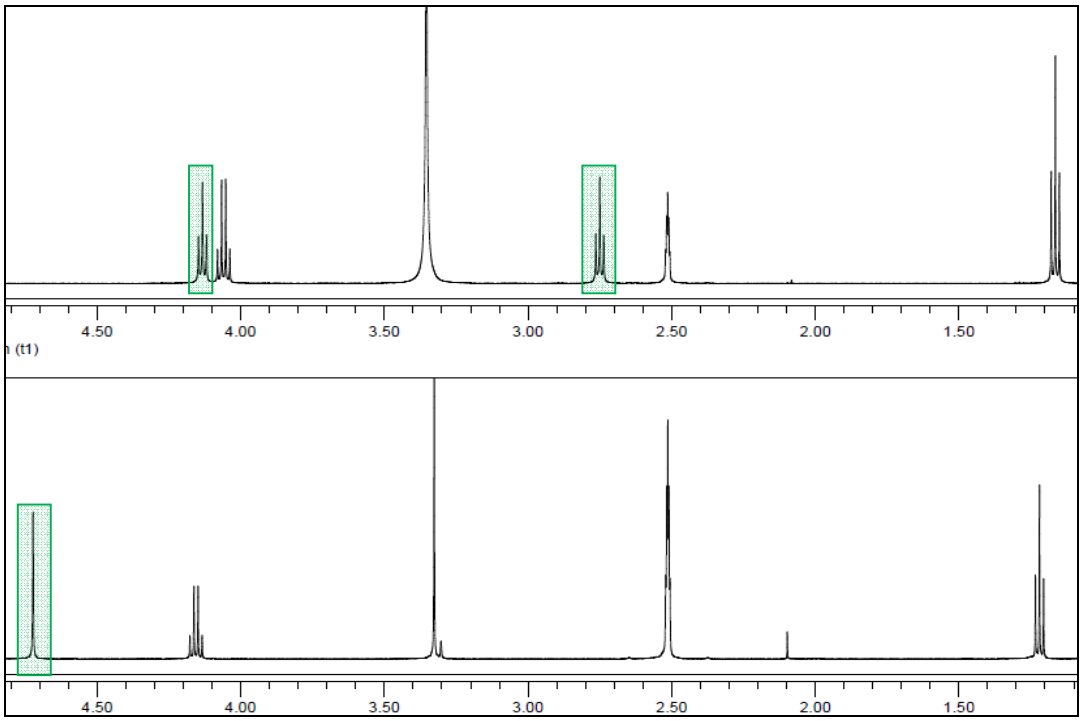

Figure 11 - ^{1}H-NMR spectra of the aliphatic area of **5a** (top) and **1a** (bottom). green marked signals represent the spacing CH_2-groups

The ^{1}H-NMR spectra of the complexes in $CDCl_3$ show doublets corresponding to each proton of the cym ring. The hydrogen atoms of the spacer group are diastereotopic, leading to the observation of two doublets, for example for compound **2b** at 3.89 and 5.12 ppm with a geminal coupling constant ^{2}J(H,H) = 16 Hz (figure 17, marked green), or four multiplets for C2-spacer complexes like **7b** between 2.7 and 4.4 ppm (figure 18, marked green). In protic solvents, the

same protons give a singlet for C1-spacer or two triplets for C2-spacer respectively. [45,56]

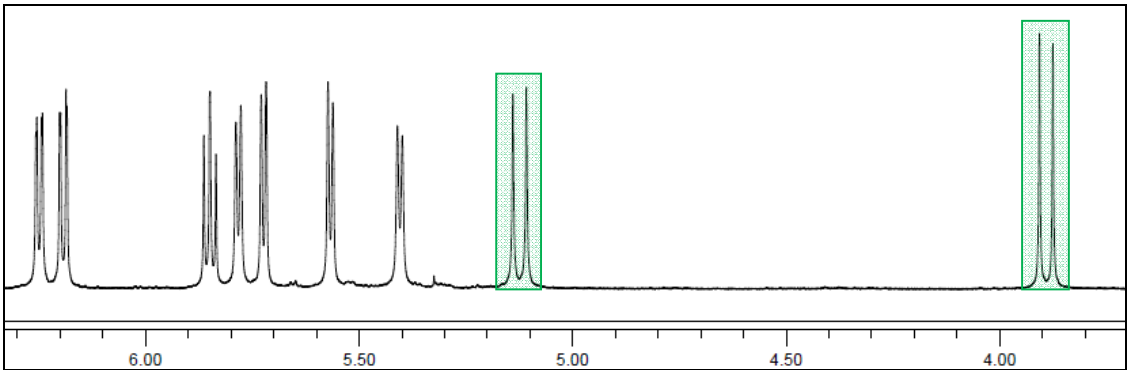

Figure 12 - ^{1}H-NMR spectra of compound **2b** in $CDCl_3$. aromatic area; splitting diastereotopic protons are marked green

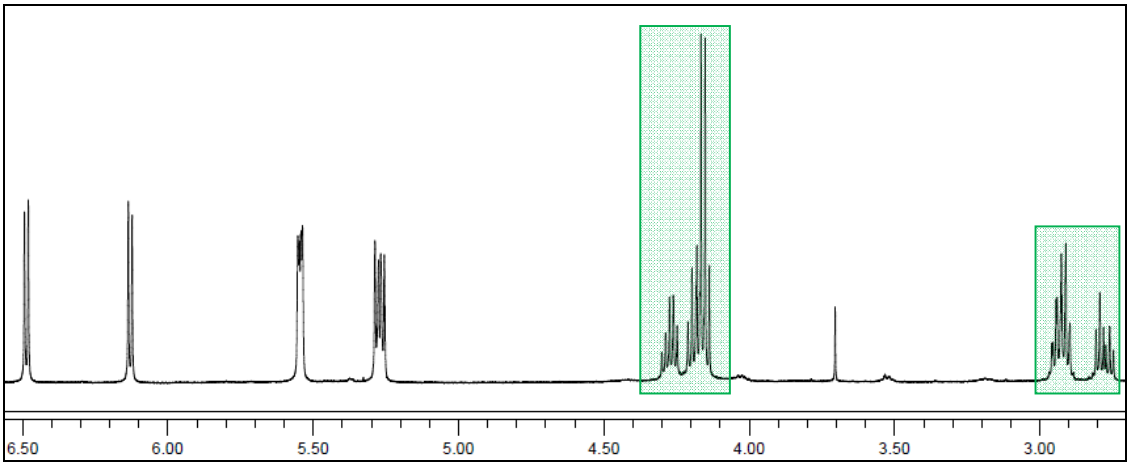

Figure 13 - ^{1}H-NMR spectra of compound **5b** in $CDCl_3$. aromatic area; splitting diastereotopic protons are marked green. At around 4.15 ppm also signal for ester-CH_2-group

2.1.3. Determination of the Molecular Structure

Single crystals of the complexes **2b**, **4c, 4d, 5d** and **8b** were obtained by the slow diffusion method with dichloromethane/Et_2O, which were suitable for x-ray diffraction analysis. All structures showed the typical "piano-stool" configuration, with ruthenium, osmium or rhodium as the central metal, where the η^6 π-bound cymene ring acts as seat and the pyridone and the chlorido/carboxylato moieties

[56] Z. Grote, M. Lehaire, R. Scopelliti, K. Severin, J. Am. Chem. Soc., **2003**, *125*, 13638–13639.

as the legs. The 3-hydroxy-2-pyridone ligands bind bidentately to the metal center *via* the lactam and alcoholate oxygens, forming a non-planar five-membered ring. The coordination of the free carboxylate to the metal center leads to dimeric structures of the complexes (figure 14, 15 and 16).

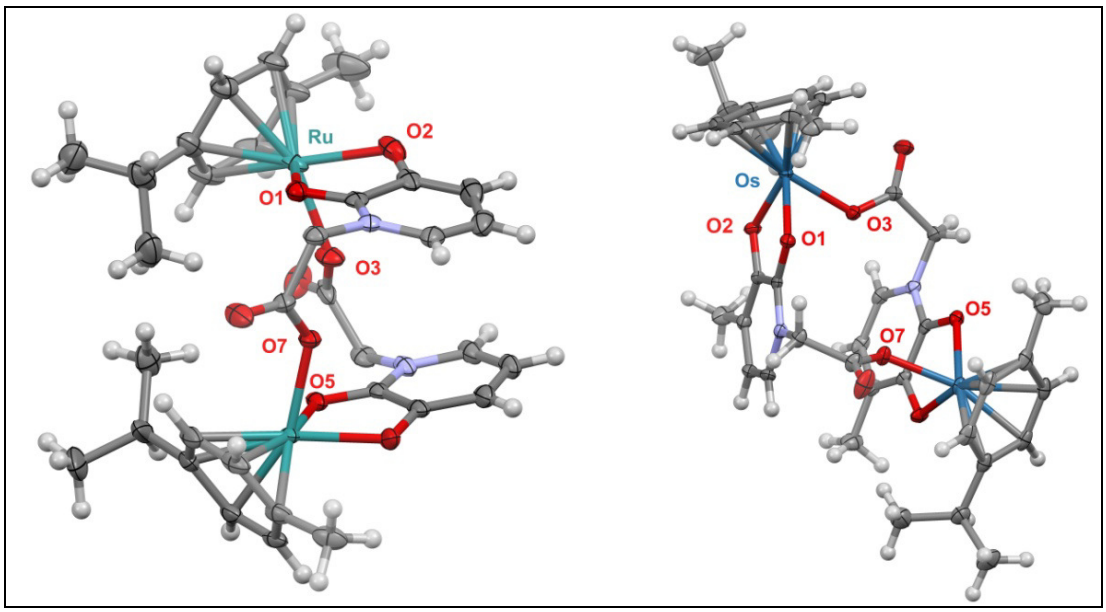

Figure 14 - Molecular structure of **2b** (left) and **4c** (right)

Both ruthenium compounds **2b** and **8b** as well as the rhodium compound **4d** crystallized in triclinic centrosymmetric space group P-1, the osmium compound **4c** and the rhodium monomer **5d** in monoclinic space group C 2/c.

The bond lengths and angles between the metal center and the oxygens are very similar to each other (listed in table 2).

Table 2 - Bond lengths and angles to the metal center. X = Cl (**5d**), O3 (**2b**, **4c**, **4d**, **8b**)

compound	2b	4c	4d	5d	8b
$r_{(M1-O1)}$ /Å	2.1029(19)	2.1147(16)	2.1013(28)	2.1270(16)	2.1055(11)
$r_{(M1-O2)}$ /Å	2.0722(19)	2.0596(17)	2.0735(27)	2.0912(19)	2.0730(13)
$r_{(M1-X)}$ /Å	2.0790(17)	2.0835(16)	2.1078(32)	2.4214(7)	2.0715(12)
$r_{(M2-O5)}$ /Å	2.1001(19)	2.1147(16)	2.1203(29)	-	2.1055(11)
$r_{(M2-O6)}$ /Å	2.0760(22)	2.0596(17)	2.0586(29)	-	2.0730(13)
$r_{(M2-O7)}$ /Å	2.0877(20)	2.0835(16)	2.1264(31)	-	2.0715(12)
$\varphi_{(O1-M1-O2)}$ /°	79.29(8)	76.83(6)	80.42(11)	78.13(5)	78.89(5)
$\varphi_{(O2-M1-X)}$ /°	79.34(7)	79.22(7)	81.10(11)	89.12(5)	80.73(5)
$\varphi_{(X-M1-O1)}$ /°	79.69(7)	78.75(6)	78.05(12)	84.68(5)	77.95(5)
$\varphi_{(O5-M2-O6)}$ /°	79.32(8)	76.83(6)	80.01(11)	-	78.89(5)
$\varphi_{(O6-M2-O7)}$ /°	78.75(8)	79.22(7)	81.05(11)	-	80.73(5)
$\varphi_{(O7-M2-O5)}$ /°	80.16(8)	78.75(6)	77.98(11)	-	77.95(5)

The four oxygen atoms O1, O3, O5 and O7 of the dimeric metal complexes form a twisted tetragon (in case of compound **8b** a parallelogram) with different distances and angles (listed in table 3), which is confined by the arene ligands (C1 spacer) of the complex, leading to the formation of a cavity.

Table 3 - Distances and angles of the oxygen tetragon

compound	2b	4c	4d	8b
$r_{(O1-O7)}$ /Å	3.289	3.797	3.623	2.627
$r_{(O3-O5)}$ /Å	3.390	3.797	3.607	2.627
$r_{(O5-O7)}$ /Å	2.696	2.609	2.650	4.982
$r_{(O1-O3)}$ /Å	2.676	2.609	2.672	4.982
$\varphi_{(O1-O7-O5)}$ /°	94.99	97.00	98.64	108.26
$\varphi_{(O3-O5-O7)}$ /°	83.96	82.48	81.65	71.74
$\varphi_{(O1-O3-O5)}$ /°	93.03	97.00	98.61	108.26
$\varphi_{(O3-O1-O7)}$ /°	86.22	82.48	81.06	71.74
τ/°	9.12	6.43	1.79	0

Metal ions or (solvent) molecules could be attached by interaction with the oxygen atoms. During crystallization of **4c** and **4d**, a dichloromethane molecule was incorporated into this cavity (see figure 15).

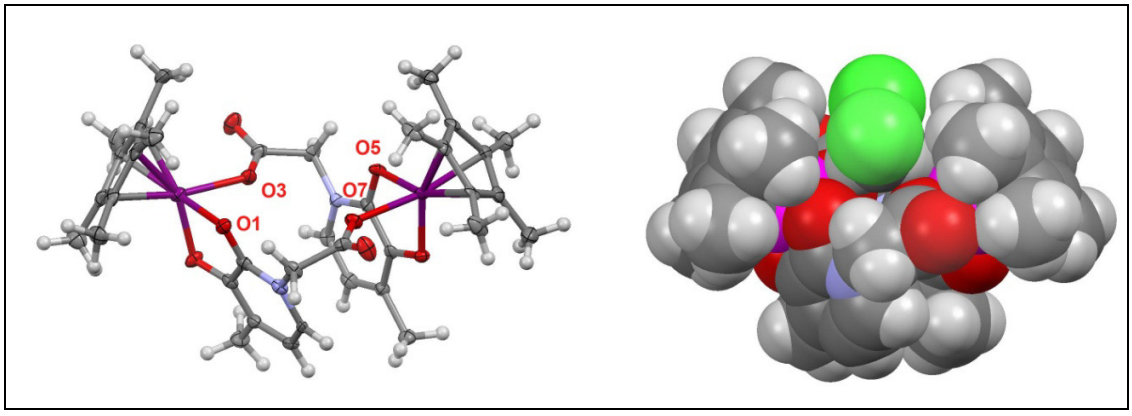

Figure 15 - Molecular structure of **4d**, coordination of dichloromethane to the cavity of **4d** (right)

Another possibility for intercalation is by π-stacking between the aromatic rings of the pyridone ligands of the C1 spacer complexes with a distance between the centroids of 3.949 Å for **2b**, 3.798 Å for **2d**, and 3.747 Å for **4d**.

In case of the C2-spacer complexes, the lactam moiety point in opposite directions, therefore no intercalation through π-stacking might be possible (see figure 16).

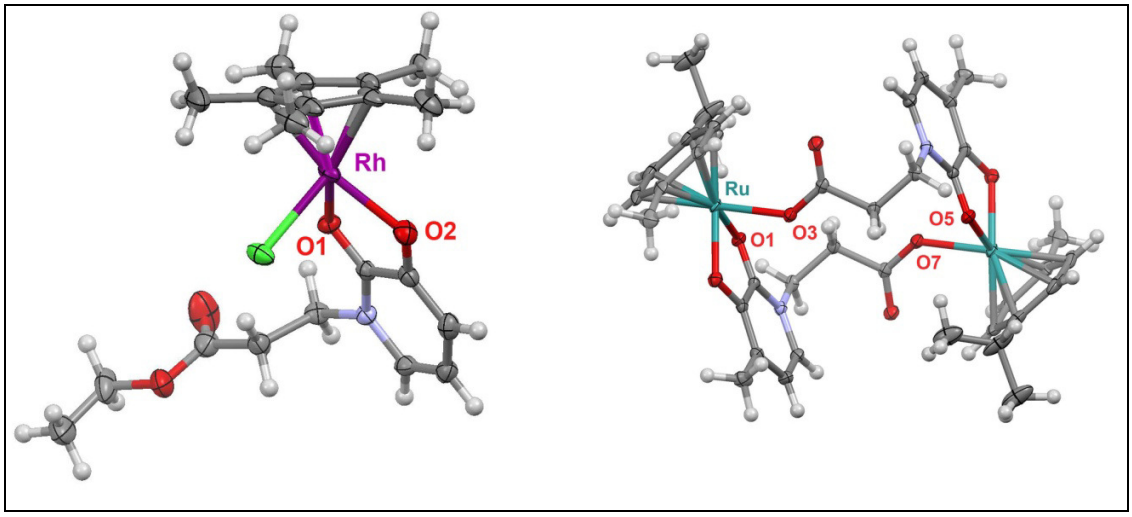

Figure 16 - Molecular structure of **5d** (left) and **8b** (right)

The crystal data and details of data collection corresponding to the complexes **2b**, **4c** and **4d** are listed in table 4, to **5d** and **8d** in table 5.

Table 4 – Crystal data and details of data collection for **2b**, **4c** and **4d**

compound	2b	4c	4d
Chemical formula	$C_{34}H_{38}N_2O_8Ru_2$	$C_{37}H_{44}Cl_2N_2O_8Os_2$	$C_{37}H_{50}Cl_2N_2O_{10}Rh_2$
M (g mol^{-1})	809.78	1011.19	959.51
Temperature (K)	100(2)	100(2)	100(2)
Crystal size (mm)	0.50 x 0.30 x 0.20	0.10 x 0.10 x 0.04	0.18 x 0.15 x 0.05
Crystal color, shape	orange, block	green, block	red, block
Crystal system	triclinic	monoclinic	Triclinic
Space group	P-1	C2/c	P-1
a (Å)	10.3118(5)	16.0277(4)	11.0352(7)
b (Å)	12.8875(7)	11.1724(4)	12.6088(11)
c (Å)	13.3610(7)	20.8953(7)	14.7170(13)
α (°)	85.021(2)	90	110.472(2)
β (°)	69.737(2)	95.157(2)	91.228(2)
γ (°)	74.725(2)	90	91.012(2)
V (Å^3)	1606.84(14)	3726.5(2)	1917.3(3)
Z	2	4	2
D_c (g cm^{-3})	1.674	1.954	1.662
μ (mm^{-1})	0.997	7.01	1.060
F (000)	818	2120	980
θ range (°)	2.17 – 30.15	2.23 – 28.00	2.33 – 25.50
h range	-14/14	-21/20	-13/13
k range	-18/18	-14/13	-15/15
l range	-18/18	-27/27	-17/17
no. reflections	52298	45315	31862
no. parameters	434	233	490
R_{int}	0.0293	0.0398	0.0760
R_1[a]	0.0388	0.0185	0.0435
wR_2[b]	0.0956	0.0389	0.0999
GOF[c]	1.056	1.060	1.037
Residuals (e$^-$ Å^{-3})	1.466, -1.379	0.919, -0.802	1.050, -0.737

[a]: $R_1 = \Sigma||F_0| - |F_c||/ \Sigma|F_0|$ [b]: $wR_2 = \{\Sigma[w(F_0^2 - F_c^2)^2]/w\Sigma[(F_0^2)^2\}^{½}$
[c]: GOF = $\{\Sigma[w(F_0^2 - F_c^2)^2]/(n - p)^{½}$

Table 5 - Crystal data and details of data collection for **5d** and **8b**

compound	**5d**	**8b**
Chemical formula	$C_{20}H_{27}ClNO_4Rh$	$C_{19}H_{23}NO_4Ru$
M (g mol^{-1})	483.79	430.45
Temperature (K)	150(2)	100(2)
Crystal size (mm)	0.20 x 0.10 x 0.05	0.65 x 0.44 x 0.07
Crystal color, shape	dark red, block	dark red, block
Crystal system	Monoclinic	triclinic
Space group	C2/c	P-1
a (Å)	36.4313(18)	9.7980(4)
b (Å)	8.0432(4)	10.1383(4)
c (Å)	15.3744(7)	10.5159(4)
α (°)	90	70.104(2)
β (°)	114.725(4)	75.025(2)
γ (°)	90	67.311(2)
V (Å^3)	4092.1(3)	896.45(6)
Z	8	2
D_c (g cm^{-3})	1.571	1.595
μ (mm^{-1})	0.990	0.897
F (000)	1984	440
θ range (°)	2.46 – 30.17	2.26 – 30.15
h range	-51/51	-13/13
k range	-11/11	-14/14
l range	-21/21	-14/14
no. reflections	64032	26875
no. parameters	249	232
R_{int}	0.0703	0.0446
R_1[a]	0.0380	0.0245
wR_2[b]	0.0869	0.0652
GOF[c]	1.022	1.008
Residuals (e$^-$ Å^{-3})	0.795, -0.858	0.851, -0.786

2.2. Investigations

The water stability, the corresponding pK_a-values and their interaction of the complexes with the DNA-model compound 5'-GMP were investigated by ^{1}H-NMR for selected compounds.

2.2.1. Water Stability and pH Dependency

Nearly all complexes (except **3b**, **3c**, **4c**, and **5d** because of their insufficient solubility in water) were dissolved in D_2O and ^{1}H-NMR-spectra were recorded after 5 minutes, 24 and 48 hours to monitor their stability in aqueous solution. Formation of smaller amounts of another species, probably the hydroxido dimer was observed for all compounds after 24 hours. This amount didn't increase significantly after additional 24 hours (marked peaks figure 17). In case of the rhodium compounds (see figure 18) the formation of a new signal at 2.17 ppm was observed.

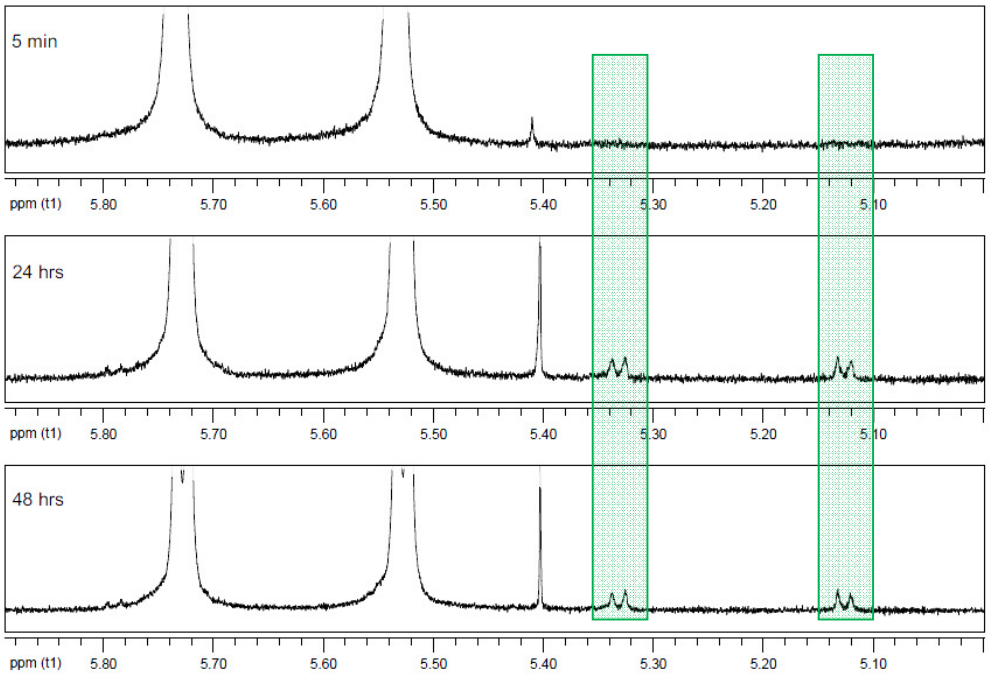

Figure 17 – ^{1}H-NMR spectra of compound **2b** in D_2O, *p*-cym signals

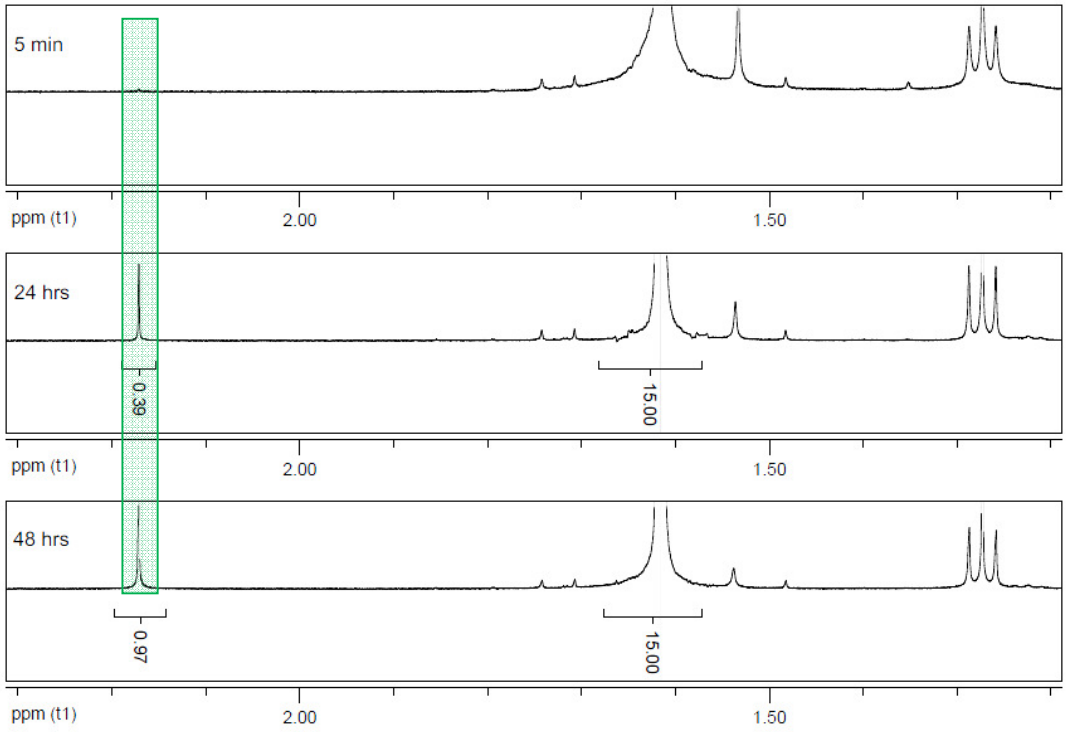

Figure 18 – ^{1}H-NMR-spectra of compound **1d** in D_2O, cp* signals

The ruthenium and rhodium complexes dissolves faster than their osmium counterparts, implying a fast hydrolysis to the charged aqua species by exchanging of the carboxylate-group of the pyridone ligand or chlorido ligand (in case of the mononuclear complexes) by a water molecule which is in accordance to the result of the water stability experiment.[45]

The pH dependent monomerization of the dimeric complexes **2b**, **2d**, **6b** and **6d** was investigated by measuring proton spectra at different pD values, which were adjusted by addition of DNO_3 or NaOD to the sample dissolved in D_2O. In theory at high pD (respectively pH) the dimeric structure should be intact, while at low pD values the coordinated carboxylate should be protonated to the corresponding free acid leading to the cleavage of the macrocylce and formation of a monomeric complex that can be monitored by arising of additional signals. But instead formation of new signals in the proton spectra at low pD a shift of the signals was observed. This result also indicated that the dimeric complexes were

quickly hydrolyzed to their monomeric charged aqua analogues by protonation of the carboxylate-group and coordination of a water molecule to the metal core.
Through these experiments the pK_a values of the aqua species of the two ruthenium compounds **2b** and **6b** and the rhodium compounds **2d** and **6d** were determined by plotting the chemical shifts of the aromatic pyridone signals against the pD value.

$$\mathbf{pK_a = 0.929\ pK_{a^*} + 0.42} \qquad (1)$$

The inflection point of the sigmoid titration curve represents the pK_{a^*} value, which were converted to the corresponding pK_a values (see table 6) by applying equation 1. [57]

Table 6 - pK_a values

compound	pKa
2b	9.84
2d	10.20

No sigmoid curve was observed for compound **6b** and **6d** in the pD range between 2.90 and 10.24. The infliction point may be at higher pD, as it is for compounds **2b** and **2d**.

While adding NaOD or DNO_3 to the rhodium compounds new signals were found in the ^{1}H-NMR-spectra between 3.30 and 3.80 ppm (see figure 19) that are still present when changing the pD back to neutral.

[57] A. Krezel, W. Bal, *J. Inorg. Biochem.* **2004**, *98*, 161–166.

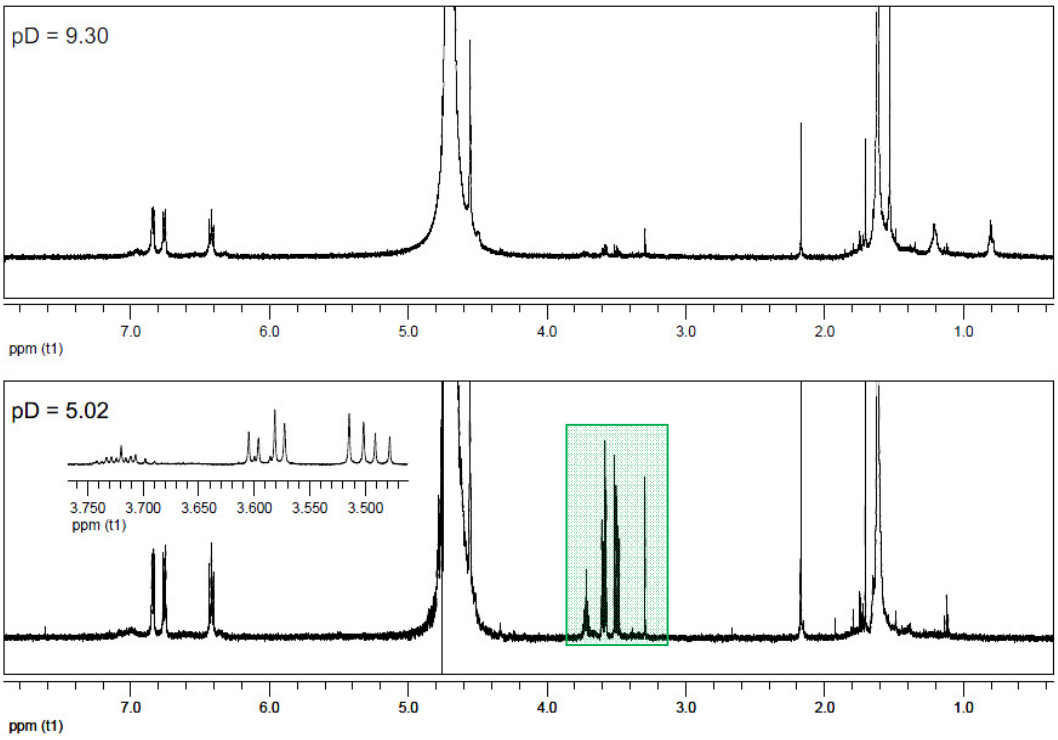

Figure 19 – ^{1}H-NMR of **2d** at different pD-values. Arising of new signals between 3 and 4 ppm (marked green)

2.2.2. Behavior in Alkali Salt Solutions

The water stability tests and pK_a determination of the dimeric complexes **2b**, **2d**, **6b** and **6d** indicated the dimeric structure was not stable in protic solvents and quick hydrolysis of the compound was observed. In organic solvents such as chloroform the dimeric structure was intact, proven by crystal structure analyses and ^{1}H-NMR spectra in $CDCl_3$. According to the molecular structures of **2b**, **4c** and **8b** (see figure 14 and figure 15 in section 2.1.3.) a binding of metal ions on the side of the oxygen tetragon might be possible.

To investigate the sensitivity for alkali metal ions of the compounds **2b**, **2d**, **6b** and **6d**, two different experimental setups (experimental part, section 3.1.3.),

were applied, developed by Kay Severin and coworkers.[58] Based on their research more signals in ^{1}H-NMR of the incorporated metal salts are expected compared the experiments without salts. However in all experimental setups no interaction with lithium, sodium and potassium ions could be observed.

2.2.3. GMP-Experiments

For DNA-interaction studies, D_2O solutions of compounds **1b–d** and **2b–d** were treated with a slightly excess of 5'-GMP (10 mg/mL in D_2O).A shift of *H8* proton of the purine ring was monitored for ruthenium and osmium complexes by ^{1}H-NMR, which indicates coordination of the nucleobase over the *N7* of the heterocycle. For rhodium no such binding was observed. Also no binding *via* the oxygens of the phosphate moiety was monitored by ^{31}P-NMR spectroscopy.

2.2.4. Intercalation Experiments

The possibility of intercalation between the pyridone rings by π-stacking was investigated by treating the dimeric compounds **2b–d** in $CDCL_3$ with an excess of toluene. The experiment was monitored by ^{1}H-NMR, but no signal shifts in the aromatic area was observed as it would be expected in case of intercalation.

[58] H. Piotrowski, G. Hilt, A. Schulz, P. Mayer, K. Polborn, K. Severin, *Chem. Eur. J.* **2001**, *7*(15), 3196-3208.

3. Experimental Part

3.1. Equipment, Materials and Methods

3.1.1. Chemicals

All solvents were dried and distilled prior to use.

2,3-DHP (Aldrich), bromo ethyl acetate (Fischer), morpholine (Fluka), aqueous formaldehyde solution (30%, Merck), cyclohexene (Fluka), palladium on activated charcoal (10%, Aldrich), sodium methoxide (Aldrich), α-terpinene (Acros), ruthenium(III) chloride trihydrate (Johnson Matthey), osmiumtetroxide (Degussa), rhodium(III) chloride trihydrate (Johnson Matthey), hydrazine hydrochloride (Fluka), pentamethylcyclopentadiene (95%, Aldrich), lithium chloride (Aldrich), sodium chloride, potassium chloride (Aldrich) deuterated sodium hydroxide (euriso-top) and deuterated nitirc acid (euriso-top), guanosine monophosphate (Aldrich) were purchased and used without further purification.

3.1.2. Equipment

NMR spectra were recorded at 25 °C using a *Bruker FT-NMR spectrometer Avance III™ 500 MHz* Proton NMR spectra were measured at 500.10 MHz, ^{13}C-NMR spectra at 125.75 MHz in deuterated solvents. 2D NMR spectra were measured using a gradient-enhanced mode. Elemental analyses were carried out with a *Perkin Elmer 2400 CHN* elemental analyzer at the microanalytical laboratory of the University of Vienna. Melting Points were determined by using a *Büchi Melting Point B-540*. The X-ray diffraction measurement was performed with single crystals of **2b**, **4c**, **4d**, **5d** and **8b** on a Bruker X8 APEX II CCD diffractometer at 100 K. A *Bruker esquire 3000 ion trap mass spectrometer* with an orthogonal ESI source was used for ESI-MS measurements. The pD values were determined directly in the NMR tubes using a pH-meter Eco Scan pH6

equipped with a glass microcombination pH electrode (Orion 9826BN) that was calibrated with standard buffer solutions of pH 4.00, 7.00 and 10.00.

3.1.3. Procedures to determine Sensitivity to Alkaline Metal Ions

Method A

Complex (1 mg) was solved in 1 mL of $CDCl_3$, 1 mL of a 10 mM MCl solution (M = lithium, sodium, potassium) in D_2O was added and stirred for 24 hours. The aqueous phase and the organic phase were measured by ^{1}H-NMR.

Method B

Complex (1 mg) was solved in 1 mL of a 0.1 M LiCl solution in CD_3OD, stirred for 15 hours and measured by ^{1}H-NMR.

3.2. General Procedures

3.2.1. General Procedure for the Ester Hydrolysis

Pyridone ester (1 eq.) was stirred in sodium hydroxide (4M, 2.36 eq.) for 45 minutes which yielded a clear solution. Hydrochloric acid (30%) was added dropwise at 0 °C until a faint precipitate appeared. Two more drops were added and the suspension was stored at 4 °C for 2 hours. The colorless solid was filtered off, washed with ice-cold water and dried *in vacuo*.

3.2.2. General Procedure for Pyridone-based Metal Complexes

Pyridone ligand (1.1 eq) and sodium methoxide (1.1 eq for ester, 2.5 eq for acid) were dissolved in 10 mL dry methanol and stirred for 1 hour under an argon atmosphere to give a clear solution. Precursor complex (1.0 eq) was added in one portion and the reaction mixture was stirred for further 4–16 hours at room temperature. The solution was concentrated to dryness and the residue was extracted with dichloromethane, filtered and concentrated to a final volume of about 3 mL. Upon addition of *n*-hexane or diethyl ether the desired product was precipitated, isolated by filtration and dried *in vacuo*.

3.3. Synthesis of Precursor Metal Complexes

3.3.1. Synthesis of Bis[dichlorido(η^6-p-cymene)ruthenium(II)] - p1

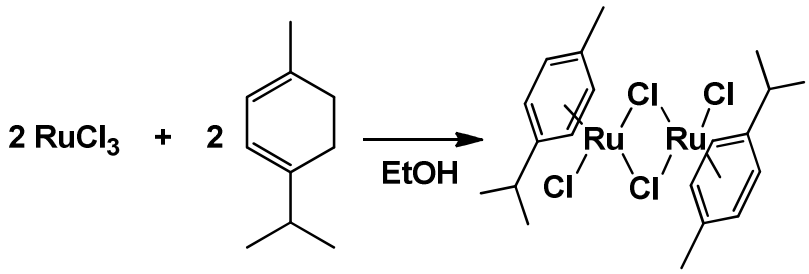

Synthesis:

α-Terpinene (12.5 mL, 77 mmol) was added to a solution of the $RuCl_3*3H_2O$ (2.00 g, 7.6 mmol) in dry EtOH (75 mL) and the reaction mixture was refluxed for 4 h. The mixture was cooled to room temperature, the volume was reduced to 30 mL and diethyl ether (40 mL) was added whereas precipitation occurred. The obtained red solid was filtered off, washed with diethyl ether (3 x 10 mL) and dried in vacuum.

Yield: 2.14 g (92%)

3.3.2. Synthesis of Bis[dichlorido(η^6-p-cymene)osmium(II)] - p2

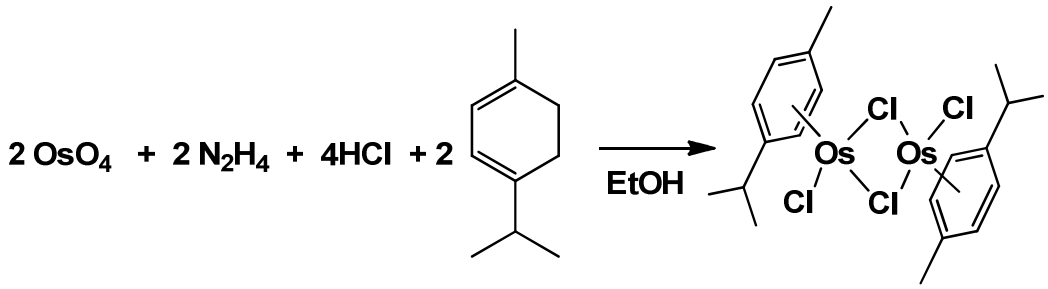

Synthesis:

Hydrochloric acid (50 mL) was added to hydrazine-hydrochloride (840 mg, 8 mmol) in a 100 mL round-bottom flask, equipped with a $CaCl_2$ drying tube. Afterwards, osmiumtetroxide (2.00 g) was added and the mixture was stirred for 2 weeks under light exposure.

After this time the red solution was filtered and the solvent was evaporated. The residue was dissolved in EtOH (20 mL) and concentrated to dryness (3x) and finally three times with dry EtOH. The obtained red oil was flushed 3 times with argon and dissolved in dry EtOH (40 mL). α-Terpinene was added to the red solution and refluxed for three days with exclusion of light and under an argon atmosphere.

After that, the solution was allowed to cool to room temperature and stored at -20 °C for 2 more days. The formed orange solid was filtered off and washed with dry EtOH (3x 3 mL) and *in vacuo*.

Yield: 2.42 g (79%)

3.3.3. Synthesis of Bis[dichlorido(η^5-pentamethylcyclopentadiene) rhodium(III)] - p3

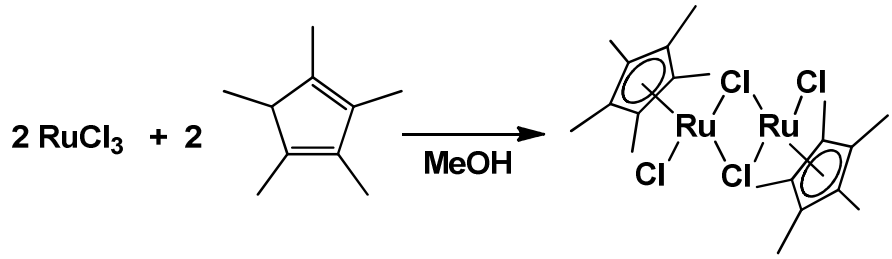

Synthesis:

Pentamethylcyclopentadiene (1.00 mL, 7.20 mmol) was added to a solution of the $RhCl_3 \cdot 3H_2O$ (1.02 g, 3.90 mmol) in dry methanol (25 mL) and the reaction mixture was refluxed for 24 h. After cooling the mixture to 4 °C, the so formed red precipitate was filtered off, washed with diethyl ether (3 x 10 mL) and dried *in vacuo*.

Yield: 0.98 g (82%)

3.4. Ligand Synthesis

3.4.1. 1-Ethoxycarbonylmethyl-3-hydroxy-2(*1H*)-pyridone - 1a

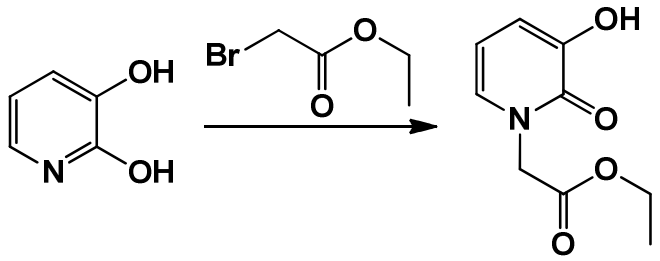

Synthesis:

Ethyl bromoacetate (75 mL, 0.66 mol) and 2,3-DHP (15.0 g, 0.13 mol) were refluxed under an argon atmosphere for 24 hours. Afterwards the brown solution was allowed to cool to room temperature and then stored at 4 °C for 24 hours. The formed solid was filtered off and recrystallized from EtOH (96%) in the presence of charcoal. The colorless product was separated by filtration, washed with cold EtOH and dried *in vacuo*.

Yield: 8.01 g (31% of theory, 49% of literature[54])

Melting point: 142 – 143 °C

Elemental analysis: calculated for $C_9H_{11}NO_4 \cdot 0.25H_2O$

1a	C[%]	H[%]	N[%]
calculated	53.59	5.75	6.94
found	53.80	5.53	7.13
Δ	0.21	0.22	0.19

NMR-spectroscopy:

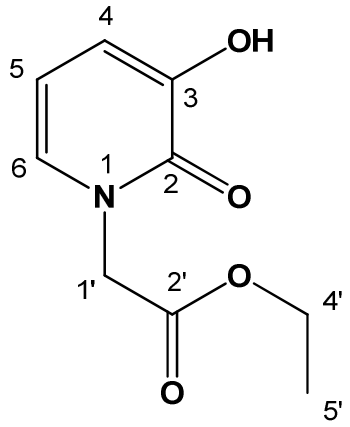

^{1}H NMR (500 MHz, d^{6}-DMSO): δ = 1.22 (t, ^{3}J(H,H) = 7 Hz, 3H, H5'), 4.15 (q, ^{3}J(H,H) = 7 Hz, 2H, H4'), 4.72 (s, 2H, H1'), 6.13 (dd, ^{3}J(H,H) = 7 Hz, ^{3}J(H,H) = 7 Hz, 1H, H5), 6.74 (dd, ^{3}J(H,H) = 7 Hz, ^{4}J(H,H) = 2 Hz, 1H, H4), 6.87 (dd, ^{3}J(H,H) = 7 Hz, ^{4}J(H,H) = 2 Hz, 1H, H6), 9.12 (s, 1H, Pyr-OH) ppm.

^{13}C NMR (75 MHz, d^{6}-DMSO): δ = 14.5 (C5'), 50.7 (C1'), 61.4 (C4'), 105.6 (C5), 115.8 (C4), 129.3 (C6), 147.2 (C3), 158.4 (C2), 168.5 (C2') ppm.

3.4.2. 1-Carboxylmethyl-3-hydroxy-2(*1H*)-pyridone - 2a

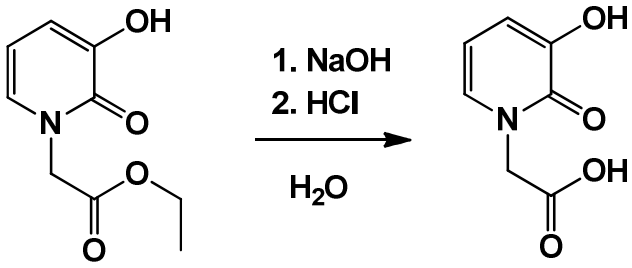

Synthesis:

The synthesis was performed according to the general procedure for the ester hydrolysis using 5 g (25.4 mmol) of compound **1a**.

Yield: 3.38 g (80% of theory, 96% of literature[55])

Melting Point: 213–215 °C

Elemental analysis: calculated for $C_7H_7NO_4$

2a	C[%]	H[%]	N[%]
calculated	49.71	4.17	8.28
found	49.38	4.16	8.20
Δ	0.33	0.01	0.08

NMR-spectroscopy:

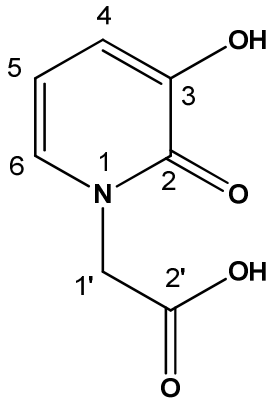

^{1}H NMR (500 MHz, d^{6}-DMSO): δ = 4.64 (s, 2H, H1'), 6.10 (dd, ^{3}J(H,H) = 7 Hz, ^{3}J(H,H) = 7 Hz, 1H, H5), 6.73 (dd, ^{3}J(H,H) = 6 Hz, ^{4}J(H,H) = 2 Hz, 1H, H4), 7.14 (dd, ^{3}J(H,H) = 5 Hz, ^{4}J(H,H) = 2 Hz, 1H, H6), 9.07 (s, 1H, Pyr-O*H*), 12.98 (brs, 1H, COOH) ppm.

3.4.3. 1-Ethyoxycarbonylmethyl-3-hydroxy-4-morpholinomethyl-2(*1H*)-pyridone - 1i

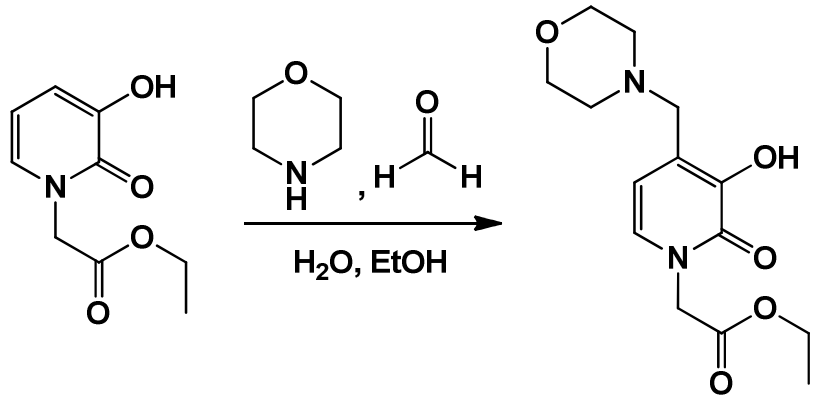

Synthesis:

To an aqueous formaldehyde solution (35%, 5.70 g, 57.8 mmol) morpholine (5.02 mL, 57.8 mmol) was added slowly at ca. 0° C. The solution was stirred for 15 minutes at 0 °C and additionally 15 minutes at room temperature. The formed mannich reagent was added dropwise to compound **1a** (3.80 g, 19.3 mmol) in 30 mL EtOH (96%). The mixture was stirred for 24 hours yielding a clear solution. The reaction mixture was stored at 4 °C whereas the product precipitated. The crude product was filtered and recrystallized from EtOH (96%). The desired product was isolated as a colorless solid by filtration and, dried *in vacuo*.

Yield: 4.36 g (76% of theory, 96% of literature[55])

NMR-spectroscopy:

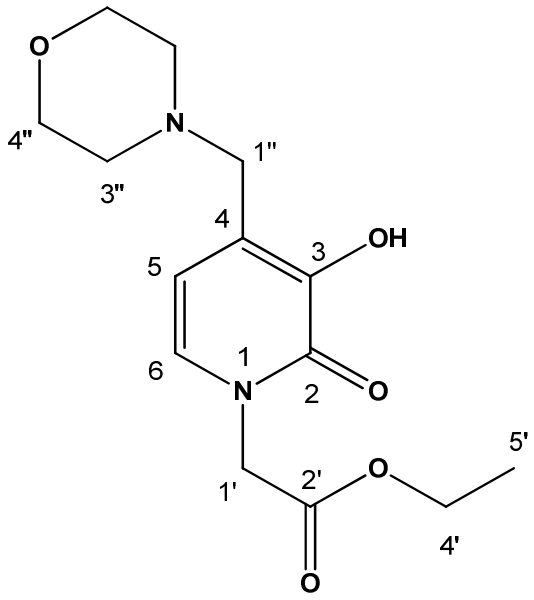

^{1}H NMR (500 MHz, d^{6}-DMSO): δ = 1.22 (t, ^{3}J(H,H) = 7 Hz, 3H, H5'), 2.39 (t, ^{3}J(H,H) = 4 Hz, 4H, H3''), 3.39 (s, 2H, H1''), 3.36 (t, ^{3}J(H,H) = 5 Hz, 4H, H4''), 4.15 (q, ^{3}J(H,H) = 7 Hz, 2H, H4'), 4.71 (s, 2H, H1'), 6.22 (d, ^{3}J(H,H) = 7 Hz, 1H, H5), 7.12 (d, ^{3}J(H,H) = 7 Hz, 1H, H6), 9.17 (brs, 1H, Pyr-OH) ppm.

3.4.4. 1-Ethyoxycarbonylmethyl-3-hydroxy-4-methyl-2-(*1H*)-pyridone - 3a

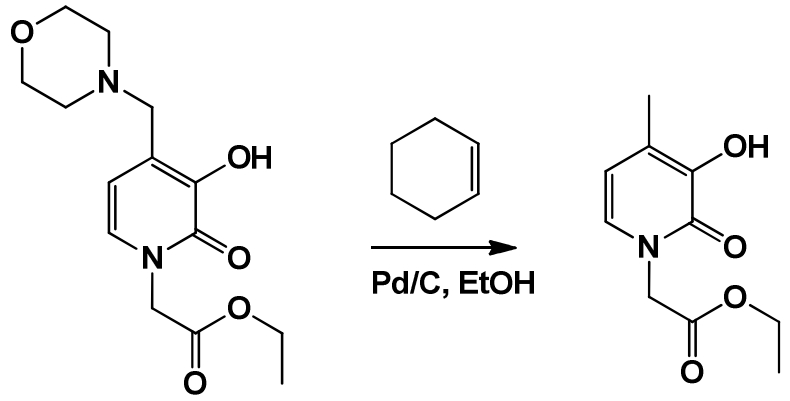

Synthesis:

Compound **1i** (4 g, 13.5 mmol) was suspended in dry EtOH (32 mL) and cyclohexene (65 mL). After 30 minutes Pd/C catalyst (10%, 0.8 g) was added and the mixture was refluxed for 24 hours. The catalyst was filtered off and the solvent was removed under reduced pressure to give a colorless solid, which was recrystallized from dry EtOH yielding colorless needles.

Yield: 1.96 g (69% of theory, 95% of literature[55])

Melting point: 158 – 160 °C

NMR-spectroscopy:

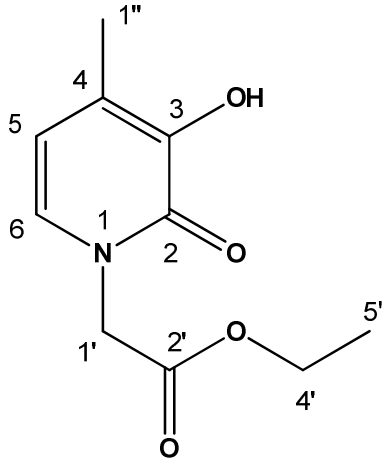

^{1}H NMR (500 MHz, d^{6}-DMSO): δ = 1.22 (t, ^{3}J(H,H) = 7 Hz, 3H, H5'), 2.04 (s, 3H, H1''), 4.14 (q, ^{3}J(H,H) = 7 Hz, 2H, H4'), 4.69 (s, 2H, H1'), 6.08 (d, ^{3}J(H,H) = 7 Hz, 1H, H5), 7.07 (d, ^{3}J(H,H) = 7 Hz, 1H, H6), 8.73 (brs, 1H, Pyr-O*H*) ppm.

3.4.5. 1-Carboxylmethyl-3-hydroxy-2(*1H*)-4-methyl-pyridone - 4a

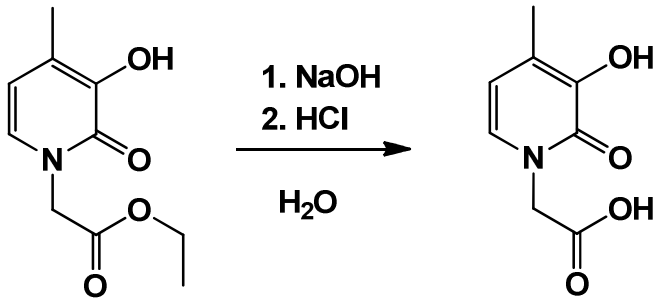

Synthesis:

Synthesis was performed according to the general procedure for the ester hydrolysis using 448 mg (2.12 mmol) of compound **1d**.

Yield: 299 mg (77% of theory, 96% of literature[55])

Melting point: 245 – 247 °C

Elemental analysis: calculated for $C_8H_9NO_4$

4a	C[%]	H[%]	N[%]
calculated	51.69	5.04	7.57
found	51.50	4.51	7.54
Δ	0.19	0.53	0.03

NMR-spectroscopy:

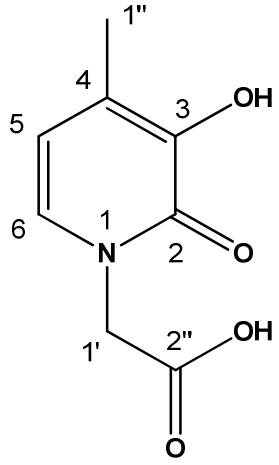

^{1}H NMR (500 MHz, d^{6}-DMSO): δ = 2.03 (s, 3H, H1''), 4.61 (s, 2H, H1'), 6.05 (d, ^{3}J(H,H) = 7 Hz, 1H, H5), 7.06 (d, ^{3}J(H,H) = 7 Hz, 1H, H6), 8.68 (s, 1H, Pyr-O*H*), 12.95 (brs, 1H, -COO*H*) ppm.

3.4.6. 1-Ethoxycarbonylethyl-3-hydroxy-2(*1H*)-pyridone - 5a

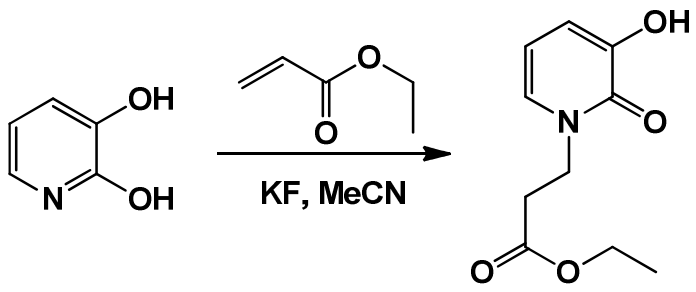

Synthesis:

Anhydrous KF and 2,3-DHP (5 g, 44 mmol) were dissolved in dry acetonitrile (60 mL) under an argon-atmosphere. Afterwards, ethyl acrylate (6 mL, 49 mmol) was added in one portion to the reaction mixture and the solution was heated to reflux for 24 hours.

In the next step the solvent was removed under reduced pressure, water was added to the residue and stirred for 5 minutes. The lightly green, brown solid was filtered off and washed with water yielding a beige powder.

Yield: 8.34 g (90%)

Melting point: 97 – 98 °C

Elemental analysis: calculated for $C_{10}H_{13}NO_4$

5a	C[%]	H[%]	N[%]
calculated	56.86	6.20	6.63
found	56.51	6.00	6.63
Δ	0.35	0..20	0

NMR-spectroscopy:

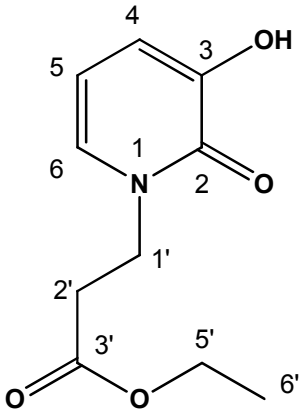

^{1}H NMR (500 MHz, d^{6}-DMSO): δ = 1.16 (t, ^{3}J(H,H) = 7 Hz, 3H, H6'), 2.75 (t, ^{3}J(H,H) = 7 Hz, 2H, H2'), 4.06 (q, ^{3}J(H,H) = 7 Hz, 2H, H5'), 4.13 (t, ^{3}J(H,H) = 7 Hz, 2H, H1'), 6.09 (dd, ^{3}J(H,H) = 7 Hz, ^{3}J(H,H) = 7 Hz, 1H, H5), 6.69 (dd, ^{3}J(H,H) = 6 Hz, ^{4}J(H,H) = 2 Hz, 1H, H4), 7.13 (dd, ^{3}J(H,H) = 5 Hz, ^{4}J(H,H) = 2 Hz, 1H, H6), 9.01 (brs, 1H, Pyr-O*H*) ppm.

^{13}C NMR (75 MHz, d^{6}-DMSO): δ = 14.5 (C6'), 33.4 (C2'), 45.7 (C1'), 60.7 (C5'), 105.7 (C5), 115.2 (C4), 128.9 (C6), 147.1 (C3), 158.2 (C2), 171.2 (C3) ppm.

3.4.7. 1-Carboxylethyl-3-hydroxy-2(*1H*)-pyridone - 6a

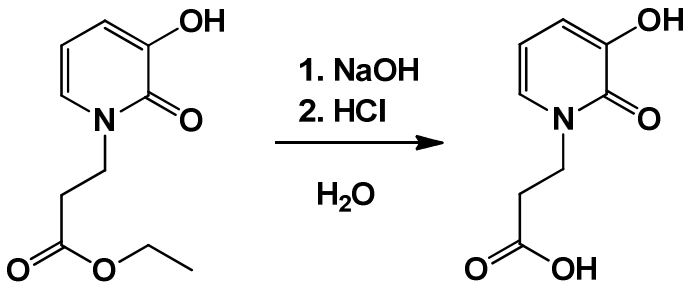

Synthesis:

Synthesis was performed according to the general procedure for the ester hydrolysis using 600 mg (2.80 mmol) of compound **5a**.

Yield: 445 mg (87%)

Melting point: 192 – 193 °C

Elemental analysis: calculated for $C_8H_9NO_4$

6a	C[%]	H[%]	N[%]
calculated	52.46	4.95	7.65
found	52.35	4.85	7.60
Δ	0.11	0.10	0.05

NMR-spectroscopy:

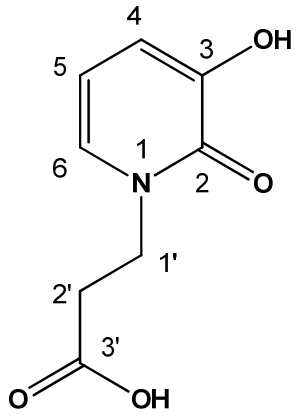

^{1}H NMR (500 MHz, d^{6}-DMSO): δ = 2.68 (t, ^{3}J(H,H) = 7 Hz, 2H, H2'), 4.10 (t, ^{3}J(H,H) = 7 Hz, 2H, H1'), 6.09 (dd, ^{3}J(H,H) = 7 Hz, ^{3}J(H,H) = 7 Hz, 1H, H5), 6.70 (dd, ^{3}J(H,H) = 6 Hz, ^{4}J = 2 Hz, 1H, H4), 7.14 (dd, ^{3}J(H,H) = 5 Hz, ^{4}J(H,H) = 2 Hz, 1H, H6), 9.00 (s, 1H, Pyr-O*H*), 12.43 (s, 1H, -COO*H*) ppm.

^{13}C NMR (75 MHz, d^{6}-DMSO): δ = 33.4 (C2'), 45.8 (C1'), 105.6 (C5), 115.2 (C4), 129.0 (C6), 147.1 (C3), 158.1 (C2), 172.7 (C3') ppm.

3.4.8. 1-Ethyoxycarbonylethyl-3-hydroxy-4-morpholinomethyl-2(*1H*)-pyridone - 5i

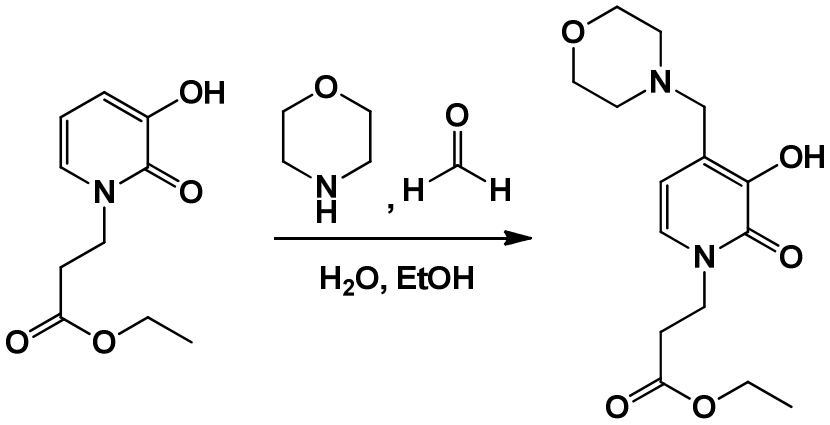

Synthesis:

To an aqueous formaldehyde-solution (35%, 5.70 g, 57.8 mmol) morpholine (5.02 mL, 57.8 mmol) was added slowly at 0 °C. The solution was stirred for 15 minutes at 0 °C and an additional 15 minutes at room temperature. The formed mannich reagent was added dropwise to compound **5a** (3.80 g, 19.3 mmol) in 30 mL EtOH (96%). The mixture was stirred for 24 hours, during that time it became a clear solution. The solvent was removed under reduced pressure, water was added and the solid was filtered off and washed with water yielding a colorless powder.

Yield: 3.59 g (60%)

Melting point: 113 – 115°C

Elemental analysis: calculated for $C_{15}H_{22}N_2O_5$

	C[%]	H[%]	N[%]
calculated	58.05	7.15	9.03
found	58.01	7.24	9.02
Δ	0.04	0.09	0.01

NMR-spectroscopy:

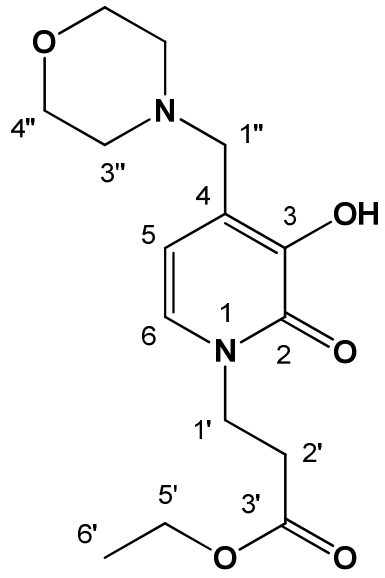

^{1}H NMR (500 MHz, d^6-DMSO): δ = 1.16 (t, ^3J(H,H) = 7 Hz, 3H, H6'), 2.37 (t, ^3J(H,H) = 4 Hz, 4H, H3''), 2.75 (t, ^3J(H,H) = 7 Hz, 2H, H2'), 3.36 (s, 1H, H1''), 3.58 (t, ^3J(H,H) = 5 Hz, 4H, H4''), 4.06 (q, ^3J(H,H) = 7 Hz, 2H, H5'), 4.12 (t, ^3J(H,H) = 7 Hz, 2H, H1'), 6.18 (d, ^3J(H,H) = 7 Hz, 1H, H5), 7.11 (d, ^3J(H,H) = 7 Hz, 1H, H6), 9.04 (s, 1H, Pyr-O*H*) ppm.

3.4.9. 1-Ethyoxycarbonylethyl-3-hydroxy-4-methyl-2-(*1H*)-pyridone - 7a

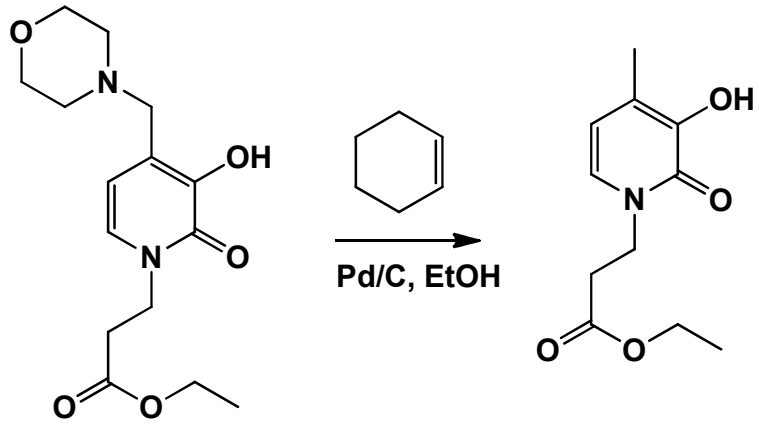

Synthesis:

Compound **5i** (4.00 g, 12.9 mmol) was suspended in dry EtOH (25 mL) and cyclohexene (50 mL). After 30 minutes of stirring the Pd/C catalyst (10%, 1.28 g) was added and the mixture was refluxed for 24 hours. The catalyst was filtered off and solvent was removed under reduced pressure yielding a colorless solid, which was washed with water and dried *in vacuo*.

Yield: 2.26 g (78%)

Melting point: 108 – 109 °C

Elemental analysis: calculated for $C_{11}H_{15}NO_4$

7a	C[%]	H[%]	N[%]
calculated	58.66	6.71	6.22
found	58.53	6.69	6.16
Δ	0.13	0.02	0.06

NMR-spectroscopy:

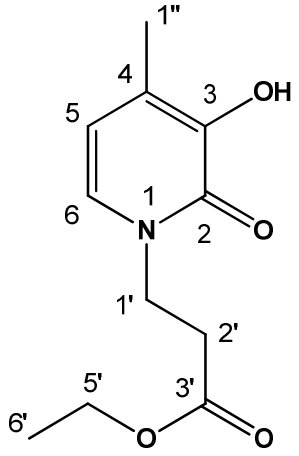

^{1}H NMR (500 MHz, d^{6}-DMSO): δ = 1.17 (t, ^{3}J(H,H) = 7 Hz, 3H, H6'), 2.01 (s, 3H, H1''), 2.74 (t, ^{3}J(H,H) = 7 Hz, 2H, H2'), 4.06 (q, ^{3}J(H,H) = 5 Hz, 2H, H5'), 4.11 (t, ^{3}J(H,H) = 7 Hz, 2H, H1'), 6.04 (d, ^{3}J(H,H) = 7 Hz, 1H, H5), 7.06 (d, ^{3}J(H,H) = 7 Hz, 1H, H6), 8.82 (brs, 1H, Pyr-O*H*) ppm.

3.4.10. 1-Carboxylethyl-3-hydroxy-2(*1H*)-4-methyl-pyridone - 8a

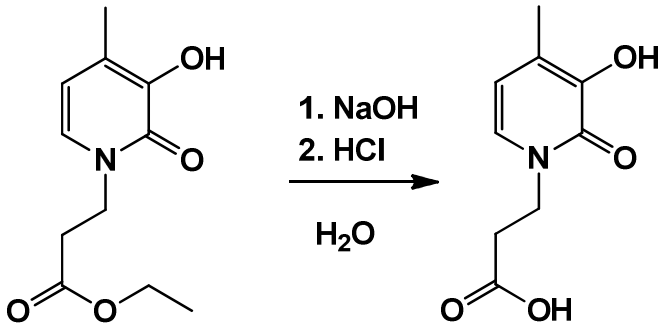

Synthesis:

The synthesis was performed according to the general procedure for the ester hydrolysis using 1.00 g (4.40 mmol) of compound **7a**.

Yield: 0.662 g (76%)

Melting point: 165 – 166 °C

Elemental analysis: calculated for $C_9H_{11}NO_4$

8a	C[%]	H[%]	N[%]
calculated	54.82	5.62	7.10
found	54.71	5.43	6.97
Δ	0.11	0.19	0.13

NMR-spectroscopy:

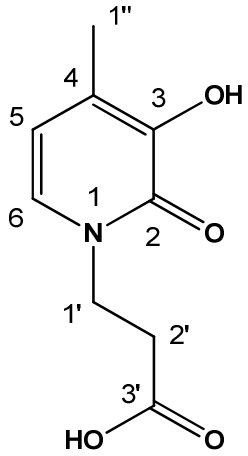

^{1}H NMR (500 MHz, d^{6}-DMSO): δ = 2.01 (s, 3H, H1''), 2.67 (t, ^{3}J(H,H) = 7 Hz, 2H, H2'), 4.07 (t, ^{3}J(H,H) = 7 Hz, 2H, H1'), 6.04 (d, ^{3}J(H,H) = 7 Hz, 1H, H5), 7.07 (d, ^{3}J(H,H) = 7 Hz, 1H, H6), 8.62 (s, 1H, Pyr-O*H*), 12.41 (brs, 1H, -COO*H*) ppm.

3.5. Synthesis of Pyridone-based Metal Complexes

3.5.1. [Chlorido(η^6-p-cymene){N-[(ethylcarbonyl)methyl]-3-oxo-κO-2-(*1H*)-pyridonato-κO}ruthenium(II)] - 1b

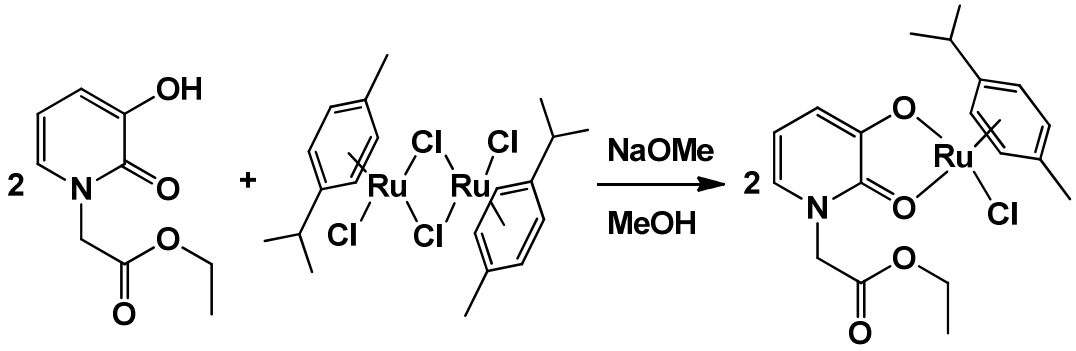

Synthesis:

The synthesis was performed according to the general procedure using 120 mg (0.196 mmol) of ruthenium precursor **p1**, 85 mg (0.431 mmol) of compound **1a** and 28 mg (0.49 mmol) of NaOMe. The resolved crude product was precipitated by addition of Et_2O (20 mL).

Yield: 170 mg (92%)

Melting point: >205 °C (decomposition

Water solubility: 5.16 mg/mL

Elemental analysis: calculated for $C_{19}H_{24}ClNO_4Ru$

1b	C[%]	H[%]	N[%]
calculated	48.87	5.18	3.00
found	48.56	5.26	2.97
Δ	0.31	0.08	0.03

NMR-spectroscopy:

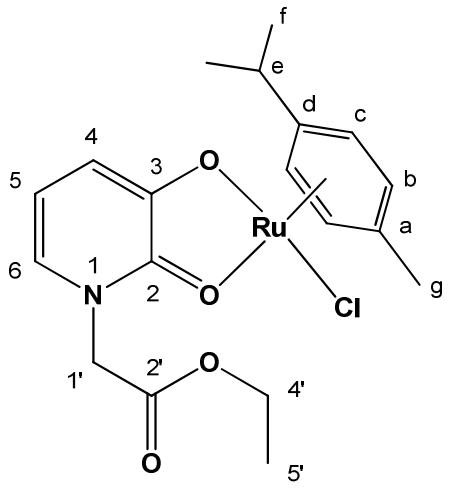

^{1}H NMR (500 MHz, $CDCl_3$): δ = 1.32–1.36 (m, 9H, H*f*, H5'), 2.31 (s, 3H, H*g*), 2.87–2.93 (m, 1H, H*e*), 4.23–4.31 (m, 3H, H4', H1'), 5.15 (d, ^{2}J(H,H) = 17 Hz, 1H, H1'), 5.31 (d, ^{3}J(H,H) = 6 Hz, 1H, H*b*), 5.32 (d, ^{3}J(H, H) = 6 Hz, 1H, H*b*), 5.52 (d, ^{3}J(H, H) = 6 Hz, 1 H, H*c*), 5.53 (d, ^{3}J(H, H) = 6 Hz, 1 H, H*c*), 6.28 (dd, ^{3}J(H,H) = 7 Hz, ^{3}J(H,H) = 7 Hz, 1H, H5), 6.40 (dd, ^{3}J(H,H) = 7 Hz, ^{4}J(H,H) = 1 Hz, 1H, H4), 6.69 (dd, ^{3}J(H,H) = 8 Hz, ^{4}J(H,H) = 1 Hz, 1H, H6) ppm.

3.5.2. [Chlorido(η^6-p-cymene){N-[(ethylcarbonyl)methyl]-3-oxo-κO-2-(*1H*)-pyridonato-κO}osmium(II)] - 1c

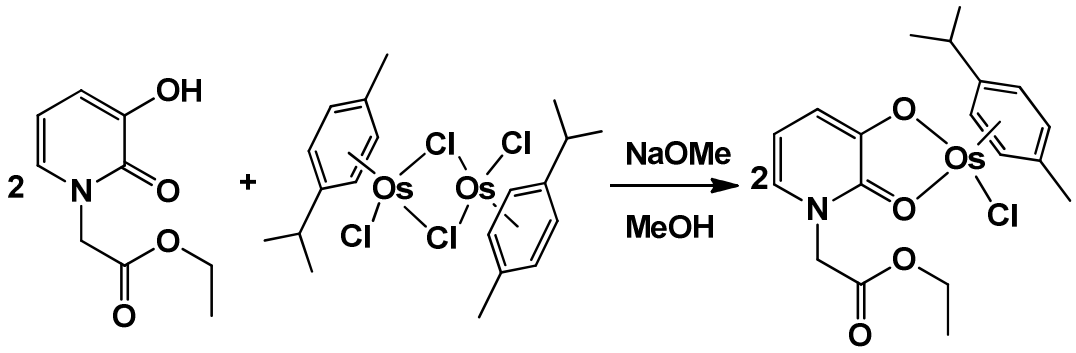

Synthesis:

The synthesis was performed according to the general procedure using 100 mg (0.16 mmol) of osmium precursor **p2**, 67 mg (0.34 mmol) of compound **1a** and 22 mg (0.37 mmol) of NaOMe. The resolved crude product was precipitated by addition of *n*-hexane (20 mL).

Yield: 105 mg (59%)

Melting point: >144 °C (decomposition)

Water solubility: 0.26 mg/mL

Elemental analysis: calculated for: $C_{19}H_{24}ClNO_4Os \cdot 0.1C_4H_{10}O$

1c	C[%]	H[%]	N[%]
calculated	41.35	4.47	2.49
found	41.54	4.39	2.71
Δ	0.19	0.08	0.22

NMR-spectroscopy:

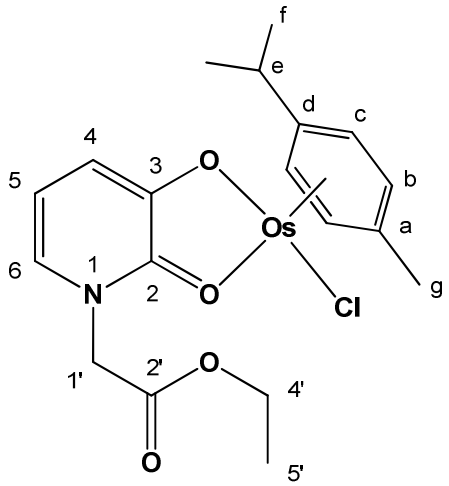

^{1}H NMR (500 MHz, $CDCl_3$) δ = 1.29–1.35 (m, 9H, H*f*, H5'), 2.34 (s, 3H, H*g*), 2.71–2.78 (m, 1H, H*e*), 4.25–4.35 (m, 3H, H4', H1'), 5.15 (d, ^{2}J(H,H) = 17 Hz, 1H, H1'), 5.77 (d, ^{3}J(H,H) = 6 Hz, 1H, H*b*), 5.84 (d, ^{3}J(H,H) = 5 Hz, 1H, H*b*), 6.02 (d, ^{3}J(H,H) = 5 Hz, 1H, H*c*), 6.06 (d, ^{3}J(H,H) = 6 Hz, 1H, H*c*), 6.33 (dd, ^{3}J(H,H) = 7 Hz, ^{3}J(H,H) = 7 Hz, 1H, H5), 6.46 (dd, ^{3}J(H,H) = 7 Hz, ^{4}J(H,H) = 1 Hz, 1H, H4), 6.75 (dd, ^{3}J(H,H) = 8 Hz, ^{4}J(H,H) = 2 Hz, 1H, H6) ppm.

3.5.3. [Chlorido(η^5-pentamethylcyclopentadiene){N-[(ehtylcarbonyl)-methyl)]-3-oxo-κO-2-(*1H*)-pyridonato-κO}rhodium(III)] - 1d

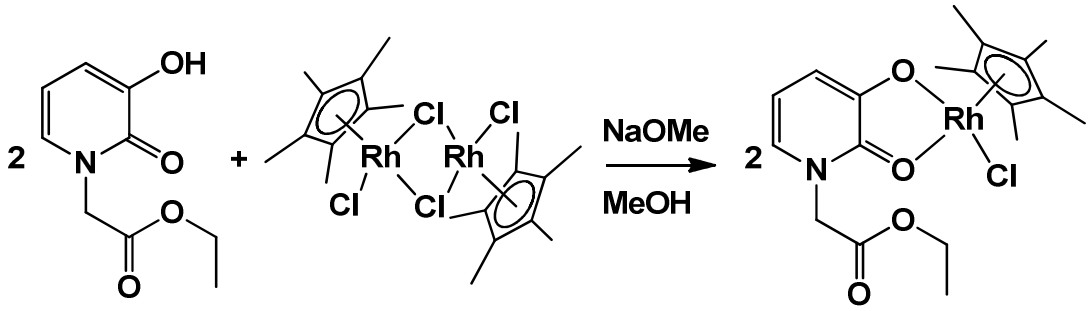

Synthesis:

The synthesis was performed according to the general procedure using 100 mg (0.16 mmol) of rhodium precursor **p3**, 70 mg (0.36 mmol) of compound **1a** and 35 mg (0.64 mmol) of NaOMe. The resolved crude product was precipitated by addition of Et_2O (20 mL).

Yield: 78 mg (54%)

Melting point: >198 °C (decomposition)

Water solubility: 11.25 mg/mL

Elemental analysis: calculated for $C_{19}H_{25}ClNO_4Rh$

1d	C[%]	H[%]	N[%]
calculated	48.39	5.39	2.97
found	48.44	5.06	2.94
Δ	0.05	0.33	0.03

NMR-spectroscopy:

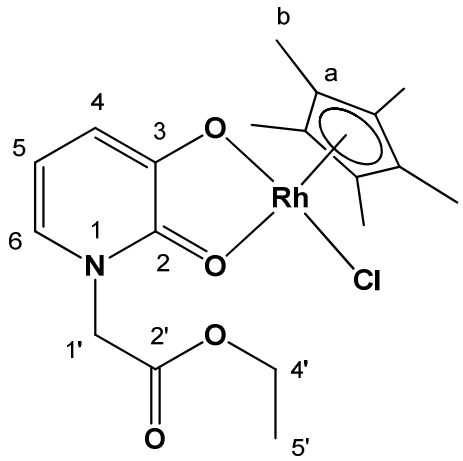

^{1}H NMR (500 MHz, d_4-CD_3OD): δ = 1.33 (t, 3H, ^{3}J(H,H) = 7 Hz, H5'), 1.69 (s, 15H, H*b*), 4.30 (q, ^{3}J(H,H) = 7Hz, 2H, H4'), 4.86 (s, 2H, H1'), 6.37 (dd, ^{3}J(H,H) = 7 Hz, ^{3}J(H,H) = 7 Hz, 1H, H5), 6.66 (d, ^{3}J(H,H) = 7 Hz, 1H, H4), 6.81 (d, ^{3}J(H,H) = 7 Hz, 1H, H6) ppm.

3.5.4. Bis[(η^6-p-cymene){N-[(carboxyl-κO)methyl]-3-oxo-κO-2-(*1H*)-pyridonato-κO}ruthenium(II)] - 2b

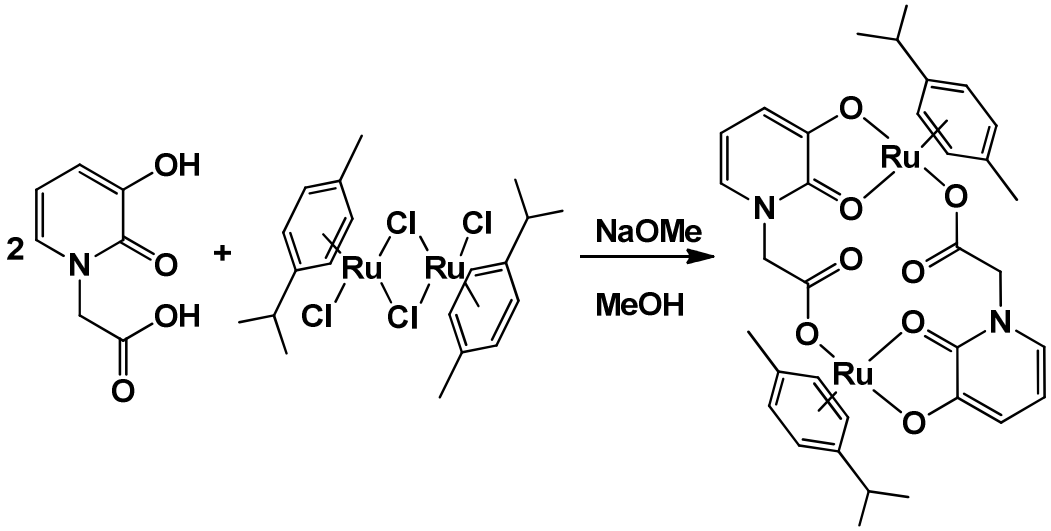

Synthesis:

The synthesis was performed according to the general procedure using 245 mg (0.40 mmol) of ruthenium precursor **p1**, 150 mg (0.88 mmol) of compound **2a** and 102 mg (1.80 mmol) of NaOMe. The resolved crude product was precipitated by addition of Et_2O (20 mL).

Yield: (45%)

Melting point: >188 °C (decomposition)

Water solubility: 5.77 mg/mL

Elemental analysis: calculated for $C_{34}H_{38}N_2O_8Ru_2 \cdot 2H_2O$

2b	C[%]	H[%]	N[%]
calculated	48.57	5.03	3.33
found	48.54	4.79	3.43
Δ	0.03	0.24	0.10

NMR-spectroscopy:

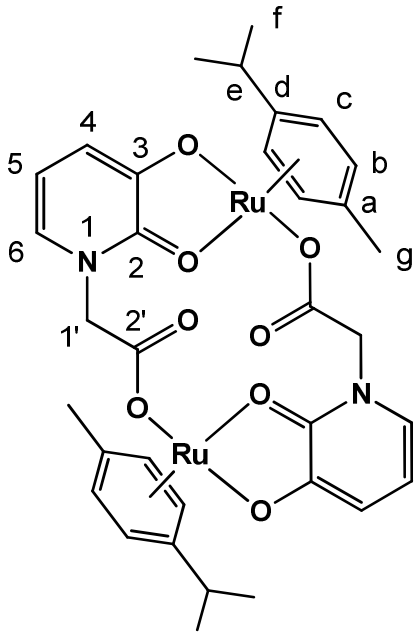

^{1}H NMR (500 MHz, $CDCl_3$): δ = 1.28–1.33 (m, 6H, H*f*), 2.26 (s, 3H, H*g*), 2.87–2.92 (m, 1H, H*e*), 3.89 (d, ^2J(H,H) = 16 Hz, 1H, H1'), 5.12 (d, ^2J(H,H) = 16 Hz, 1H, H1'), 5.40 (d, ^3J(H,H) = 6 Hz, 1H, H*b*), 5.57 (d, ^3J(H,H) = 6 Hz, 1H, H*b*), 5.72 (d, ^3J(H,H) = 6 Hz, 1H, H*c*), 5.78 (d, ^3J(H,H) = 6 Hz, 1H, H*c*), 5.85 (dd, ^3J(H,H) = 7 Hz, ^3J(H,H) = 7 Hz, 1H, H5), 6.19 (dd, ^3J(H,H) = 8 Hz, ^4J(H,H) = 1 Hz, 1H, H4), 6.25 (dd, ^3J(H,H) = 7 Hz, ^4J(H,H) = 1 Hz, 1H, H6) ppm.

3.5.5. Bis[(η^6-p-cymene){N-[(carboxyl-κO)methyl]-3-oxo-κO-2-(*1H*)-pyridonato-κO}osmium(II)] - 2c

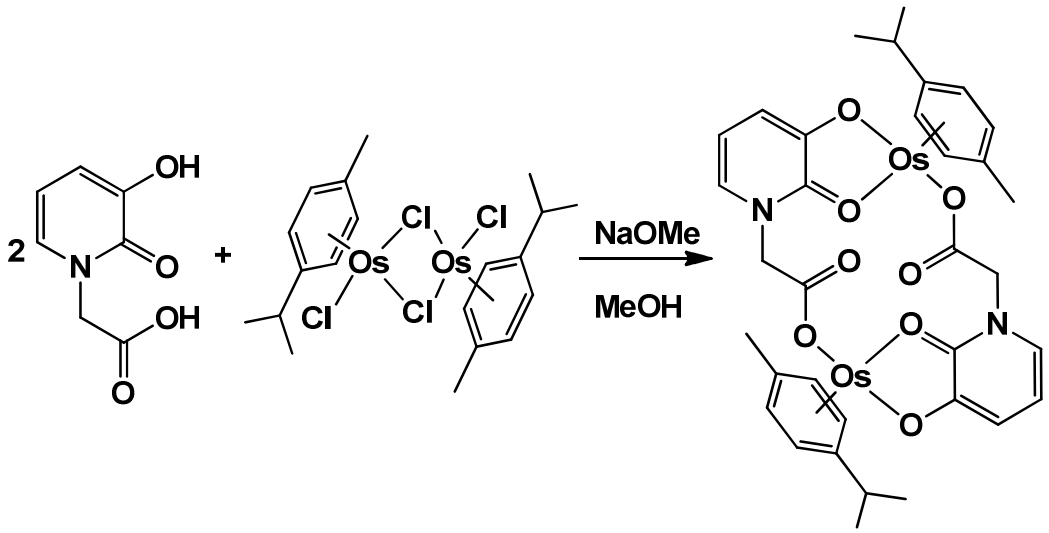

Synthesis:

The synthesis was performed according to the general procedure using 119 mg (0.15 mmol) of osmium precursor **p2**, 61 mg (0.36 mmol) of compound **2a** and 51 mg (0.89 mmol) of NaOMe. The resolved crude product was precipitated by addition of *n*-hexane (20 mL).

Yield: 84 mg (57%)

Melting point: >170 °C (decomposition)

Water solubility: 1.37 mg/mL

Elemental analysis: calculated for $C_{34}H_{38}N_2O_8Os_2 \cdot 0.25C_4H_{10}O$

2c	C[%]	H[%]	N[%]
calculated	41.97	4.07	2.80
found	42.23	4.29	2.71
Δ	0.26	0.22	0.09

NMR-spectroscopy:

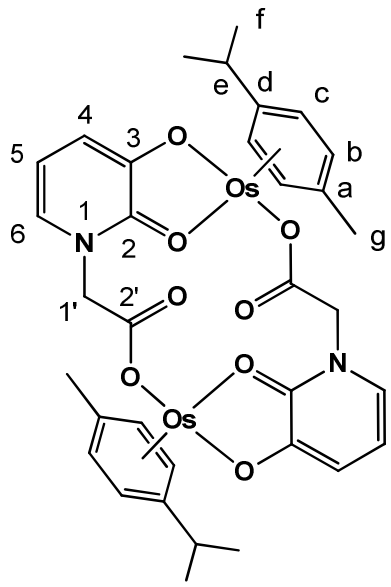

^{1}H NMR (500 MHz, CD_3OD): δ = 1.29–1.34 (m, 6H, H*f*), 2.30 (s, 3H, H*g*), 2.72–2.77 (m, 1H, H*e*), 4.18 (d, ^2J(H,H) = 16 Hz, 1H, H1'), 4.94 (d, ^2J(H,H) = 16 Hz, 1H, H1'), 5.92 (d, ^3J(H,H) = 5 Hz, 1H, H*b*), 5.95 (d, ^3J(H,H) = 5 Hz, 1H, H*b*), 6.09 (dd, ^3J(H,H) = 7 Hz, ^3J(H,H) = 7 Hz, 1H, H5), 6.24 (d, ^3J(H,H) = 5 Hz, 1H, H*c*), 6.28 (d, ^3J(H,H) = 5 Hz, 1H, H*c*), 6.36 (dd, ^3J(H,H) = 8 Hz, ^4J(H,H) = 1 Hz, 1H, H4), 6.52 (dd, ^3J(H,H) = 7 Hz, ^4J(H,H) = 1 Hz, 1H, H6) ppm.

^{13}C NMR (125.75 MHz, CD_3OD): δ = 17.7 (C*g*), 21.5 (C*f*), 22.4 (C*f*), 31.8 (C*e*), 51.8 (C1'), 67.0 (C*b*), 67.1 (C*b*), 70.5 (C*c*), 71.1 (C*c*), 83.8 (C*a*), 87.7 (C*d*), 111.6 (C5), 117.5 (C6), 124.2 (C4), 158.9 (C2'), 167.3 (C3), 172.9 (C2) ppm.

3.5.6. Bis[(η^5-pentamethylcyclopentadiene){N-[(ethoxycarbonyl)-methyl]-3-oxo-κO-2-(*1H*)-pyridonato-κO}rhodium(III)] - 2d

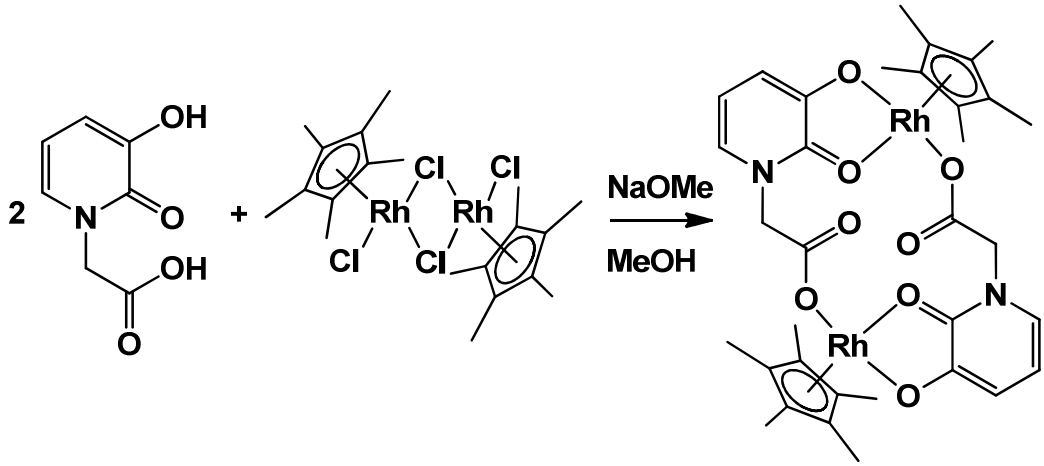

Synthesis:

The synthesis was performed according to the general procedure using 100 mg (0.16 mmol) of rhodium precursor **p3**, 57 mg (0.34 mmol) of compound **2a** and 48 mg (0.85 mmol) of NaOMe. The resolved crude product was precipitated by addition of *n*-hexane (20 mL).

Yield: 90 mg (69%)

Melting point: >185 °C (decomposition)

Water solubility: 15.00 mg/mL

Mass spectrometry: m/z = 428 ($C_{17}H_{20}NO_4Rh + Na^+$)
833 ($C_{34}H_{40}N_2O_8Rh_2 + Na^+$)

NMR-spectroscopy:

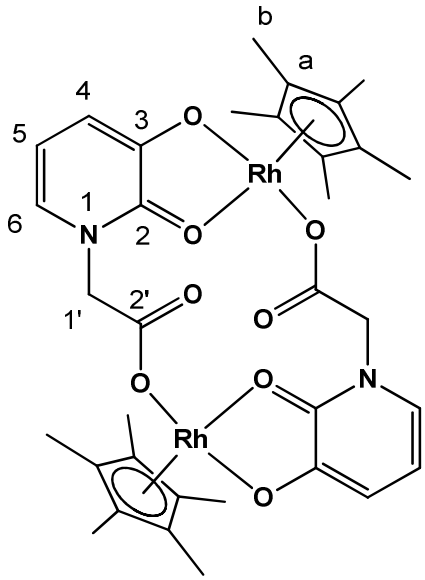

^{1}H NMR (500 MHz, d_4-CD_3OD): δ = 1.71 (s, 15H, H*b*), 4.60 (brs, 2H, H1'), 6.35 (dd, ^{3}J(H,H) = 7 Hz, ^{3}J(H,H) = 7 Hz, 1H, H5), 6.68 (d, ^{3}J(H,H) = 8 Hz, 1H, H4), 6.82 (d, ^{3}J(H,H) = 7 Hz, 1H, H6) ppm.

3.5.7. [Chlorido(η^6-p-cymene){N-[(ethylcarbonylmethyl]-3-oxo-κO-4-methyl-2-(*1H*)-pyridonato-κO}ruthenium(II)] - 3b

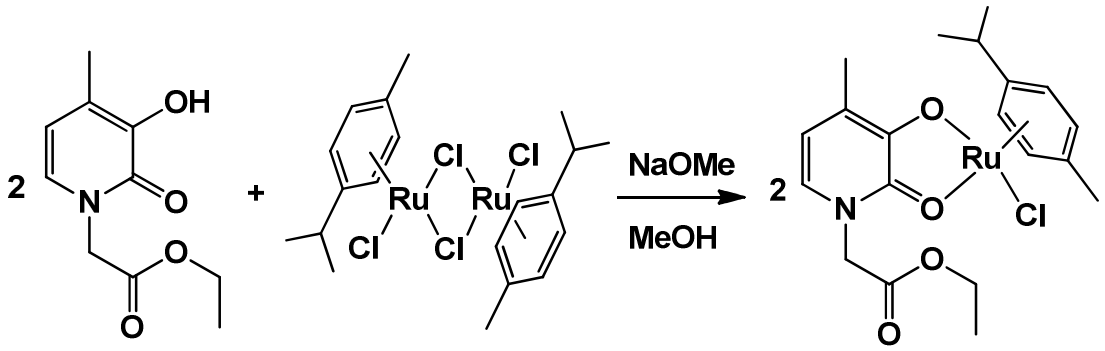

Synthesis:

The synthesis was performed according to the general procedure using 122 mg (0.20 mmol) of ruthenium precursor **p1**, 85 mg (0.40 mmol) of compound **3a** and 25 mg (0.44 mmol) of NaOMe. A red solid was formed after 3 hours reaction, filtered off, which was washed with methanol and dried in vacuo.

Yield: 110 mg (75%)

Melting point: >205 °C (decomposition)

Water solubility: 1.13 mg/mL

Elemental analysis: calculated for $C_{20}H_{26}ClNO_4Ru \cdot 0.75H_2O$

3a	C[%]	H[%]	N[%]
calculated	48.58	5.61	2.83
found	48.53	5.30	2.89
Δ	0.05	0.31	0.06

NMR-spectroscopy:

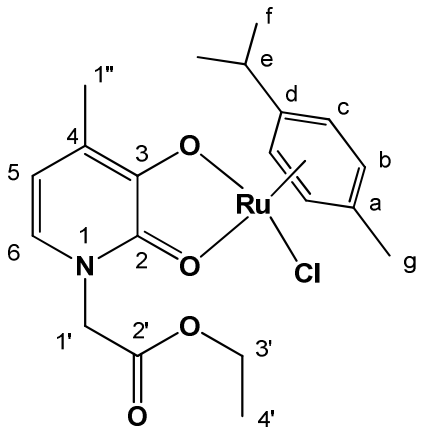

^{1}H NMR (500 MHz, $CDCl_3$): δ = 1.29–1.35 (m, 9H, H*f*, H4'), 2.18 (s, 3H, H1''), 2.30 (s, 3H, H*g*), 2.85–2.91 (m, 1H, H*e*), 4.17–4.29 (m, 3H, H3', H1'), 5.12 (d, ^{2}J(H,H) = 17 Hz, 1H, H1'), 5.24 (d, ^{3}J(H,H) = 6 Hz, 2H, H*b*), 5.48–5.52 (m, 2H, H*c*), 6.18 (d, ^{3}J(H,H) = 7 Hz, 1H, H5), 6.33 (d, ^{3}J(H,H) = 7 Hz, 1H, H6) ppm.

^{13}C NMR (125.75 MHz, $CDCl_3$): δ = 14.2 (C4'), 15.5 (C1''), 18.5 (C*g*), 22.3 (C*f*), 22.4 (C*f*), 31.1 (C*e*), 51.1 (C1'), 61.8 (C7), 77.1 (C*b*), 77.6 (C*b*), 80.4 (C*c*), 80.6 (C*c*), 95.8 (C*a*), 98.5 (C*d*), 115.4 (C5), 120.0 (C6), 128.9 (C4), 158.2 (C2'), 164.4 (C3), 167.2 (C2) ppm.

3.5.8. [Chlorido(η^6-p-cymene){N-[(ethylcarbonylmethyl]-3-oxo-κO-4-methyl-2-(*1H*)-pyridonato-κO}osmium(II)] - 3c

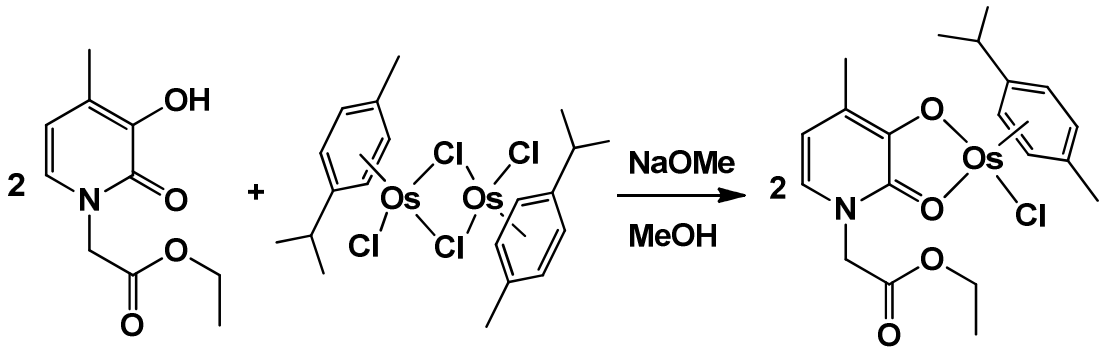

Synthesis:

The synthesis was performed according to the general procedure using 126 mg (0.16 mmol) of osmium precursor **p2**, 72 mg (0.34 mmol) of compound **3a** and 22 mg (0.85 mmol) of NaOMe. The resolved crude product was precipitated by addition of Et_2O (20 mL).

Yield: 80 mg (44%)

Melting point: >184 °C (decomposition)

Water solubility: <0.1 mg/mL

Elemental analysis: calculated for $C_{20}H_{26}ClNO_4Os \cdot H_2O$

3c	C[%]	H[%]	N[%]
calculated	40.84	4.80	2.38
found	40.98	4.50	2.32
Δ	0.14	0.3	0.06

NMR-spectroscopy:

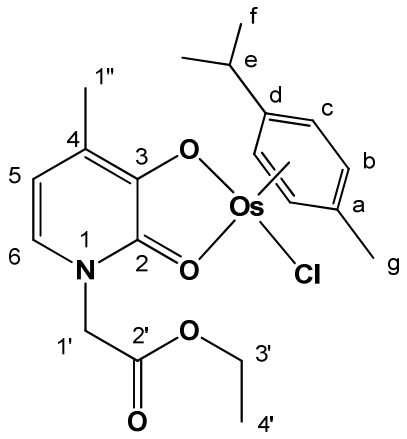

^{1}H NMR (500 MHz, $CDCl_3$): δ = 1.28–1.35 (m, 9H, H*f*, H4'), 2.22 (s, 3H, H1''), 2.35 (s, 3H, H*g*), 2.69–2.77 (m, 1H, H*e*), 3.81 (s, 1H, H1'), 4.26–4.35 (m, 2H, H3'), 5.10–5.15 (m, 1H, H1'), 5.76–5.79 (m, 2H, H*b*), 6.01–6.04 (m, 2H, H*c*), 6.24 (d, ^{3}J(H,H) = 7 Hz, 1H, H5), 6.40 (d, ^{3}J(H,H) = 7 Hz, 1H, H6) ppm.

3.5.9. [Chlorido(η^5-pentamethylcyclopentadiene){N-[(ehtylcarbonyl)-methyl)]-3-oxo-κO-4-methyl-2-(*1H*)-pyridonato-κO}rhodium(III)] - 3d

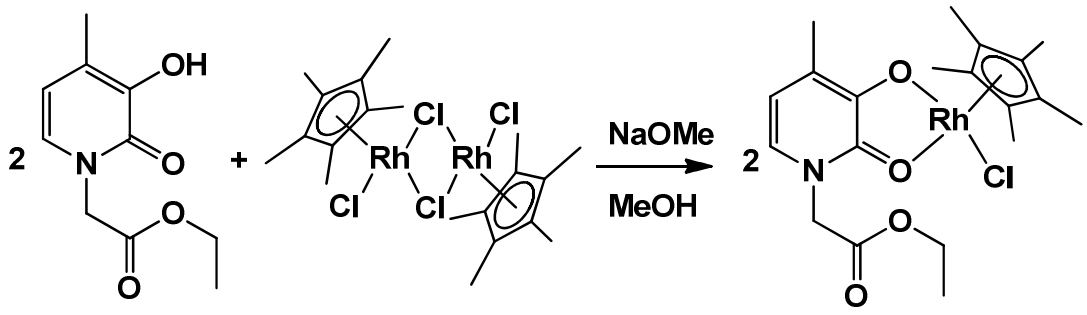

Synthesis:

The synthesis was performed according to the general procedure using 100 mg (0.16 mmol) of rhodium precursor **p3**, 76 mg (0.36 mmol) of compound **3a** and 35 mg (0.64 mmol) of NaOMe. The resolved crude product was precipitated by addition of *n*-hexane (20 mL).

Yield: 86 mg (57%)

Melting point: >152 °C (decomposition)

Elemental analysis: calculated for $C_{20}H_{27}ClNO_4Rh \cdot 0.1CH_2Cl_2$

3d	C[%]	H[%]	N[%]
calculated	49.00	5.55	2.85
found	49.24	5.17	2.90
Δ	0.24	0.38	0.05

NMR-spectroscopy:

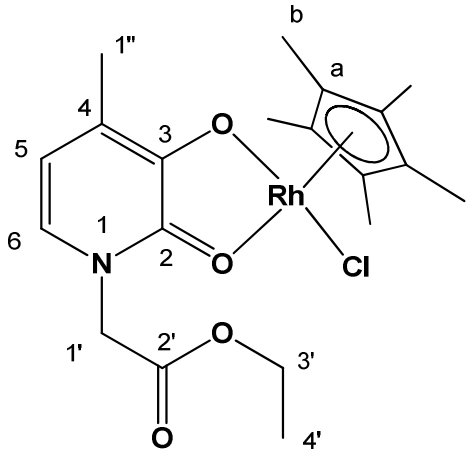

^{1}H NMR (500 MHz, d_4-CD_3OD): δ = 1.34 (t, ^{3}J(H,H) = 7 Hz, 3H, H4'), 1.69 (s, 15H, H*b*), 2.21 (s, 1H, H1''), 3.37 (s, 1H, H1'), 3.83 (s, 1H, H1'), 4.30 (q, ^{3}J(H,H) = 7 Hz, 2H, H3'), 6.35 (t, ^{3}J(H,H) = 7 Hz, 1H, H5), 6.79 (d, ^{3}J(H,H) = 7 Hz, 1H, H5) ppm.

3.5.10. Bis[(η^6-p-cymene){N-[(carboxyl-κO)ethyl]-3-oxo-κO-4-methyl-2-(*1H*)-pyridonato-κO}ruthenium(II)]- 4b

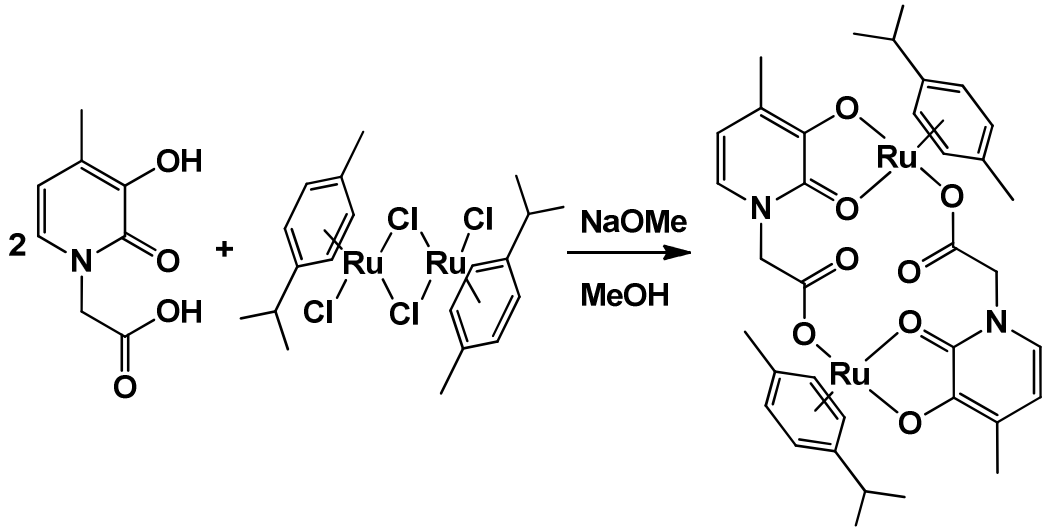

Synthesis:

The synthesis was performed according to the general procedure using 153 mg (0.25 mmol) of ruthenium precursor **p1**, 100 mg (0.55 mmol) of compound **4a** and 81 mg (1.50 mmol) of NaOMe. The resolved crude product was precipitated by addition of *n*-hexane (20 mL).

Yield: 156 mg (75%)

Melting point: >200 °C (decomposition)

Water solubility: 0.59 mg/mL

Elemental analysis: calculated for $C_{36}H_{42}N_2O_8Ru_2 \cdot 1.25CH_2Cl_2$

4b	C[%]	H[%]	N[%]
calculated	47.64	4.78	2.98
found	47.97	4.74	3.07
Δ	0.33	0.04	0.09

NMR-spectroscopy:

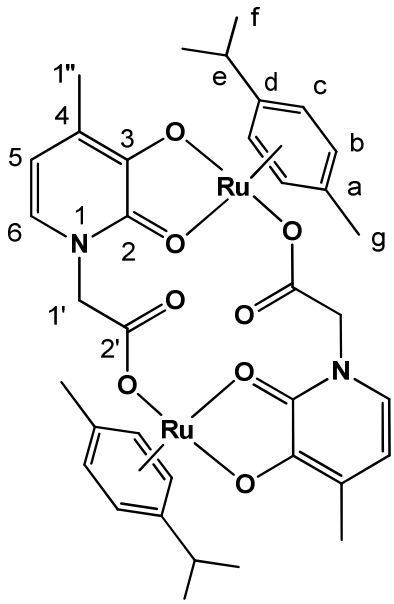

^{1}H NMR (500 MHz, CD_3OD): δ = 1.29–1.35 (m, 6H, H*f*), 1.98 (s, 3H, H1''), 2.26 (s, 3H, H*g*), 2.85–2.90 (m, 1H, H*e*), 4.02 (d, ^2J(H,H) = 16 Hz, 1H, H1'), 4.93 (d, ^2J(H,H) = 16 Hz, 1H, H1'), 5.51 (d, ^3J(H,H) = 6 Hz, 1H, H*b*), 5.57 (d, ^3J(H,H) = 6 Hz, 1H, H*b*), 5.80 (d, ^3J(H,H) = 6 Hz, 2H, H*c*), 5.87 (d, ^3J(H,H) = 7 Hz, 1H, H5), 6.34 (d, ^3J(H,H) = 7 Hz, 1H, H6) ppm.

^{13}C NMR (125.75 MHz, CD_3OD): δ = 14.4 (C1''), 17.1 (C*g*), 21.1 (C*f*), 21.8 (C*f*), 31.1 (C*e*), 51.7 (C1'), 77.1 (C*b*), 77.4 (C*b*), 79.1 (C*c*), 79.8 (C*c*), 94.1 (C*a*), 98.3 (C*d*), 113.1 (C5), 122.6 (C6), 127.9 (C4), 154.8 (C2'), 162.8 (C3), 173.0 (C2) ppm.

3.5.11. Bis[(η^6-p-cymene){N-[(carboxyl-κO)ethyl]-3-oxo-κO-4-methyl-2-(*1H*)-pyridonato-κO}ruthenium(II)]- 4c

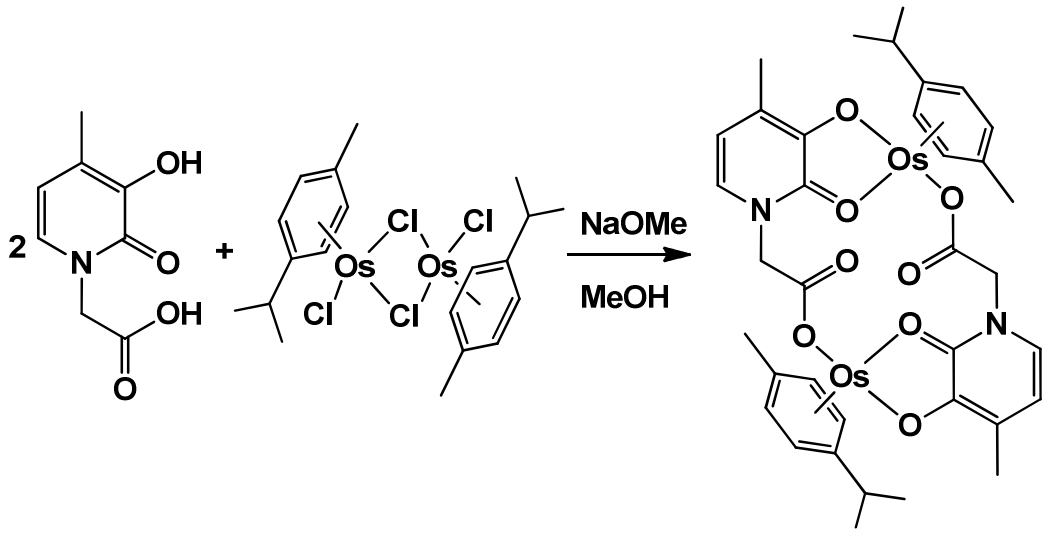

Synthesis:

The synthesis was performed according to the general procedure using 198 mg (0.25 mmol) of osmium precursor **p2**, 100 mg (0.55 mmol) of compound **4a** and 81 mg (1.50 mmol) of NaOMe. The resolved crude product was precipitated by addition of Et_2O (20 mL).

Yield: 119 mg (47%)

Melting point: >200 °C (decomposition)

Water solubility: <0.1 mg/mL

Elemental analysis: calculated for $C_{36}H_{42}N_2O_8Os_2 \cdot H_2O$

4c	C[%]	H[%]	N[%]
calculated	42.01	4.31	2.72
found	42.19	4.38	2.76
Δ	0.18	0.07	0.04

NMR-spectroscopy:

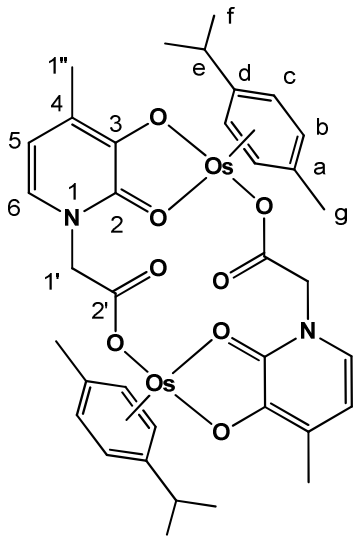

^{1}H NMR (500 MHz, CD_3OD): δ = 1.27–1.30 (m, 6H, H*f*), 1.98 (s, 3H, H1''), 2.31 (s, 3H, H*g*), 2.72–2.76 (m, 1H, H*e*), 3.89 (d, ^2J(H,H) = 16 Hz, 1H, H1'), 5.08 (d, ^2J(H,H) = 16 Hz, 1H, H1'), 5.79–5.81 (m, 3H, H5, H*b*), 6.16–6.22 (m, 3H, H*c*, H6) ppm.

^{13}C NMR (125.75 MHz, CD_3OD): δ = 15.4 (C1''), 18.8 (C*g*), 23.0 (C*f*), 23.1 (C*f*), 32.0 (C*e*), 51.6 (C1'), 66.1 (C*b*), 66.5 (C*b*), 71.1 (C*c*), 71.8 (C*c*), 84.3 (C*a*), 87.0 (C*d*), 114.0 (C5), 121.4 (C6), 127.0 (C4), 158.0 (C2'), 166.3 (C3), 172.0 (C2) ppm.

3.5.12. Bis[(η^5-pentamethylcyclopentadiene){N-[(ethoxycarbonyl)-methyl]-3-oxo-κO-4-methyl-2-(*1H*)-pyridonato-κO}rhodium(III)] - 4d

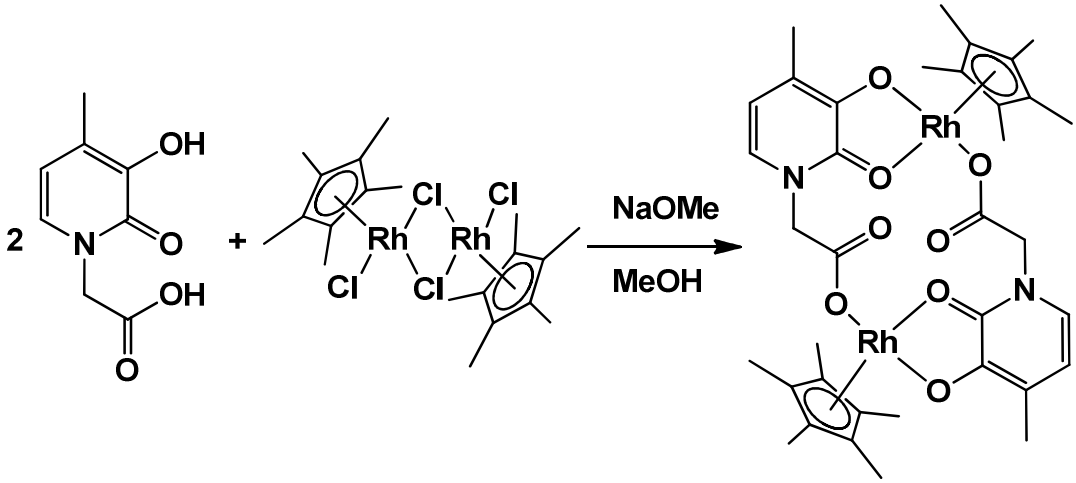

Synthesis:

The synthesis was performed according to the general procedure using 100 mg (0.16 mmol) of rhodium precursor **p3**, 63 mg (0.34 mmol) of compound **4a** and 35 mg (0.70 mmol) of NaOMe. The resolved crude product was precipitated by addition of *n*-hexane (20 mL).

Yield: 101 mg (75%)

Melting point: >170 °C (decomposition)

Water solubility: 10 mg/mL

NMR-spectroscopy:

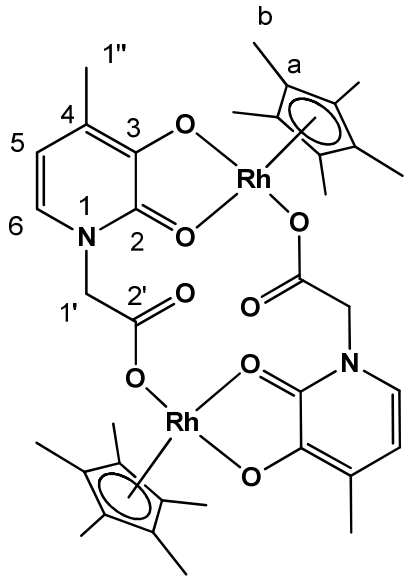

^{1}H NMR (500 MHz, d_4-CD_3OD): δ = 1.70 (s, 15H, H*b*), 2.20 (s, 3H, H1''), 4.58 (brs, 2H, H1'), 6.30 (d, ^{3}J(H,H) = 7 Hz, 1H, H5), 6.76 (d, ^{3}J(H,H) = 7 Hz, 1H, H6) ppm.

^{13}C NMR (125.75 MHz, d_4-CD_3OD): δ = 7.3 (C*b*), 14.3 (C1''), 53.6 (C1'), 91.8 (C*a*), 113.9 (C5), 122.8 (C6), 129.2 (C4), 156.3 (C2'), 163.7 (C3), 172.3 (C2) ppm.

3.5.13. [Chlorido(η^6-p-cymene){N-[(ethylcarbonyl)ethyl]-3-oxo-κO-2-(*1H*)-pyridonato-κO}ruthenium(II)] - 5b

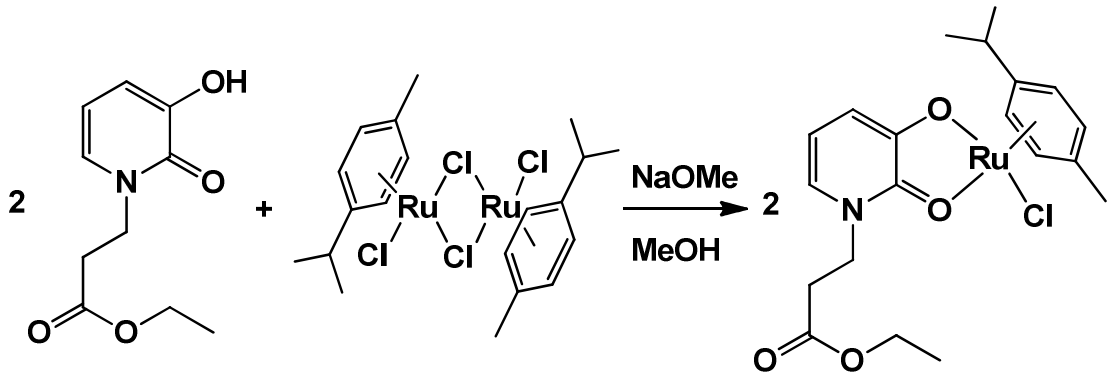

Synthesis:

The synthesis was performed according to the general procedure using 245 mg (0.4 mmol) of ruthenium precursor **p1**, 186 mg (0.88 mmol) of compound **5a** and 80 mg (1.40 mmol) of NaOMe. The resolved crude product was precipitated by addition of *n*-hexane (20 mL).

Yield: 88 mg (23%)

Melting point: >101 °C (decomposition)

Water solubility: 1.76 mg/mL

Elemental analysis: calculated for $C_{20}H_{26}ClNO_4Ru \cdot 0.25H_2O$

5b	C[%]	H[%]	N[%]
calculated	49.48	5.50	2.89
found	49.55	5.44	3.02
Δ	0.07	0.06	0.13

NMR-spectroscopy:

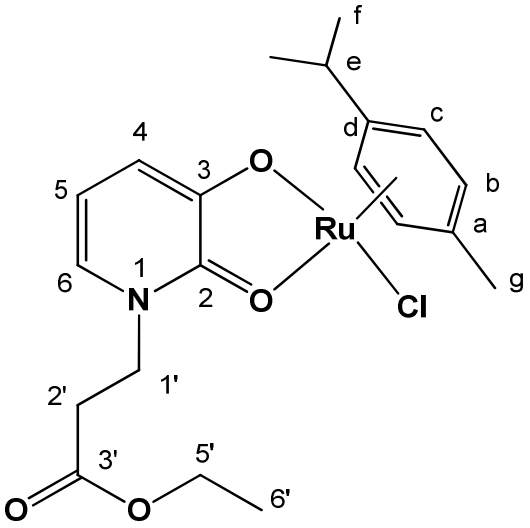

^{1}H NMR (500 MHz, $CDCl_3$): δ = 1.26 (t, ^{3}J(H, H) = 7 Hz, 3H, H6'), 1.33–1.38 (m, 6H, H*f*), 2.34 (s, 3H, H*g*), 2.76–2.81 (m, 1H, H2'), 2.86–2.97 (m, 2H, H*e*, H2'), 4.16 (q, 2H, ^{3}J(H, H) = 7 Hz, H5'), 4.19–4.32 (m, 2H, H1'), 5.32 (t, ^{3}J(H,H) = 5 Hz, 2H, H*b*), 5.52–5.56 (m, 2H, H*c*), 6.21 (dd, ^{3}J(H,H) = 7 Hz, ^{3}J(H,H) = 7 Hz, 1H, H5), 6.55 (dd, ^{3}J(H,H) = 7 Hz, ^{4}J(H,H) = 2 Hz, 1H, H4), 6.65 (dd, ^{3}J(H,H) = 8 Hz, ^{4}J(H,H) = 2 Hz, 1H, H6) ppm.

^{13}C NMR (125.75 MHz, $CDCl_3$): δ = 13.1 (C6'), 17.2 (C*g*), 21.2 (C*f*), 31.1 (C*e*), 32.7 (C2') 46.5 (C1'), 60.5 (C5'), 76.0 (C*b*), 79.5 (C*c*), 95.3 (C*a*), 99.2 (C*d*), 111.8 (C5), 123.2 (C6), 128.3 (C4), 158.9 (C3'), 165.2 (C3), 170.9 (C2) ppm.

3.5.14. [Chlorido(η^5-pentamethylcyclopentadiene){N-[(ehtylcarbonyl)ethyl)]-3-oxo-κO-2-(*1H*)-pyridonato-κO}rhodium(III)] - 5d

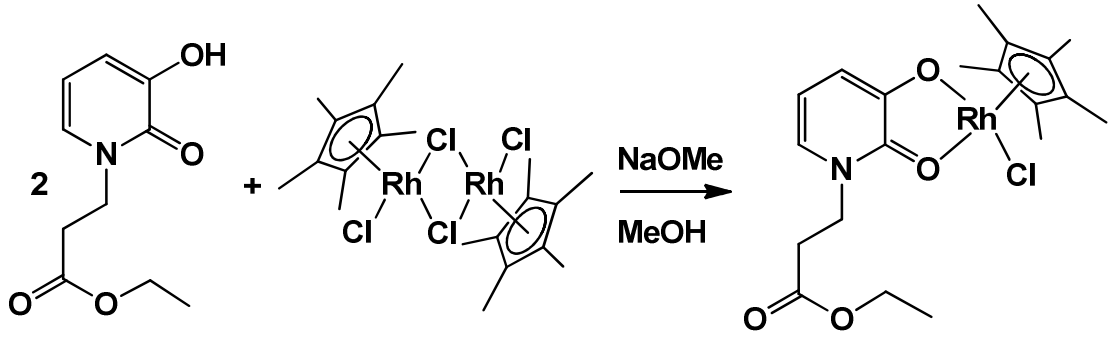

Synthesis:

The synthesis was performed according to the general procedure using 100 mg (0.16 mmol) of rhodium precursor **p3**, 72 mg (0.34 mmol) of compound **5a** and 22 mg (0.37 mmol) of NaOMe. The resolved crude product was precipitated by addition of *n*-hexane (20 mL).

Yield: (39%)

Melting point: >164 °C (decomposition)

Water solubility: 8.00 mg/mL

Elemental analysis: calculated for $C_{20}H_{27}ClNO_4Rh \cdot 0.5H_2O$

5d	C[%]	H[%]	N[%]
calculated	48.74	5.73	2.84
found	48.69	5.55	2.88
Δ	0.05	0.18	0.04

NMR-spectroscopy:

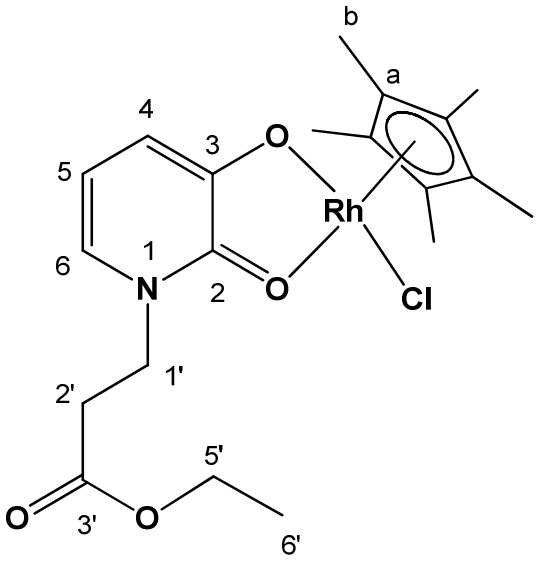

^{1}H NMR (500 MHz, $CDCl_3$): δ = 1.27 (t, ^{3}J(H,H) = 7 Hz, 3H, H6'), 1.75 (s, 15H, H*b*), 2.77–2.83 (m, 1H, H2'), 2.92–2.96 (m, 1H, H2'), 4.13–4.19 (m, 3H, H5', H1'), 4.33–4.39 (m, 1H, H1'), 6.19 (dd, ^{3}J(H,H) = 7 Hz, ^{3}J(H,H) = 7 Hz, 1H, H5), 6.51 (dd, ^{3}J(H,H) = 7 Hz, ^{4}J = 2 Hz, 1H, H4), 6.61 (dd, ^{3}J(H,H) = 8 Hz, ^{4}J(H,H) = 2 Hz, 1H, H6)

^{13}C NMR (125.75 MHz, d_4-CH_3OD): δ = 7.5 (Hb), 13.1 (C6'), 32.8 (C2') 46.4 (C1'), 60.5 (C5'), 91.9 (C*b*), 92.0 (C*b*), 111.5 (C5), 117.2 (C6), 122.8 (C4), 159.0 (C3'), 165.0 (C3), 171.0 (C2) ppm.

3.5.15. Bis[([(η^6-p-cymene){N-(Carboxyl-ethyl)-3-oxo-κO-2-(*1H*)-pyridonato-κO}ruthenium(II)] - 6b

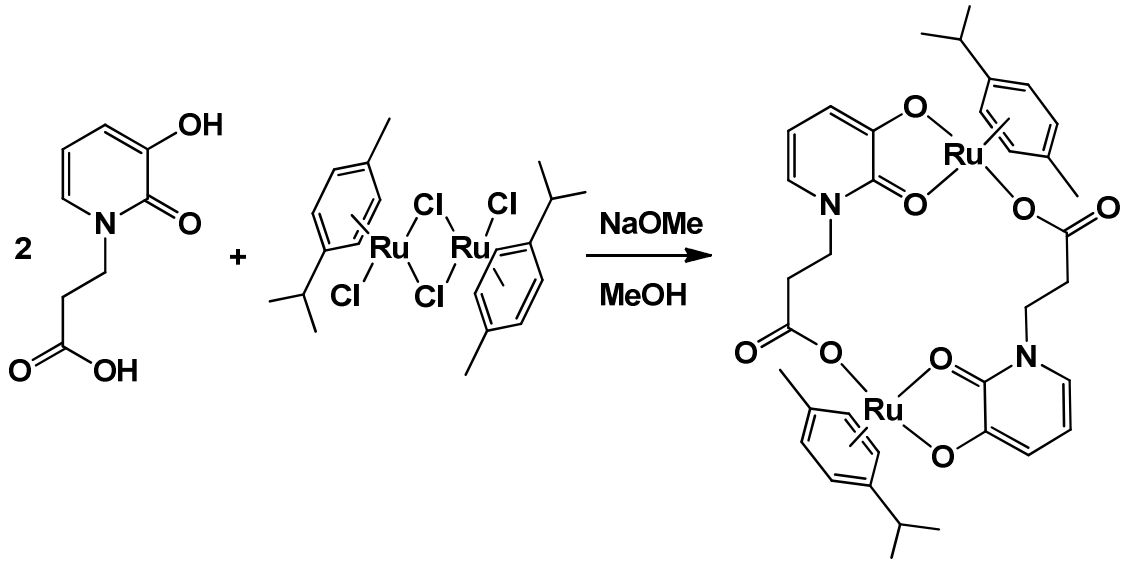

Synthesis:

The synthesis was performed according to the general procedure using 100 mg (0.16 mmol) of ruthenium precursor **p1**, 63 mg (0.34 mmol) of compound **6a** and 41 mg (0.72 mmol) of NaOMe. The resolved crude product was precipitated by addition of *n*-hexane (20 mL).

Yield: 45 mg (34%)

Melting point: >150 °C (decomposition)

Water solubility: 0.66 mg/mL

Elemental analysis: calculated for $C_{36}H_{42}N_2O_8Ru_2 \cdot CH_2Cl_2$

6b	C[%]	H[%]	N[%]
calculated	48.42	4.83	3.05
found	48.51	4.91	3.16
Δ	0.09	0.08	0.11

NMR-spectroscopy:

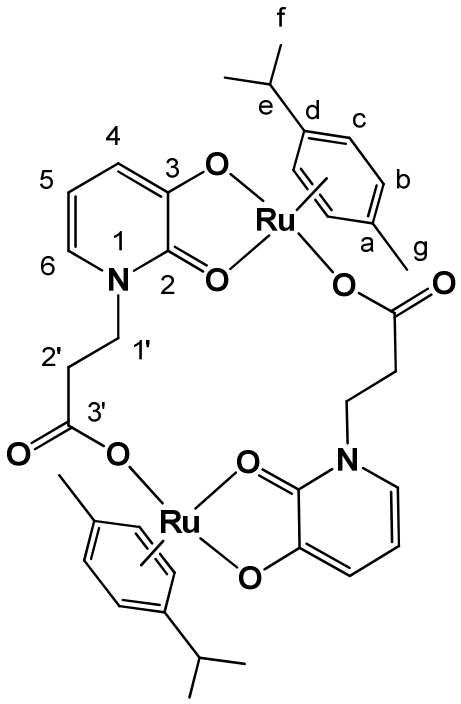

^{1}H NMR (500 MHz, $CDCl_3$): δ = 1.20 (t, ^3J(H, H) = 7 Hz, 6H, H*f*), 2.24–2.36 (m, 5H, H2', H*g*), 2.74–2.79 (m, 1H, H*e*), 3.92 (td, 1H, ^3J(H, H) = 7 Hz, ^4J(H,H) = 2 Hz, H1'), 4.18 (ddd, ^2J(H,H) = 13 Hz, ^3J(H,H) = 5 Hz, ^4J(H,H) = 2 Hz, 1H, H1'), 5.24 (d, ^3J(H,H) = 6 Hz, 1H, H*b*), 5.49 (d, ^3J(H,H) = 6 Hz, 1H, H*b*), 5.58 (d, ^3J(H,H) = 6 Hz, 1H, H*c*), 6.10 (d, ^3J(H,H) = 6 Hz, 1H, H*c*), 6.13 (dd, ^3J(H,H) = 7 Hz, ^3J(H,H) = 7 Hz, 1H, H5), 6.55 (dd, ^3J(H,H) = 8 Hz, ^4J(H,H) = 2 Hz, 1H, H4), 6.90 (dd, ^3J(H,H) = 7 Hz, ^4J(H,H) = 1 Hz, 1H, H6) ppm.

3.5.16. Bis[([(η^5-pentamethylcyclopentadiene){N-[(ethoxycarbonyl)ethyl]-3-oxo-κO-2-(*1H*)-pyridonato-κO}rhodium(III)] - 6d

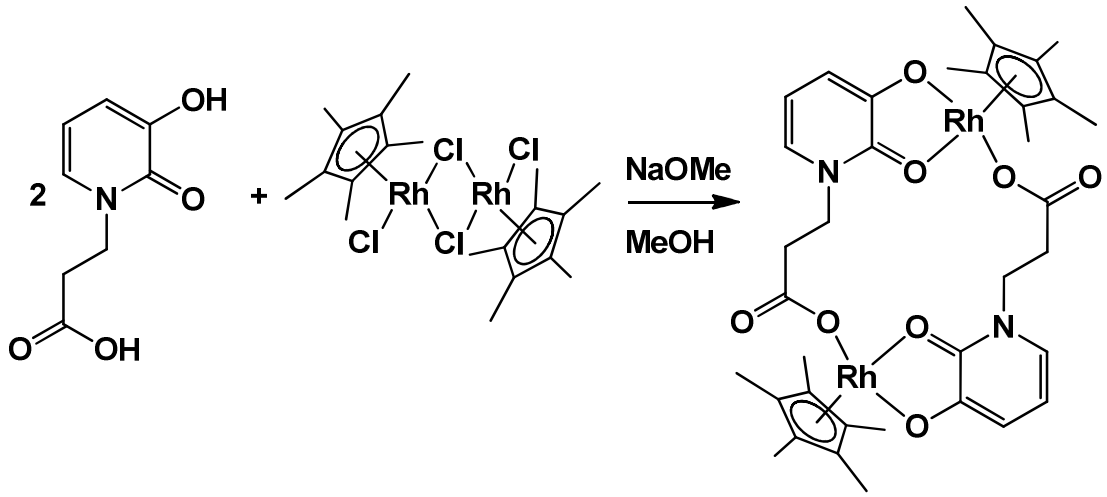

Synthesis:

The synthesis was performed according to the general procedure using 100 mg (0.16 mmol) of ruthenium precursor **p3**, 62 mg (0.34 mmol) of compound **6a** and 41 mg (0.72 mmol) of NaOMe. The resolved crude product was precipitated by addition of *n*-hexane (20 mL).

Yield: 71 mg (53%)

Melting point: >103 °C (decomposition)

Water solubility: 4.17 mg/mL

Mass spectrometry: m/z = 420 ($C_{18}H_{22}NO_4Rh$)
442 ($C_{18}H_{22}NO_4Rh + Na^+$)
839 ($C_{36}H_{44}N_2O_8Rh_2$)
861 ($C_{36}H_{44}N_2O_8Rh_2 + Na^+$)

NMR-spectroscopy:

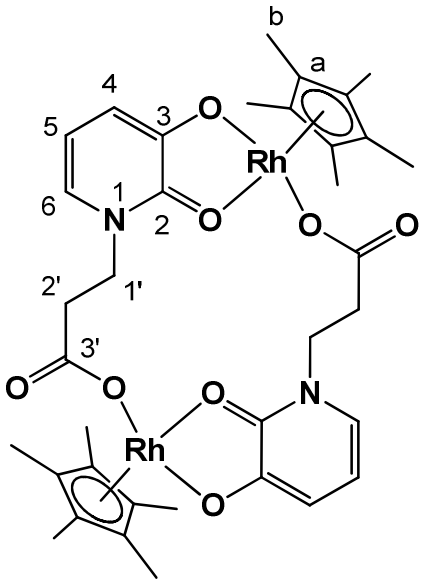

^{1}H NMR (500 MHz, d_4-CD_3OD): δ = 1.74 (s, 15H, H*b*), 2.68 (t, ^{3}J(H,H) = 7 Hz, 2H, H2'), 4.29 (brs, 2H, H1'), 6.32 (dd, ^{3}J(H,H) = 7 Hz, ^{3}J(H,H) = 7 Hz, 1H, H5), 6.66 (d, ^{3}J(H,H) = 7 Hz, 1H, H4), 6.90 (d, ^{3}J= 6 Hz, 1H, H6) ppm.

3.5.17. [Chlorido(η^6-p-cymene){N-[(ethylcarbonyl)ethyl]-3-oxo-κO-4-methyl-2-(*1H*)-pyridonato-κO}ruthenium(II)] - 7b

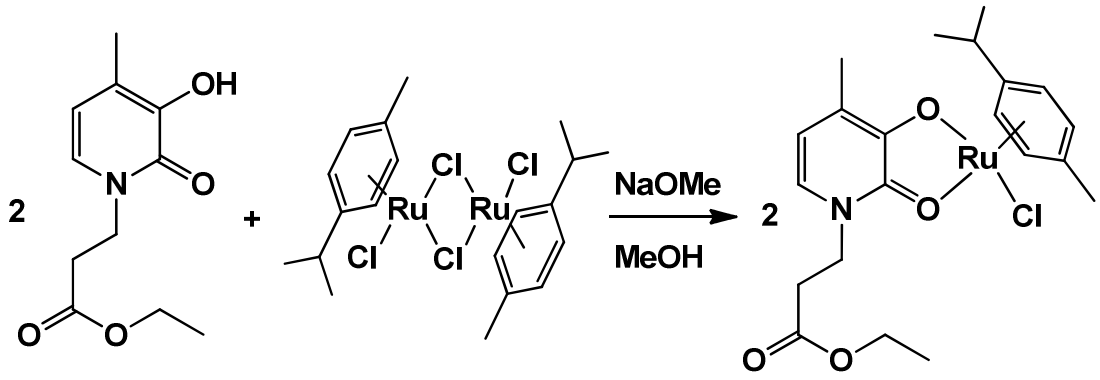

Synthesis:

The synthesis was performed according to the general procedure using 245 mg (0.4 mmol) of ruthenium precursor **p1**, 198 mg (0.88 mmol) of compound **7a** and 80 mg (1.40 mmol) of NaOMe. The resolved crude product was precipitated by addition of Et_2O (20 mL).

Yield: 212 mg (54%)

Melting point: >133 °C (decomposition)

Water solubility: 0.60 mg/mL

Elemental analysis: calculated for $C_{21}H_{28}NO_4ClRu \cdot 0.4CH_2Cl_2$

7b	C[%]	H[%]	N[%]
calculated	48.59	5.49	2.65
found	48.33	5.45	3.11
Δ	0.26	0.04	0.46

NMR-spectroscopy:

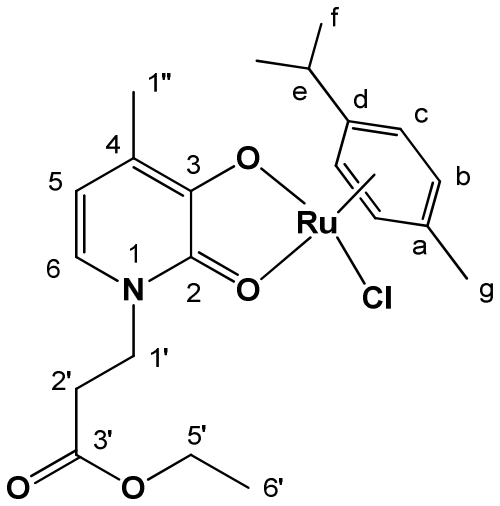

^{1}H NMR (500 MHz, $CDCl_3$): δ = 1.27 (t, ^3J(H, H) = 7 Hz, 3H, H6'), 1.35–1.37 (m, 6H, H*f*), 2.17 (s, 3H, H1''), 2.36 (s, 3H, H*g*), 2.75–2.81 (m, 1H, H2'), 2.90–2.96 (m, 2H, H*e*, H2'), 4.14–4.21 (m, 3H, H5', H1'), 4.25–4.30 (m, 1H, H1'), 5.26–5.29 (m, 2H, H*b*), 5.54–5.55 (m, 2H, H*c*), 6.13 (d, ^3J(H,H) = 7 Hz, 1H, H5), 6.49 (d, ^3J(H,H) = 7 Hz, 1H, H6) ppm.

3.5.18. [Chlorido(η^6-p-cymene){N-[(ethylcarbonyl)ethyl]-3-oxo-κO-4-methyl-2-(*1H*)-pyridonato-κO}osmium(II)] - 7c

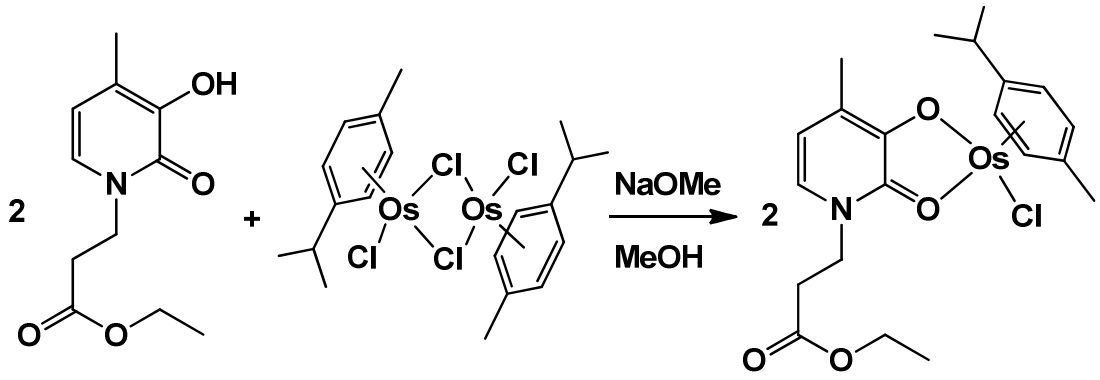

Synthesis:

The synthesis was performed according to the general procedure using 126 mg (0.16 mmol) of osmium precursor **p2**, 77 mg (0.34 mmol) of compound **7a** and 22 mg (0.39 mmol) of NaOMe. The resolved crude product was precipitated by addition of *n*-hexane (20 mL).

Yield: 48 mg (51%)

Melting point: >142 °C (decomposition)

Elemental analysis: calculated for $C_{21}H_{28}NO_4ClOs$

7b	C[%]	H[%]	N[%]
calculated	43.18	4.83	2.40
found	43.16	4.83	2.51
Δ	0.02	0.00	0.11

NMR-spectroscopy:

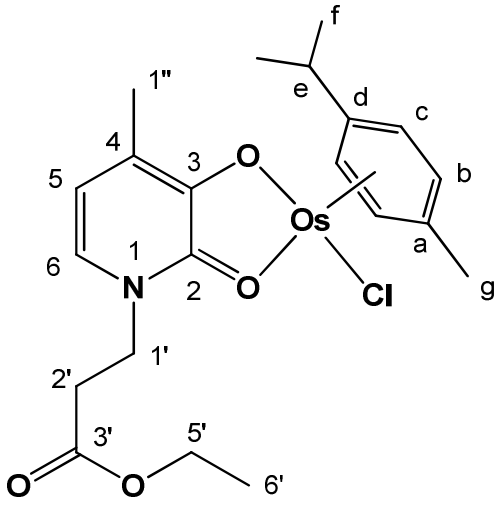

^{1}H NMR (500 MHz, $CDCl_3$): δ = 1.27 (t, ^{3}J(H, H) = 8 Hz, 3H, H6'), 1.33 (d, ^{3}J(H,H) = 7 Hz, 6H, H*f*), 2.19 (s, 3H, H1''), 2.39 (s, 3H, H*g*), 2.73–2.86 (m, 2H, H*e*, H2'), 2.90–2.96 (m, 1H, H2'), 4.16 (q, ^{3}J(H,H) = 7 Hz, 2H, H5'), 4.21–4.33 (m, 2H, H1'), 4.25–4.30 (m, 1H, H1'), 5.78 (t, ^{3}J(H,H) = 5 Hz, 2H, H*b*), 6.04 (d, ^{3}J(H,H) = 5 Hz, 2H, H*c*), 6.17 (d, ^{3}J(H,H) = 7 Hz, 1H, H5), 6.56 (d, ^{3}J(H,H) = 7 Hz, 1H, H6) ppm.

3.5.19. [Chlorido(η^5-pentamethylcyclopentadiene){N-[(ehtylcarbonyl)ethyl)]-3-oxo-κO-4-methyl-2-(*1H*)-pyridonato-κO}rhodium(III)] - 7d

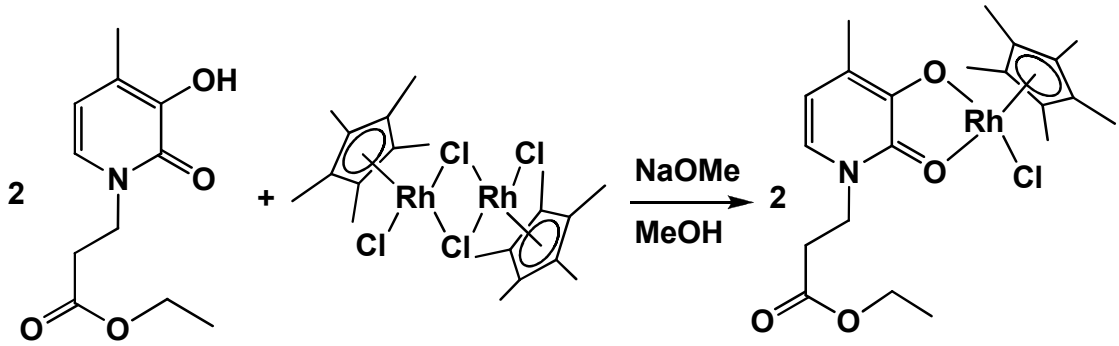

Synthesis:

The synthesis was performed according to the general procedure using 100 mg (0.16 mmol) of rhodium precursor **p3**, 77 mg (0.34 mmol) of compound **7a** and 22 mg (0.37 mmol) of NaOMe. The resolved crude product was precipitated by addition of *n*-hexane (20 mL).

Yield: 100 mg (63%)

Melting point: >170 °C (decomposition)

Water solubility: 7.14 mg/mL

Elemental analysis: calculated for $C_{21}H_{29}ClNO_4Rh \cdot 0.5H_2O$

1c	C[%]	H[%]	N[%]
calculated	49.77	5.97	2.76
found	49.63	5.82	2.79
Δ	0.14	0.16	0.03

NMR-spectroscopy:

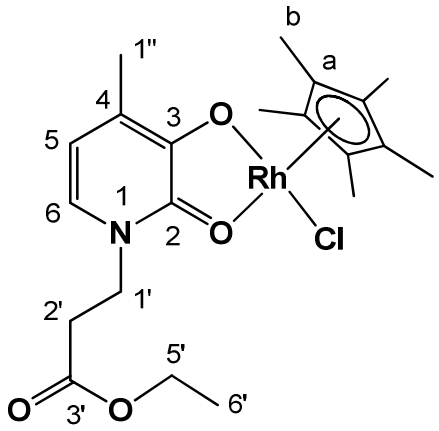

^{1}H NMR (500 MHz, $CDCl_3$): δ = 1.27 (t, ^{3}J(H,H) = 7 Hz, 3H, H6'), 1.74 (s, 15H, H*b*), 2.18 (s, 3H, H1''), 2.77–2.85 (m, 1H, H2'), 2.93–2.99 (m, 1H, H2'), 4.08–4.18 (m, 3H, H5', H1'), 4.37–4.41 (m, 1H, H1'), 6.14 (d, ^{3}J(H,H) = 7 Hz, 1H, H5), 6.46 (d, ^{3}J(H,H) = 7 Hz, 1H, H6) ppm.

3.5.20. Bis[([(η^6-p-cymene){N-(Carboxyl-ethyl)-3-oxo-κO-4-methyl-2-(*1H*)-pyridonato-κO}ruthenium(II)] - 8b

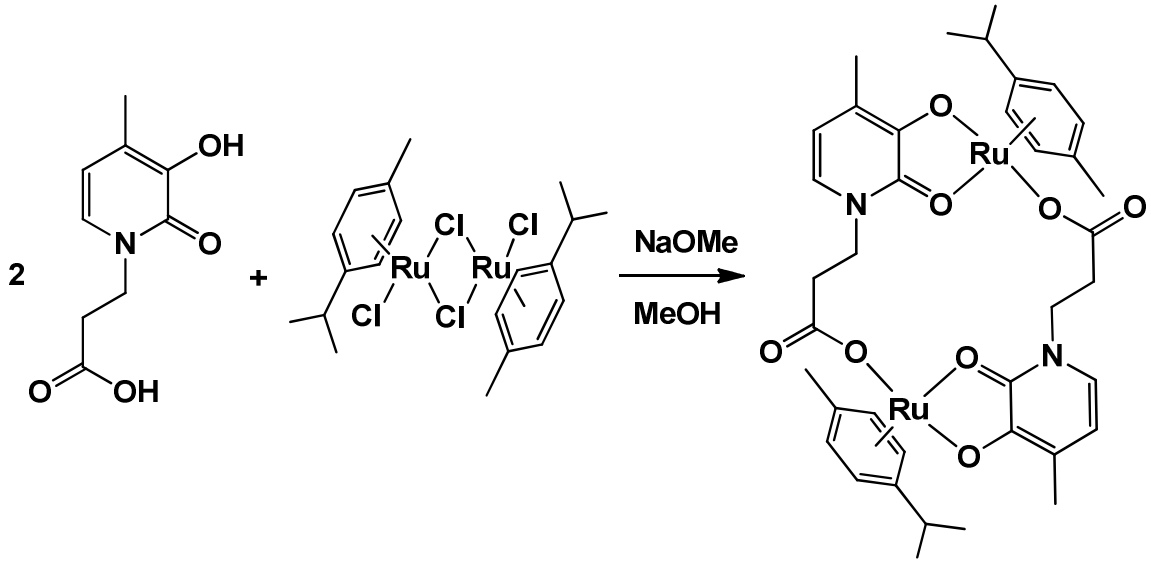

Synthesis:

The synthesis was performed according to the general procedure using 100 mg (0.16 mmol) of ruthenium precursor **p1**, 71 mg (0.36 mmol) of compound **8a** and 42 mg (0.73 mmol) of NaOMe. No product was formed upon precipitation by addition of Et_2O nor by *n*-hexane.

Yield: >5 mg, dark red crystals (crystallization experiment)

3.5.21. Bis[([(η^5-pentamethylcyclopentadiene){N-[(ethoxycarbonyl)ethyl]-3-oxo-κO-4-methyl-2-(*1H*)-pyridonato-κO}rhodium(III)] - 8d

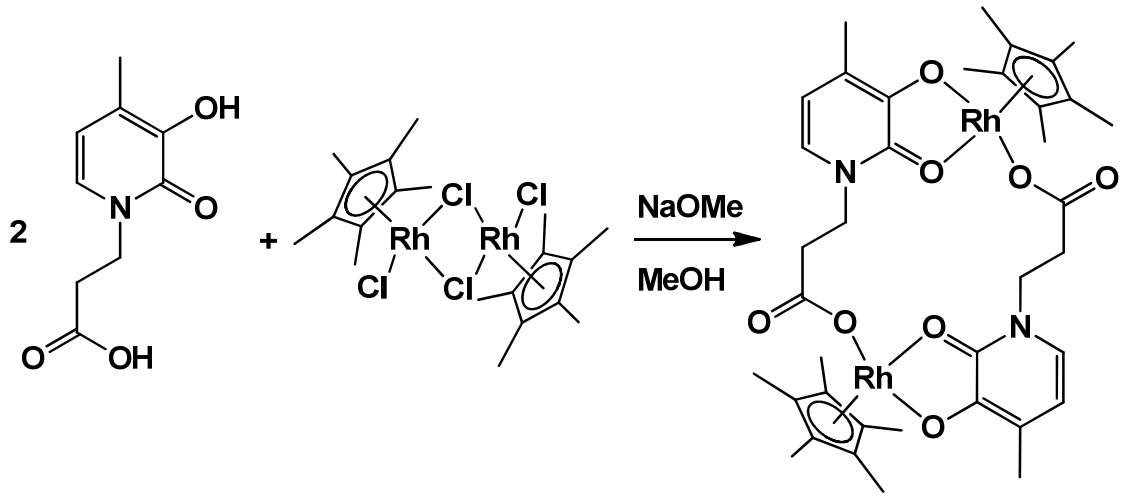

Synthesis:

The synthesis was performed according to the general procedure using 100 mg (0.16 mmol) of ruthenium precursor **p3**, 67 mg (0.34 mmol) of compound **8a** and 41 mg (0.72 mmol) of NaOMe. The resolved crude product was precipitated by addition of *n*-hexane (20 mL).

Yield: 78 mg (56%)

Melting point: >164 °C (decomposition)

Water solubility: 5.00 mg/mL

Mass spectrometry: m/z = 434 ($C_{19}H_{24}NO_4Rh$)
456 ($C_{18}H_{22}NO_4Rh + Na^+$)
867 ($C_{36}H_{44}N_2O_8Rh_2$)
889 ($C_{36}H_{44}N_2O_8Rh_2 + Na^+$)

NMR-spectroscopy:

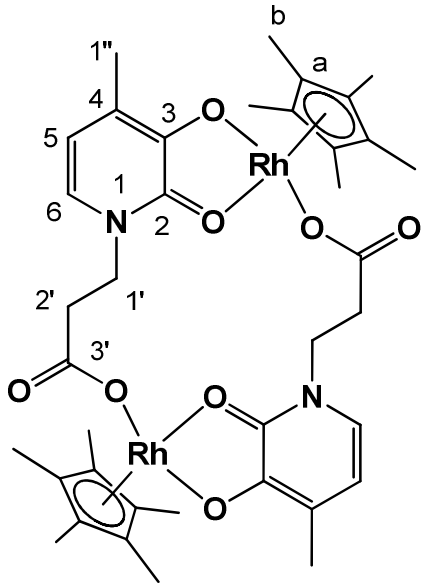

^{1}H NMR (500 MHz, d_4-CD_3OD): δ = 1.74 (s, 15H, H*b*), 2.17 (s, 3H, H1''), 2.70 (t, ^3J(H,H) = 7 Hz, 2H, H2'), 4.31 (t, 2H, H1'), 6.29 (d, ^3J(H,H) = 7 Hz, 1H, H5), 6.87 (d, ^3J(H,H) = 7 Hz, 1H, H6) ppm.

4. Conclusion and Outlook

Beside established platinum based drugs for chemotherapy, other metal complexes became potential candidates for cancer treatment such as the ruthenium(III)-based compounds KP1019 and NAMI-A. In this master thesis several “piano-stool” configured mono and dimerc ruthenium, osmium and rhodium complexes bearing 3-hydroxy-2-pyridones were synthesized and characterized. The chelating ligand system was modified through *N*-alkylation, Mannich reaction, followed by hydrogenation and hydrolysis of the ester moiety. X-ray diffraction analysis showed the formation of two possible intercalation sites for the C1 spacer complexes *via* π-stacking or interaction with the oxygens inside the cavity. With the used experimental setups no intercalation of alkali metals was observed. In water ruthenium and rhodium complexes showed good to excellent solubility, the osmium analogues only moderate or in some cases low solubility. Water stability tests revealed the immediately monomerization of the dimeric compounds to their charged aqua species, which was proven by variation of pH during pK_a determination. Coordination to the DNA model compound 5'-GMP *via N7* of the purine ring was demonstrated for selected ruthenium and osmium compounds, while rhodium showed no interaction with the nucleobase.

The *in vitro* activity of the dimeric complexes and the monomeric rhodium compounds should be investigated to compare the cytotoxicity between monomeric and dimeric compounds and between the transition metals for this ligand system. By switching to thionated pyridones the complex stability and the *in vitro* activity could be increased as it was reported for the (thio)maltolato-ruthenium(II) arene complexes.[26] Exchanging the carboxyl moiety e.g. by an amine group could be an opportunity to stabilize the dimeric structure.

Curriculum Vitae

Leo Schranzhofer B.Sc.

Address: **Wurlitzergasse 61/33**
1160 Wien
Phone number: **+436503323836**
Email-address: **leo.schranzhofer@univie.ac.at**

Nationality: Austria
Date of Birth: 03. March 1983, Hallein

Education

08. 2011 – 08.2012	Master Thesis, Institute of Inorganic Chemistry, University of Vienna
12. 2011 – 04. 2012	Master Program Chemistry, University of Vienna
11. – 12. 2011	Bachelor Program Chemistry, University of Vienna
10. 2004 – 11. 2011	Diploma Program Chemistry, University of Vienna
10. 2003 – 08. 2004	Bachelor Program Biology, University of Salzburg
09. 1993 – 07. 2002	Gymnasium, BRG Akademiestrasse, Salzburg
09. 1989 – 07. 1993	Ground School, Leopoldskron Moos, Salzburg

Work Experience

02. and 07. 2010 07. 2009	Member of the working group of Prof. Keppler, Institute of Inorganic Chemistry, University of Vienna

08. 2009	Marktgemeinde Grödig, Office Work
07. - 08. 2008	
07. - 08. 2007	
07. 2006	
07. – 08. 2005	
07. – 08. 2004	
08. – 09. 2002	
08. – 09. 2006	Zementwerk Leube GmbH., laboratory activities
10. 2003 – 09. 2004	Seniorenheim Grödig, civilian service

workshops and congresses

04. 2012	WACÖ Innsbruck 2012 (oral presentation)

Language Skills

German (mother language)
English
Latin (basic knowledge)

Other Skills

MS Office
Hardware knowledge